ALBERTA BOREAL DEER PROJECT

ALBERTA BOREAL DEER PROJECT
FINAL REPORT
Jason T. Fisher, A. Cole Burton, Luke Nolan, Michelle Hiltz, Laurence D. Roy
Alberta Innovates - Technology Futures, Ecosystem Management Group

Contents

Acknowledgements

The Alberta Boreal Deer Project Team:
Alberta Innovates – Technology Futures

Dr. Jason T. Fisher, Senior Research Scientist	Scientific Lead and Project Coordinator
Dr. Cole Burton, Research Scientist	Scientist and Data Analysis
Michelle Hiltz, Portfolio Manager	Project Administrator
Luke Nolan, Senior Wildlife Technician	Field Operations
Laurence D. Roy, Wildlife Ecologist	Advisor
Sandra Melenka, Wildlife Technician	Image Analysis
Dr. Daiyuan Pan, Research Scientist	GIS Analysis
Dr. Brian Eaton, Senior Research Scientist	GIS Analysis
Kent Richardson, Technician	GIS Analysis
Nicole Heim, Wildlife Consultant	Resource selection function analysis
Hannah Britton-Foster, University of Victoria	Step selection function analysis

Alberta Environment and Parks

Barb Maile, Senior Wildlife Biologist	Lead Advisor
Grant Chapman, Senior Wildlife Biologist	Advisor
Craig Dockrill, Asst. Fish & Wildlife Manager	Advisor
Paul MacMahon, Fish & Wildlife Manager	Advisor
Kristina Norstrom, Wildlife Biologist	Advisor. **R.I.P.**

CHAPTER 1: A BRIEF INTRODUCTION TO ALBERTA BOREAL DEER

Introduction

White-tailed deer are an evolutionary success story. Since the last glaciation, white-tailed deer (WTD; *Odocoileus virginianus*) have thrived in North American forested landscapes, spread mainly across the eastern side of the continent (Heffelfinger 2011). In the centuries following European colonization, when most North American mammal species suffered range contractions, WTD ranges were the only ungulate species to gain ground: an estimated 6% range increase across the continent (Laliberte and Ripple 2004). Population increases in white-tailed deer were a pervasive wildlife management problem throughout the later 20th century (Heffelfinger 2011) and remain so in the 21st. The impacts of deer expansion are profound and widespread, affecting forest structure, forestry yield, community composition, biodiversity, ecosystem dynamics, and predator-prey dynamics (Côté et al. 2004). Research into the impacts of WTD on forest ecosystems is abundant. Research into the factors that facilitate WTD expansion has focused mostly on population biology (DeYoung 2011), deer movement (Beier and McCullough 1990), and predator-prey dynamics (Ballard et al. 2001). The effects of the changing landscape on white-tailed deer was recognized by Leopold (1987) early on, though landscape-scale studies of the effects of landscape change on deer distribution has been limited. Moreover, these effects are typically region-specific, and little is known about white-tailed deer as they expand into northern boreal regions, with some exceptions (Patterson and Power 2002, Latham et al. 2011, Latham et al. 2013, Dawe et al. 2014). Understanding white-tailed deer distribution in the boreal forest was our primary goal, and we strove to meet these goals through a series of population and landscape "natural experiments" (Diamond 1983, Turner 1989). Each chapter in this report highlights a different examination of white-tailed deer distribution and abundance, and the implications for boreal deer expansion. These experiments are rooted in three main aspects of WTD biology: foraging ecology, movement ecology, and energetics.

Movement ecology

White-tailed deer movements vary markedly across their continental range, among terrain and habitats, and within age-sex classes (Sabine et al. 2002, Stewart et al. 2011, Massé and Côté 2013). White-tailed deer home range sizes vary markedly among regions, and within seasons (Stewart et al. 2011). Sub adults disperse from natal areas, but adult dispersal – typically an important driving factor in range expansion – is relatively rare, and typically short, although adult female dispersal frequency and distance varies geographically (Stewart et al. 2011).

In this highly adaptable species, general patterns are not always discernable, or at least do not typically hold over their whole range. In northern regions with consistently deep snow cover, adults are typically "obligatory migrants", moving from summer to winter ranges where the effects of a severe winter are ameliorated (Sabine et al. 2002). In northern regions with little snow, deer are "conditional migrators", moving when conditions compel them to do so. Within these classifications there is considerable annual and individual variability; some individuals may shift habitat selection but do not necessarily migrate (Sabine et al. 2002, Stewart et al. 2011). A deer's ability to move through a landscape is clearly a key factor in their persistence in northerly regions. Landscape alteration that enhances movement – creating roads and other

linear features – may encourage deer population increases and expansion, with some interacting effect of winter severity, and likely energetic condition.

Energetics and foraging

Like all mammals, white-tailed deer must balance energy obtained from forage with the metabolic demands of foraging, predation avoidance, gestation, lactation, growth, and homoeothermic (Parker et al. 2009, Hewitt 2011). White-tailed deer are ruminants and as such rely heavily on abundant nutritious forage (Ditchkoff 2011). Their diets are diverse, and the impacts of browsing by overabundant white-tailed deer have been extensively studied across the continent (Côté et al. 2004). Forage availability, and hence consumption, varies seasonally. In the summer, WTD primarily eat leaves and stems of deciduous woody plants, forbs, grasses, and some mast where available in the summer season, and are restricted to low-quality browse in the winter (Moen 1978, Hewitt 2011). The deciduous and mixed-transitional forests of eastern North America provide an abundance of WTD forage, which has sustained this species through evolutionary time (Heffelfinger 2011). Agricultural land covering much of the contemporary land base, as well as plants used in supplemental feeding, provides additional forage (Chapman et al. 2009, 2010). In the boreal forest, available browse has typically been viewed as limiting white-tailed deer populations to some degree (Patterson and Power 2002), but how browse has been contributing to deer expansion throughout the boreal forest remains unknown.

The cold temperatures and deep snow historically characteristic of the boreal regions of North America placed high metabolic demands on deer, limiting foraging movements and stressing homoeothermic maintenance. In mature boreal forest – where early seral vegetation is naturally restricted to burns and forest canopy caps (Fisher and Wilkinson 2005) - these metabolic demands may be greater than the energy gained from available forage; ergo WTD distribution and abundance have historically been limited in the boreal forest (Heffelfinger 2011, Hewitt 2011, Dawe et al. 2014). Forage is especially important in winter, when WTD are energetically stressed and enter "controlled starvation" (Hewitt 2011). With ongoing climate change, winters globally have become less severe (Karl and Trenberth 2003), and evidence suggests this is true of boreal regions as well, with less snow and less extreme temperatures (Dawe 2011). Concurrent with this, white-tailed deer forage has become more abundant as forestry, mining, and oil and gas activity replaces old and mature forest stands with early-successional stands (*e.g.* Fisher and Wilkinson (2005)). A profound change in the amount of early seral vegetation on the boreal landscape, in addition to warmer and drier winters, may have increased boreal WTD populations in the region and may be driving WTD expansion. However, the landscape-scale contributions of habitat alteration and winter severity remain unknown.

Demography

Like any animal, white-tailed deer are strongly affected by demographic processes. This research was never intended to study WTD demography in the boreal forest, but a few salient points of white-tailed deer population dynamics are warranted, as these provide important context for our study of distribution, habitat selection, and density.

As WTD are remarkably flexible in their habitat associations – flexibility that facilitated their distribution across the continent – so too is their population structure highly adaptable to different environments (DeYoung 2011). The seminal work of McCullough (1979) and subsequent research suggests WTD sometimes display density dependence, and sometimes do not. Rapid population increases following forest disturbance are characteristic of WTD and fawning rates are highly variable, depending on environmental conditions (DeYoung 2011). Survivorship is age-specific. The great risk of mortality comes in the first year of life (Lesage et al. 2001), decreasing markedly for 1-2 year-olds, remaining low and constant for 2-10 year olds, then increasing again (Delgiudice et al. 2006). However, mortality is also highly variable within and among populations, and depends largely on environmental factors (Delgiudice et al. 1990b, Delgiudice et al. 2002, Delgiudice et al. 2006). In particular, mortality increases markedly with winter severity – especially snow depth, a primary correlate of body condition (Garroway and Broders 2005). However, the effect of snow depth and winter severity is mediated by physiological condition – a function of nutrition, itself a function of available browse (Delgiudice et al. 2002, Parker et al. 2009). Moreover, winter severity affects males and females differently (Lesage et al. 2001), especially adult females with gestating young (Pekins et al. 1998). Finally, there appears to be a time lag – a year or more – between the period when forage is limiting and when that limitation incurs sufficient metabolic costs to succumb to severe winters, or to impact recruitment (Fryxell et al. 1991).

Predators are also obviously a primary source of mortality, with survival rates varying among landscapes as predators vary (Delgiudice et al. 2006, Turner et al. 2011). Predator mortality has a greater impact on old does than other age-sex classes, but there is a confounding effect of environment: does suffering from extreme weather are more likely predated (Delgiudice et al. 2006). Despite chronic and periodically acute mortality, Delgiudice et al. (2006) found that high survival rates of prime age deer, high pregnancy rates, and periodic twinning rates, often offset mortality and provide for population stability. In summary, responses of white-tailed deer to a novel boreal environment with variable winter severity, marked anthropogenic change, and a diverse suite of predators, are exceedingly challenging to predict.

Research motivation

White-tailed deer expansion is a pan-continental phenomenon (Laliberte and Ripple 2004). In each biome and region, WTD impact local flora, fauna, and ecological processes (Côté et al. 2004). Those impacts can be mitigated through wildlife and landscape management, but doing so effectively requires information on deer distribution, density, and movement – as well as the factors facilitating that expansion. This was our primary motivation.

In the boreal forest, WTD management takes on a more urgent tone than in our jurisdictions, and provided our secondary motivation. Alberta's woodland caribou populations are declining (Hervieux et al. 2013), and wolf predation is considered a primary cause (Wittmer et al. 2005). Predation increases where seismic line density is high (Boutin et al. 2012, McKenzie et al. 2012), so mitigation and reclamation of linear features is being undertaken to reduce predators' use of lines. However, these activities may not be effective alone. High densities of wolf alternate prey such as WTD may increase wolf abundance and caribou predation rates (*e.g.* Seip (1992)), potentially amplifying the effect of seismic line density. Elevated wolf densities have changed wolf-caribou dynamics (Latham et al. 2011, Latham et al. 2013) by increasing predation, and caribou mortality. Moreover, WTD management requires information on habitat selection and population

densities. However, although there are modelled large-scale predictions of white-tailed deer expansion in Alberta (Dawe et al. 2014), we have limited data on deer habitat selection in Alberta's boreal forest, or how they respond to the various kinds of anthropogenic disturbance occurring in this unique region. Moreover, density within the expansion zone is unknown, as aerial surveys of white-tailed deer are encumbered by dense conifer cover and differential sightability among habitats. Ground-based survey methods might provide a better method for estimated deer abundance, while simultaneously allowing an examination of the factors affecting WTD distribution in the boreal forest. We used a combination of camera trapping (O'Connell et al. 2011, Burton et al. 2015) and satellite telemetry (Millspaugh and Marzluff 2001, Kays et al. 2015) to examine (1) the relationship between WTD distribution, anthropogenic disturbance, and natural landcover; (2) the seasonal changes in WTD distribution and the role of winter severity; (3) WTD home-range and space-use in the boreal forest; and (4) deer density in this heavily modified boreal forest landscape.

We are not the first to attempt to disentangle the relative contributions of forage availability and climate on white-tailed deer. Patterson and Power (2002) asked this question for Nova Scotia white-tailed deer and Dawe et al. (2014) revisited it for Alberta boreal forests. However, we are the first to ask this question at landscape scales – where the effects of landscape composition and winter severity on distribution explicitly manifest – using continuous, longitudinal data on deer distributions and relative abundance. This novel approach allows us to test questions about the relative contributions of climate and landscape on boreal white-tailed deer expansion. If available forage and cover – especially in winter – are the principle drivers of white-tailed deer expansion in the boreal forest, then we would predict that deer distribution is correlated with the distribution of deciduous forests and those anthropogenic activities that create early-successional stands (*e.g.* forestry, seismic lines, and well pads), and that these features buffer deer distribution and deer density from fluctuations in severe winters. If winter severity is a principle factor, we would expect deer distributions and population sizes to shrink after more severe winters, irrespective of landscape composition. We test these hypotheses in the boreal forest of northeast Alberta. We do this using a combination of satellite telemetry, camera-based surveys, and spatially explicit density estimation models. Our twin goals were to learn more about the factors that contribute to white-tailed deer expansion in the boreal forest, and to create a method for estimating white-tailed deer density that overcomes the problems of poor sightability encountered in aerial surveys of this dense forest region.

Study Area

Our research was conducted in the boreal forest northeast of Lac La Biche, Alberta, Canada (Figure 1-1). The study area is approximately 3000 km^2 and encompasses the area around Christina Lake and Winefred Lakes, north of the Cold Lake Air Weapons Range. This landscape is a mosaic of lowland spruce, muskeg, upland spruce, deciduous and mixedwood, and some jack pine to the east. The area has extensive forestry to the north, with motorized access and oil and gas development by multiple companies in the area to the south, west, and north of Winefred Lake.

Experimental design

Inferences from landscape-scale habitat selection studies depend greatly on the distribution of different habitat types that are sampled within those landscapes (Aebischer et al. 1993, Fisher et al. 2005). To provide as broad an inference space – the scope within which one can reliably extrapolate experimental results – as possible, our goal was to disperse the cameras across the study area so that the major habitat types in this landscape had an equal probability of being surveyed for deer occurrence. This landscape is very heterogeneous, and contains both common and rare habitat types, so a design is needed that samples habitat types disproportionately to their availability in the landscape. To achieve this dispersion, we used a stratified-random design to select 1-km x 1-km grid cells for surveying white-tailed deer occurrence. We used this size of grid-cell as it is likely to meet the assumptions of independence among survey sites, and closure within survey periods, required of occupancy models (MacKenzie et al. 2006).
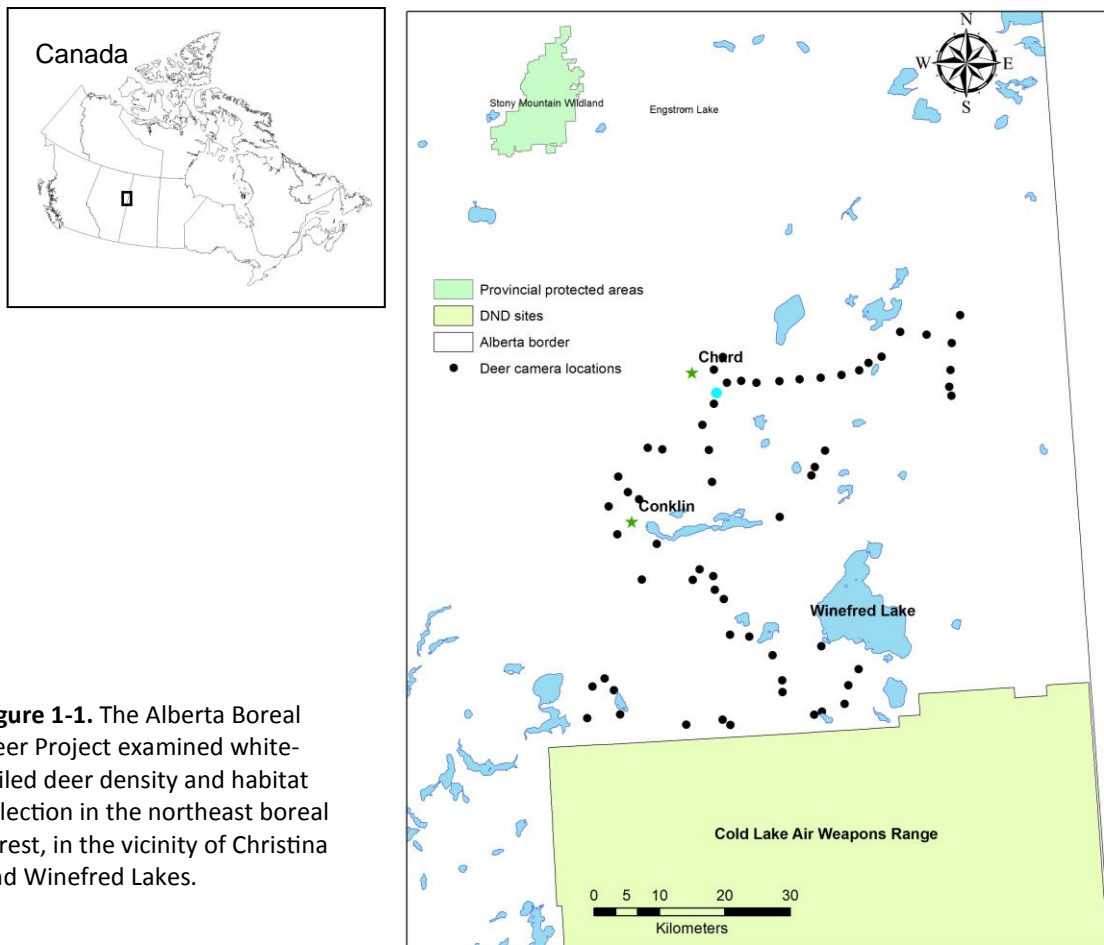
Figure 1-1. The Alberta Boreal Deer Project examined white-tailed deer density and habitat selection in the northeast boreal forest, in the vicinity of Christina and Winefred Lakes.

Cells were selected for sampling based on Alberta Vegetation Index (AVI) digital forest inventory data (AESRD 2005). We categorized tree species as coniferous [black spruce (Sb), jack pine (Pj), white spruce (Sw), and balsam fir (Fb)] or deciduous [paper birch (Bw), aspen (Aw), balsam poplar (Pb), and tamarack (Lt)]. We determined the area of each polygon within each grid cell represented by each canopy species, and multiplied that by the percentage of the canopy in that polygon. We designated each polygon as lowland if the moisture regime was designated aquatic or wet, or upland if not. For each polygon, the canopy cover designations and moisture regime information were combined to create the following categories: upland conifer, lowland conifer, upland deciduous, lowland deciduous, upland mixedwood, lowland mixedwood, non-forested.

The total area represented by each of the canopy cover/moisture regime combinations, and the non-forested category, were summarized for each 1 x 1 km grid cell, and we designated cells according to their composition. For example, we classified a cell as non-forested if more than 50% of its area was classified as non-forested at the polygon level; conifer if 70% or greater of the area was conifer polygons, and so on. Within each polygon, more than one forested category could be present, but each would have the same landscape designation (e.g. lowland or upland).

Final classification of a grid cell was based on a combination of dominant canopy cover and dominant moisture regime. Within the population of potential grid cells – defined by a systematic grid overlaying the study area - we selected those cells that intersected a navigable road to provide reliable access to survey sites. Surveying only cells with access to roads was a logistical necessity, but does constrain the inference space of our results to forested regions with roads. This selection process produced a candidate set of 406 grid cells. From this set, we randomly selected 12 grid cells to survey within each of the survey categories: lowland conifer, lowland mixedwood, upland conifer, upland mixedwood, and upland deciduous. We randomly selected an additional 5 cells in each category as back-ups in the event the primary cells could not be surveyed. The final candidate set of survey cells achieved representation across the landscape and across habitat types (Figure 1-1).

Within each grid cell, we subjectively selected a site for camera placement. We visually surveyed the cell for wildlife trails, and then selected a trail with evidence of extensive and recent wildlife travel, to maximize probabilities of detection. Cameras were deployed on the game trail, a minimum of 50 m off the road. Subjective placement is necessary to capitalise on the effect of trails in maximising probability of detection, but does not compromise the experimental design, as the grid cell is the statistical sampling unit.

Landscape reclassification

This boreal landscape is naturally very heterogeneous – a mosaic of upland and lowland forest, spruce bogs, lakes, and rivers. To quantify this natural heterogeneity in a way that constrained the independent variables going into subsequent species-habitat models to a reasonable number (Burnham and Anderson 2002), we reclassified AVI digital forest inventory data into 12 classes that we predicted were potentially important for white-tailed deer (Appendix 1).

This landscape has also experienced marked alteration for resource extraction (Figure 1-2). Forest harvesting is widespread in the north of the study area. There are industrial camps, borrow pits, sumps, and well pads. A meshwork of

traditional seismic lines (cutlines), 3-dimensional seismic lines (3D seismic), and pipelines roll across this landscape. A network of roads and trails (accessible but without gravel) cover much of the area, permitting human access. To quantify these features, we reclassified Alberta Biodiversity Monitoring Institute (ABMI) human footprint layer[1] data into 3 classes representing polygonal anthropogenic features – cutblocks, well sites, and other 'block features'. We used a high-resolution linear features layer[2] to classify anthropogenic linear features on the landscape. We buffered these linear features (Appendix 1) to assign an area of footprint to each. This reclassification formed the basis for the camera-based species distribution model analyses reported in the following chapters.
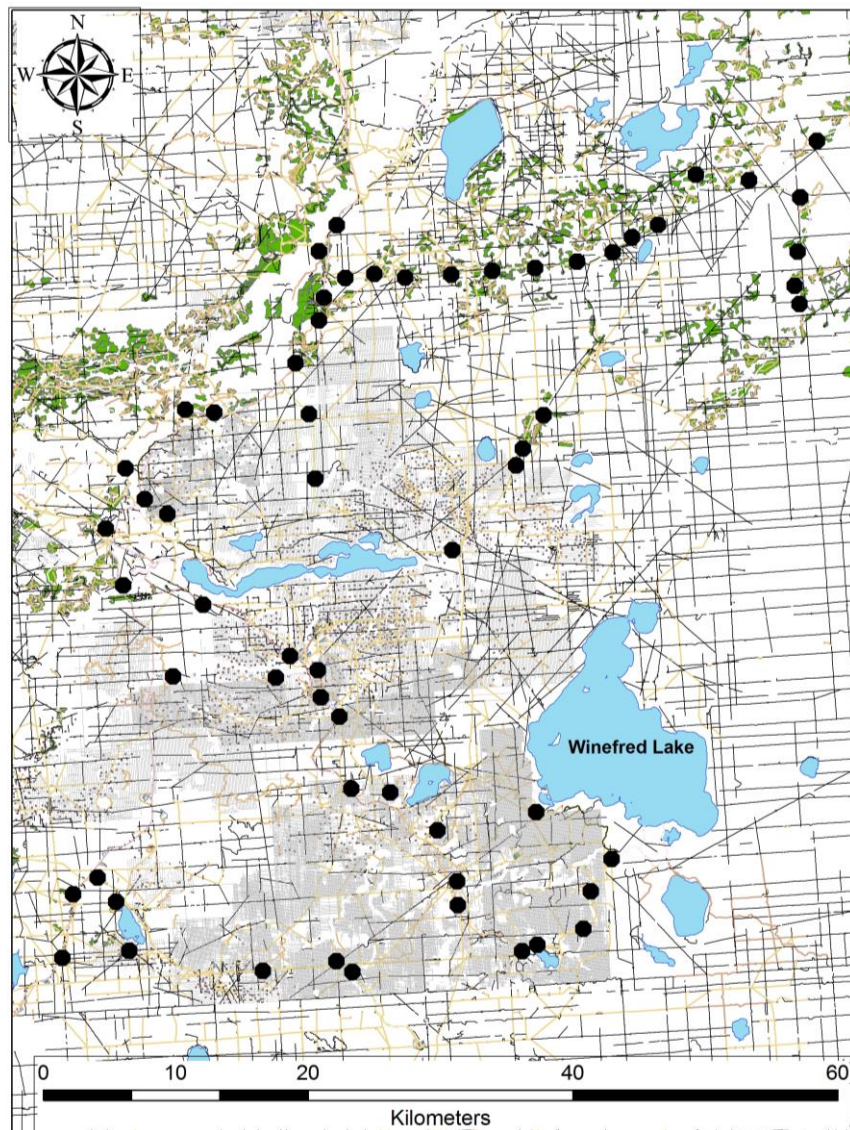
Figure 1-2. Anthropogenic footprint is extensively and intensively imposed on this landscape, including forest harvesting cutblocks (green), well sites (square dots) cutlines (black), 3D seismic (grey), and roads and trails (yellow). Large black dots are camera sites.

CHAPTER 2: OCCUPANCY DYNAMICS OF WHITE–TAILED DEER IN NORTHEAST ALBERTA: THE EFFECTS OF WINTER SEVERITY ON ANNUAL SPATIAL DISTRIBUTION

Introduction

Understanding the drivers of species distributions has been at the heart of ecological inquiry from Darwin (1859) and Grinnell (1917) to today (Scott et al. 2002). Species distributions vary in space in conjunction with habitat suitability, community assembly, abiotic and climatic variables, and a host of other factors. Identifying which factors are key drivers of distribution is the goal of niche theory (Hutchinson 1957, Hutchinson 1965, Chase and Leibold 2003, Holt 2009). Species distributions also change through time in response to temporal environmental variability. Temporal fluctuations are harder to quantify than spatial, as they require long-term data, but their importance has been brightly illuminated by pressing needs of climate change science (Kareiva et al. 1993, Pearson and Dawson 2003, Thomas et al. 2004, Lawler 2009). There are myriad ways by which climate change is expected to affect species distributions. For mammals, responses are often rooted in changing energetic demands (Humphries 2009), and this is reflected in models of future species distributions under climate change scenarios (Lawler et al. 2009).

All mammals must balance energy intake with metabolic demands, and this need is particularly pronounced for boreal species, where winters can be severe and food supplies ephemeral (Humphries et al. 2004, Humphries et al. 2005). Different species have evolved different mechanisms for dealing with energetically costly, nutrition-poor winters. White-tailed deer (WTD), for example, enter a kind of "controlled starvation" in the winter (Hewitt 2011), wherein metabolic demands exceed nutritional intake to some degree, and deer rely on fat reserves accumulated in the previous summer and fall to survive. Cold temperatures and deep snow incur a severe metabolic cost that outstrips available energy reserves, leading to high deer mortality (Ditchkoff 2011, Hewitt 2011). Deep snow, in particular, increases metabolic cost induced by drag when depth exceeds 50% of brisket height (approx. 60cm for a 50-80 kg white-tailed deer) (Parker et al. 1984, Hewitt 2011). If sufficiently severe, overwinter mortality can markedly decrease population sizes (DeYoung 2011). Historically, severe winters may have restricted WTD from extending their range into the boreal forest region (Dawe 2011, Heffelfinger 2011, Dawe et al. 2014). As the climate changes due to greenhouse gas emissions, northern winters have become less severe (Karl and Trenberth 2003). Average daytime winter temperatures have increased, and mean winter snow depth has decreased, with consequences for entire boreal and arctic communities (Walther et al. 2002, Post et al. 2009), including white-tailed deer.

The expansion of white-tailed deer into the boreal forest region is the latest in an ongoing spread of this highly adaptable species. In the centuries following European colonization of North America, while most mammal species on the continent suffered range contractions, WTD were the only ungulate species to gain ground: they effected an estimated 6%

range increase across the continent (Laliberte and Ripple 2004). Population increases in white-tailed deer were a pervasive wildlife management problem throughout the later 20th century (Heffelfinger 2011) and remain so in the 21st. The impacts of deer expansion are profound and widespread, affecting forest structure, forestry yield, community composition, biodiversity, ecosystem dynamics, and predator-prey dynamics (Côté et al. 2004). White-tailed deer expansion into the boreal forest is implicated in marked declines of threatened woodland caribou (Latham et al. 2011, Boutin et al. 2012, Latham et al. 2013). Deer are alternative prey for wolves, increasing wolf numbers, which decrease caribou populations – an example of apparent competition (Holt 1977, Holt and Kotler 1987, Holt et al. 1994). With the pressing need to stem caribou declines, white-tailed deer expansion is a topical model to examine the relative effects of winter severity and landscape change on boreal species distributions.

The relative role of winter severity and landscape change in facilitating WTD expansion is controversial. Dawe et al. (2014), using snowtracking and aerial survey data collected 2002-2009, concluded that winter severity was an important predictor of deer occurrence in Alberta's boreal forest, and thereby suggesting that the milder winters expected under climate change will continue to facilitate northward expansion of WTD range. Dawe et al. (2014) further suggested that land use change may interact with climate change, whereby landscape modifications from industrial development – forestry and oil and gas extraction – may buffer WTD against the effects of severe winters. To test this hypothesis, it is necessary to assess the spatiotemporal dynamics of deer populations. While severe winters may reduce the overall abundance of WTD, populations losses are not expected to be uniform in space (Stewart et al. 2011), and recovery may be rapid when severe conditions cease. Identifying landscape factors that allow WTD to persist in the face of severe winter conditions (i.e. spatial refugia), or facilitate their recolonization and recovery, is critical to targeting management toward minimizing the negative impacts of WTD expansion.

In this study, we assessed the spatiotemporal dynamics of WTD over three years in a 3,000 km^2 landscape within the boreal forest of Alberta, Canada. This region is not the leading edge of range expansion, but rather embedded within it; WTD are already distributed across the study area. Our goal was to investigate factors influencing distribution within this occupied boreal landscape, to help us understand those factors driving expansion. We use a relatively new method to assess WTD distribution: camera traps. Camera traps (CTs) are an increasingly popular ecological research tool that are adaptable to a variety of ecological questions (O'Connell et al. 2011, Burton et al. 2015), allowing us to cost-effectively survey species distributions over large areas and long periods. We used CT detections to model changes in WTD use of sites over time, applying an occupancy modelling framework to account for the fact that deer using a sampled area may not always be detected by a camera (i.e., imperfect detection; Mackenzie et al. 2002, 2006). In our context, we consider "occupancy" to represent deer use of a site, and "detectability" to represent availability of deer to be detected by a CT. This acknowledges that sites are not closed to changes in occupancy within a sampling period, and that detection will be influenced primarily by local deer abundance and movement in and out of the CT detection zone within a larger home range (Burton et al. 2015, Figure 2-1). This approach is cautious, but does not necessarily replace a count index if species-level detectability is shown to approach 1.0.
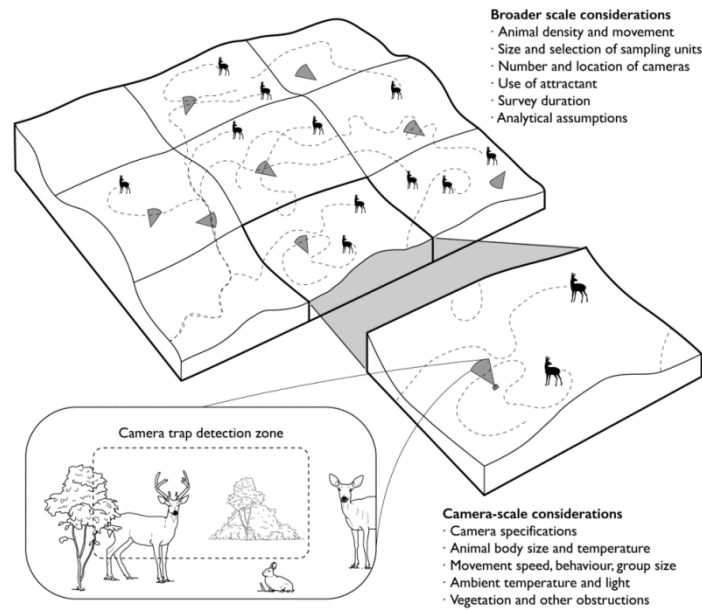
Figure 2-1. The detection of animals by camera traps is affected by ecological and observational processes occurring at both the local scale of the camera trap detection zone and the broader scale of the surrounding landscape. Explicitly accounting for these underlying processes is an important challenge for wildlife surveys with camera traps. Illustration by Jeff Dixon. From Burton *et al.* (2015).

As WTD use of the landscape changes seasonally and annually, we can estimate occupancy dynamics across time periods using multi-season occupancy models (MacKenzie et al. 2003, MacKenzie et al. 2006). Sites where WTD are absent may become occupied as the population expands or conditions change, which can be estimated as the *probability of site colonization*. Conversely, deer may stop using previously occupied sites, with some *probability of site extinction*. The sum of these processes is estimated as the *spatial growth rate*, a parameter analogous to the more familiar population growth rate (λ) but instead describes relative growth or decline in distribution, rather than abundance.

We used multi-season occupancy models to estimate WTD occupancy dynamics over three years of differing winter severity. We tested two main hypotheses:

1. Deer distribution contracts in winters, with more contraction in colder winters with deeper snow.
2. Deer quickly recolonize sites during spring and summer, leading to relatively stable annual distributions even after severe winters.

Methods

To establish the degree of seasonal and inter-annual change in temperature and snow depth in the study region, we obtained Environment Canada weather data (http://climate.weather.gc.ca) for the two closest weather stations: Lac La Biche and Fort McMurray, Alberta. We plotted daily mean temperatures and snow on ground (only available for Fort McMurray) across the three years of the study (October 2011 – September 2014).

Deer sampling

We surveyed deer occurrence across the study landscape by deploying one Reconyx™ Hyperfire PC900 camera (Holmen, WI) at each of 62 sampling sites. Cameras were set to "fast shutter" speed, as this setting reduces motion blur and provides high-resolution, detailed daytime images suitable for identifying sex and collared individuals where possible. Cameras were deployed in grid cells selected using a stratified-random design (Chapter 1). Cameras were deployed on wildlife trails chosen subjectively within the grid cell. This approach allowed us to maximize probability of detection, but did not compromise the probabilistic design as statistical inference is made with the grid cell as the sampling unit. Cameras were deployed a minimum 2-km apart. Following Burton et al. (2015), we define 'site' as the area approximating an average short-term (seasonal, 3-month) home range, centered on the camera detection zone. We assume the study area is the *ca.* 3000 km^2 area encompassing a minimum convex polygon surrounding the cameras sites.

Deployment began October 22 2011 and ended October 26 2014. We separated the continuously collected camera data into month-long (30.4 day) survey periods. Each month was treated as one survey; three surveys comprise a primary sampling season, within which sites are assumed closed to species-level changes in occupancy, similar to Pollock's robust design for capture-recapture (Pollock (1982)). As noted above, we relax the closure assumption but assume that deer use of a site is not directionally biased within the relatively short three-month sampling season; that is, there is not one-way immigration or emigration, or complete mortality, of all deer using a site during a season. Under this assumption, variation in observed deer occurrence among months within a 3-month season represents "detection error", attributed mainly to movement in and out of the camera detection zone (Figure 2-1). Deer behaviour varies seasonally, with most variation due to changes associated with mating, parturition, and dispersal (DeYoung et al. 2011). We therefore classed each "deer season" as three-month periods: rut (autumn, October – December), post-rut (winter, January – March), pre/early fawning (spring, April – June), and post-fawning (summer, July – September). The full data frame for the study is thus 12 seasons, with 3 repeated surveys within each season, for a total of 36 surveys at each site, each comprised of deer detection-nondetection within the month.

Seasonal variation in occupancy

We ran several competing models, each with different assumptions about how detectability, site occupancy, site colonization, and site extinction varied through time. We tested whether the probability of detection was either (1) constant, (2) varied among seasons, or (3) varied among surveys. We likewise tested whether site occupancy, site colonization, and site extinction were either (1) constant, or (2) varied among seasons. Our goal for this analysis was to establish mean changes in occupancy across winters for the whole study area, not estimating spatial factors affecting occupancy within the study area. Therefore, we assumed for these models that there is no spatial variability in occupancy,

an assumption we know is violated (Chapter 3). Therefore, occupancy estimates among seasons should be treated as average measures across the study area, and as relative measures for comparison among years, and not treated as a "true" single estimate of occupancy for each sampling site.

We ranked competing models using Akaike's Information Criterion (AIC) scores, which provide a balance between the variance in the deer data explained by the model, and the number of variables needed to explain that variance (Burnham and Anderson 2002). Lower AIC scores indicate a parsimonious model that explains more variance than other models. AIC scores were normalised as AIC weights (AIC_w), which are analogous to the probability that any given model is the best model of the whole set. From AIC_w we calculated evidence ratios for each variable (ER). This is the ratio of the sum of all AIC_w of all models that included a given habitat variable, *vs.* those models that did not include that variable. For example, ER=2 suggests there is twice as much evidence supporting the inclusion of a habitat variable in a deer model, than evidence supporting leaving that variable out.

Results

There were marked differences in winter severity among the three years of study (Figure 2-2). The 30-year mean annual snow depth at the Fort McMurray weather station is 30 cm (measured in February, when snow is deepest)(Environment Canada 2015). Snow depth exceeded 30 cm in 0 days in 2011-2012; 125 days in 2012-2013; and 73 days in 2013-2014, indicating that winter severity peaked during the 2nd winter of our study and differed considerably among all three. Temperature data from nearby Lac La Biche (for which no snow data were collected) were similar to Fort McMurray. Based on snow depth, we classified the three winters of the study as moderate (2011-2012) and severe (2012-2013 and 2013-2014). We expected deer distribution to differ following these three winters.
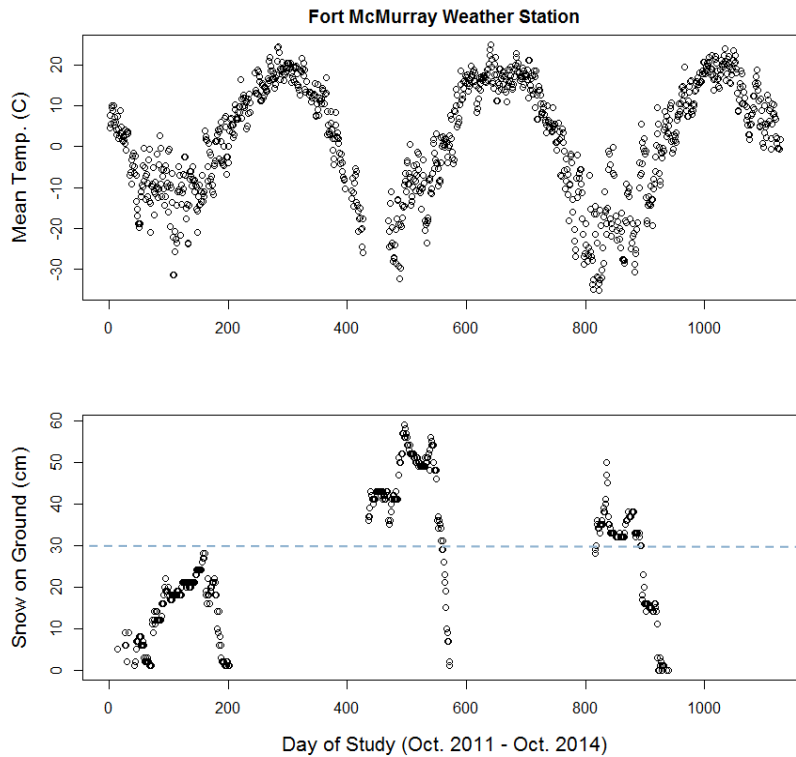
Figure 2-2. Environment Canada weather data from Fort McMurray, Alberta, 2011-2014, summarised daily. The 30-year mean maximum snow depth (blue dashed line) is 30 cm. The winter of 2011-12 exhibited average snowfall, whereas the winters of 2012-13 and 2013-14 were relatively severe.

White-tailed deer seasonal occupancy

Between October 2011 and October 2014 we achieved more than 60,000 camera trap nights from the 62 sites across the study area. We collected and analysed 141,141 camera images; 112,648 of these were of white-tailed deer. Summing across years, deer were present at all of these sites at some point during the study, although frequency of occurrence (i.e. number of months present) varied markedly.

The probability (p) of detecting deer (given they were present) varied monthly (black line, Figure 2-3). Detectability was lowest in late winter and spring, and highest in summer. In the summer, deer were almost perfectly detected, as p approached 1.0, and standard errors were relatively small. In the 2nd winter, deer were detected only half of the time that they occurred at a site, with detectability estimated to be less than 0.5. The probability of detection is a per-survey (monthly) estimate. The best-supported model carried 100% of the AIC weight, meaning that all of the weight of evidence supports this model, compared to competing models (Table 2-1).

In most seasons, PFA approached 0.0; at worst (winter 2013), PFA = 0.03 (blue lines, Figure 2-4). Thus, in the worst-case scenario, it was 97% likely that we detected deer at a site that they used at least once during a season, and usually we

approached 100% probability. These results suggest that movements in and out of the camera site within seasons do not significantly change seasonal presence-absence measures of deer occurrence.

Deer occupancy fluctuated widely among seasons (black line, Figure 2-4). In the autumn of 2011, deer were widely distributed across the study area, with occupancy near 1.0. Occupancy dropped only slightly in the first winter, which was mild, then rebounded in spring 2012. Occupancy remained mostly stable through the summer and autumn of 2012, and then dropped precipitously in the severe second winter. However, deer occupancy quickly rebounded in spring 2013. This same pattern repeated in the third winter, with a marked drop in occupancy, followed by a quick rebound in spring; occupancy remained stable in summer and early autumn.

These occupancy dynamics were driven (in part) by the probability that a camera site occupied in one season would become empty in the next season – the probability of site extinction (ε). In the mild winter of 2012, probability of site extinction was less than 0.2 (red line, Figure 2-4). Few sites became empty in summer and fall. In the severe winter of 2013, ε jumped markedly. Half the sites that had deer in the summer and fall were empty in the winter. This dynamic repeats in the third year, with occupancy dropping by half in the winter. Occupancy dynamics were also driven by the probability of site colonization (γ) – the probability that a camera site unoccupied in one season would become occupied in the next season (blue line, Figure 2-5). After the mild winter of 2012, all empty sites were recolonized (γ = 1.0, SE = 0.00). Colonization was difficult to estimate in summer and fall because most sites were occupied; standard errors were large. After the severe winter of 2013, all empty sites were again recolonized (γ = 1.0, SE = 0.00). After the severe winter of 2014, site recolonization was again very high (γ = 0.88, SE = 0.06).

In summary, although deer distribution shrank markedly in the severe winters of 2013 and 2014, high site colonization allowed deer distribution to rebound very quickly in each subsequent spring. Another way to consider these fluctuations in distribution is the spatial "growth rate" (λ), a model parameter calculated from estimates of occupancy, extinction, and colonization (Mackenzie *et al.* 2003, 2006). Spatial growth rate is analogous to population growth rate. If λ = 1.0, then the distribution remains stable; if λ <1, then distribution is shrinking, and if λ > 1, then distribution is expanding. The spatial growth rate of boreal white-tailed deer fluctuated through time (green line, Figure 2-6). Deer distribution decreased each winter, with a greater decline in the more severe winters. Deer distribution increased markedly in the subsequent springs (γ = 1.8, SE = 0.24), returning to a stable distribution (1.0) in each summer and fall season. We estimated that the spatial growth rate after the final survey was 1.01 (SE = 0.03).

Table 2-1. Multi-season occupancy models of deer detection-nondetection at cameras from October 2011 to October 2014. These models estimate the probability that a site is occupied (ψ), the probability that an empty site will be colonized (γ), and the probability that an occupied site will go "extinct" (ε). These parameters were either constant (c) or varied among 3-month SEASONs. The probability of detecting a white-tailed deer (if present), *p*, was either constant (c), varied in each SURVEY, or varied among SEASONs.

Model	AIC	ΔAIC	AIC weight	Model Likelihood	k*	-2LL**
ψ,γ(SEASON),ε(SEASON),p(SURVEY)	1210.29	0	1	1	39	1132.29
ψ,γ(c),ε(SEASON),p(SURVEY)	1244.90	34.61	0	0	33	1178.9.0
ψ,γ(SEASON),ε(c),p(SURVEY)	1246.57	36.28	0	0	33	1180.57
ψ,γ(c),ε(c),p(SURVEY)	1259.08	48.79	0	0	27	1205.08
ψ,γ(SEASON),ε(SEASON),p(SEASON)	1271.43	61.14	0	0	23	1225.43
ψ,γ(SEASON),ε(c),p(SEASON)	1305.30	95.01	0	0	17	1271.30
ψ,γ(c),ε(SEASON),p(SEASON)	1305.50	95.21	0	0	17	1271.50
ψ,γ(c),ε(c),p(SEASON)	1317.00	106.71	0	0	11	1295.00
ψ,γ(SEASON),ε(SEASON),p(c)	1347.99	137.70	0	0	16	1315.99
ψ,γ(c),ε(SEASON),p(c)	1384.73	174.44	0	0	10	1364.73
ψ,γ(SEASON),ε(c),p(c)	1410.47	200.18	0	0	10	1390.47
ψ,γ(c),ε(c),p(c)	1447.18	236.89	0	0	4	1439.18

*number of parameters; **-2 x log likelihood
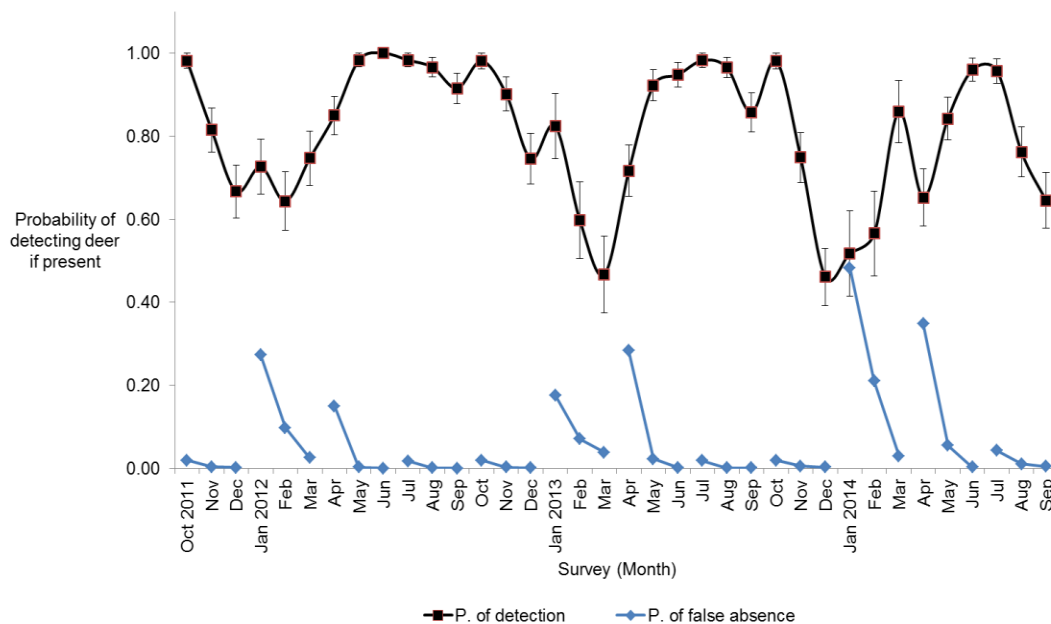
Figure 2-3. The probability of detecting deer via cameras (black line) varied monthly. The probability of false absence (blue lines) within each season approached 0.0 for most seasons and at worst (spring 2014) was 3%. Bars represent standard errors of estimates.
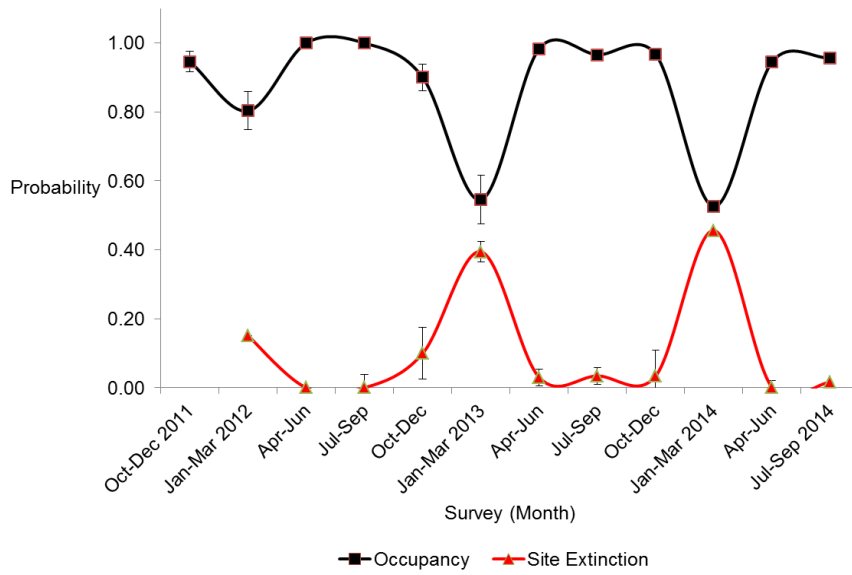
Figure 2-4. The probability of white-tailed deer occupancy (black line) and the probability of site extinction (red line) varied among seasons. Site extinction was greatest in the two severe winters. Bars represent standard errors.
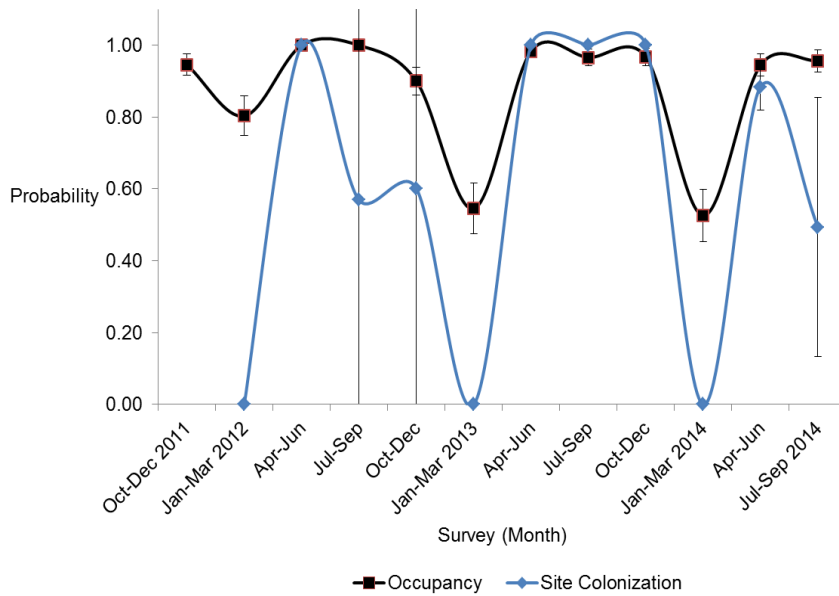
Figure 2-5. The probability of site colonization (blue line) varied among seasons, and was high in all three spring periods. Bars represent standard errors.
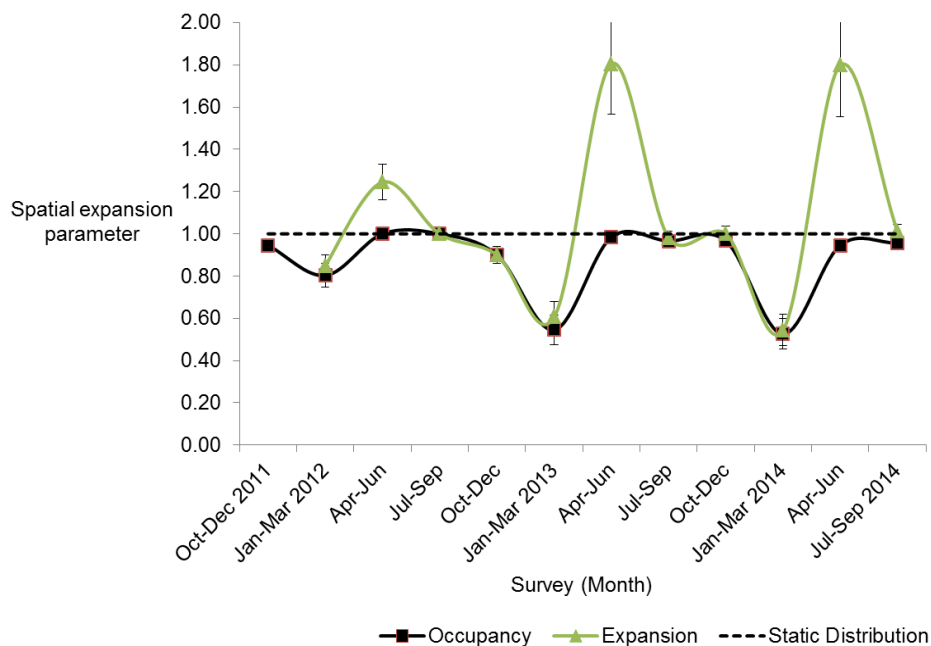
Figure 2-7. The "spatial growth rate" of boreal white-tailed deer varied among seasons, and was >1 in all three spring periods. Bars represent standard errors of estimates; the dashed line represents zero spatial growth and a stable distribution.

Discussion

Winter severity has been generally decreasing under a changing climate in western North America, with important consequences expected for biotic communities (Lawler 2009, Lawler et al. 2009, Gilman et al. 2010, Chen et al. 2011, Barnosky et al. 2012). In this first examination of white-tailed deer distribution through time, we found that WTD occupancy decreased more markedly in more severe winters when snow is deep. The moderate winter of 2012 produced a small drop in occupancy, whereas the very severe winters of 2013 and 2014 – with cold temperatures and extreme snowfalls – resulted in a nearly 50% drop in occupancy across the study area. In winter, the metabolic costs of staying warm and moving through deep snow exceed the nutrition and energy derived from available forage (Delgiudice et al. 1990b, DelGiudice et al. 1992, Delgiudice et al. 2002, Ditchkoff 2011, Hewitt 2011). If this metabolic debt exceeds available fat reserves accrued the previous winter, deer die; if reserves exceed metabolic debt (and if deer avoid predation), they survive the winter. Overwinter deer mortality leads to seasonal cycles of population decline and growth (DeYoung 2011), but the numerical effect of winter mortality on population sizes is only known from a few, well-studied populations in Minnesota and the Dakotas; it is unreliable to extrapolate their results to boreal environments. This first examination suggests that distribution of boreal populations does decrease in severe winters.

However, although we expected WTD distribution shrinkage to result from the population declines typically resulting from severe winters, distribution quickly rebounded after winter. In every spring, site occupancy rebounded to pre-winter conditions, nearing 1.0. Only half of the landscape was occupied in severe winters, but in spring, deer re-

occupied nearly the entire landscape. This finding is quite profound, and it defies expectations that severe winters would reduce WTD with some lasting effect. Even two severe winters in succession did not appreciably reduce spring deer distribution. This 'spring rebound' could result from either (1) widespread reproduction to replace losses suffered in the winter; or (2) adults surviving, and then recolonizing empty sites from local overwintering refugia. Given the rapidity of the recolonization events in all three springs, we hypothesize it is likely that both are occurring; but analysis of reproductive success (Chapter 3) and seasonal density estimates (Chapter 5) are needed to test this hypothesis.

We also show that camera data can be a robust method for estimating seasonal dynamics of species distribution, sensu (MacKenzie et al. 2003, MacKenzie et al. 2006). Estimating and accounting for the probability of detecting deer *via* cameras – given a deer was present – was potentially important, as detection probability varied monthly. For a large, wide-ranging animal such as deer, "occupancy" can be thought of as the probability of a deer spending time in the vicinity of a camera, and detectability depends on how often deer move into the range of the camera (among other things) (MacKenzie et al. 2006, Burton et al. 2015). In winter when deer yard up (Stewart et al. 2011), movement rates decrease; with fewer deer moving in front of the camera, detectability decreases even when deer are present. Movement increases in summer and fall months (Tierson et al. 1985, Grovenburg et al. 2009), and hence so does detectability. Quantifying and accounting for this detectability allows for more accurate estimates of occupancy, which are more likely to reflect true changes in distribution rather than just changes in behaviour.

For occupancy models we relegate variation in monthly occurrence at a site to "error", expecting that this variation could potentially mask a signal of distribution (Type II error) or induce a false signal (Type I error). However, this variation may itself be an ecological signal. A deer absence may not be merely a function of missed detections, but instead a measure of how deer site-use varies through time as a function of habitat quality at that site. Researchers are beginning to adopt a dualistic approach to camera-trap data analysis wherein both occupancy analysis and analysis of uncorrected data are compared for convergence (or divergence) of conclusions (Fisher et al. 2013, Banks-Leite et al. 2014, Burton et al. 2015). This approach may be useful in assessing species distributions over large scales, where variable time spent at a site can indicate differences in site quality. We adopt this approach in Chapter 3.

In conclusion, white-tailed deer were widely distributed throughout the entire study area, reflecting predictions made by Latham et al. (2011) and Dawe et al. (2014) about WTD expansion in the boreal ecosystem. However, our longitudinal study also showed that although distribution contracted after each winter – including the two severe winters – distribution recovered quickly. White-tailed deer occupied the entire study area every spring, summer, and autumn. If our study area is representative of other highly impacted areas in the northeastern boreal forest, we hypothesize that under current land-use practices, regional landscapes will support white-tailed deer populations even in the face of severe winters, and thus the continued establishment of WTD in the region may not be dependent on moderate winters induced by climate change. An examination of the relationship between white-tailed deer and anthropogenic landscape features is needed to test this hypothesis.

CHAPTER 3: NATURAL AND ANTHROPOGENIC LANDSCAPE FEATURES AFFECTING WHITE–TAILED DEER DISTRIBUTION IN NORTHEAST ALBERTA

Introduction

Habitat loss, fragmentation, and alteration are a primary cause of many species' declines and can profoundly affect ecological systems (Taylor et al. 1993, Fahrig 1997, 1999). Determining the correlates of a species' spatial distribution across heterogeneous (and fragmented) landscapes is a key precursor to elucidating the ecological processes creating those patterns. In particular, disentangling natural from anthropogenic correlates of species distribution is a necessary requirement for effective conservation and management, and is often demanded when species conservation potentially conflicts with economically important landscape development. This task is further complicated as pattern and process can change markedly among landscapes as ecological and spatial contexts change, potentially preventing reliable inference from other landscapes (Fisher et al. 2005, Wheatley and Johnson 2009, Fisher et al. 2011). The challenge of linking changes in wildlife populations and ecological processes to landscape features is therefore a daunting one, especially in the highly complex boreal forest landscapes of northeastern Alberta.

Alberta's oil sands are among the world's largest hydrocarbon deposits, a key component of the Canadian economy (Bayoumi and Mhleisen 2006), and a major factor in North American geopolitics. Open-pit bitumen mines are an oil sands icon, but in-situ drilling's footprint is markedly more extensive (Schneider et al. 2006). Natural boreal forest heterogeneity has been augmented by a diversity of different anthropogenic features, including cutblocks, roads, trails, linear seismic lines, 3D seismic lines, well sites, and polygonal industrial features. *etc.* (Appendix 1). These features are typically covered with grasses, forbs, and browse – primary food sources for WTD (Moen 1978, Hewitt 2011) which we collectively term "early seral vegetation" hereafter. Petroleum extraction's footprint has pushed boreal forest disturbance patterns well outside the historical range of natural variation (Pickell et al. 2013, Pickell et al. 2015), and is without analog elsewhere in the globe, making these patterns a unique observational experimental system. Moreover, these features are additive to the patterns of forest harvesting across the boreal landscape which have their own effects on wildlife (Fisher and Wilkinson 2005). Petroleum extraction, timber harvesting, and road infrastructure have cumulatively and rapidly increased disturbance rates in Canada's boreal forests (Spaling et al. 2000, Hansen et al. 2010).

The effects of landscape alteration vary from species to species. For some species, removal of old, mature forest represents habitat loss; for others, it is a habitat gain (Thomas et al. 2001, Fisher and Wilkinson 2005, Ewers and Didham 2006). In the boreal forest, a heterogeneous mix of deciduous and conifer of various stand ages, landscape alteration typically removes mature forest and replacing it with either early-seral vegetation such as forest harvesting cutblocks, or introducing novel anthropogenic structures on the landscape, such as well pads, seismic lines for petroleum exploration, and roads. The effects of forest harvesting – until the last decade, the primary form of anthropogenic landscape alteration in the boreal forest – has been extensively studied, and reviews show these effects vary widely among species (Fisher and Wilkinson 2005, Schieck and Song 2006). The ecological effects of roads and linear features have been less studied, but are

catching up. Road effects differ from cutblocks, often posing a barrier to movement (Forman 2003). For some species, roads and other linear features may actually expedite movement (Whittington et al. 2011, McKenzie et al. 2012). Road verges are also a source of early-seral vegetation. Roads and trails provide human access which can increase the success rates for legal licensed and unlicensed harvest of wildlife (Gratson and Whitman 2000) (B. Maile, pers. comm). Access may also increase poaching mortality (Trombulak and Frissell 2000). Access can lead to substantial pressure on highly sought-after game species.

Very little is known about how these various anthropogenic features might interact with natural landcover to affect species distributions in this landscape. We predicted that, since most anthropogenic features are associated with WTD forage, that these features may be facilitating WTD expansion across the boreal forest. Dawe et al. (2014) used predictive models to examine the contribution of landscape alteration to WTD expansion at provincial spatial scales. However, they did not have empirical data on deer distribution to quantify these relationships at landscape scales. Our goal was to empirically estimate the relative contribution of natural landcover and anthropogenic disturbance to white-tailed deer distribution in the northeast boreal forest, at landscape scales.

We used camera trapping (O'Connell et al. 2011) to survey deer distribution over three years. Cameras are widely used for surveying mammals (Burton et al. 2015) and have been used to characterize species density (Trolle et al. 2006, Sollmann et al. 2013), diversity (Tobler et al. 2008), habitat selection (Fisher et al. 2011, Fisher et al. 2013), and to estimate population and community changes through time (Karanth et al. 2004, O'Brien 2008). Species distribution models make the assumption that the frequency of a species' use of a site is related to the landscape within some defined area around that site (Morrison et al. 2006). Defining the appropriate scale of this area is difficult, because different processes operate at different spatial scales (Figure 3-1). The area affecting a deer's occurrence at a camera site may be smaller than a home range, reflecting the influence of small-scale, local patch choices by individuals. Conversely, the size of the landscape affecting distribution may be larger than a home-range, since a variety of ecological factors – predators, competitors *etc*. – occurring well beyond the home-range affect the quality of a site for a species (Kotliar and Wiens 1990, Bowyer and Kie 2006, Boyce 2006, Fisher et al. 2011, Fisher et al. 2012). Because we don't know the size of the landscape that might affect a species' occurrence – and getting the size wrong can lead to incorrect conclusions – a rigorous approach is to test several different landscape sizes and determine which best predicts that occurrence (Fisher et al. 2011).

Complicating matters, white-tailed deer habitat selection and space-use varies seasonally, in response to changing nutritional requirements and metabolic demands (Ditchkoff 2011, Hewitt 2011, Stewart et al. 2011). Deer distribution is also expected to change seasonally, as winter mortality depletes some habitats across a landscape, and then rebounds in the spring. Therefore, one might predict that the scale of the deer-landscape relationship may also change seasonally, with local factors becoming more important in the wintertime. Finally, deer-landscape relationships might change depending on how deer distribution is measured. Deer occurrence (presence or absence) through time may not reflect deer abundance, if a few deer are scattered widely throughout a landscape whereas most deer are clustered at a few sites.
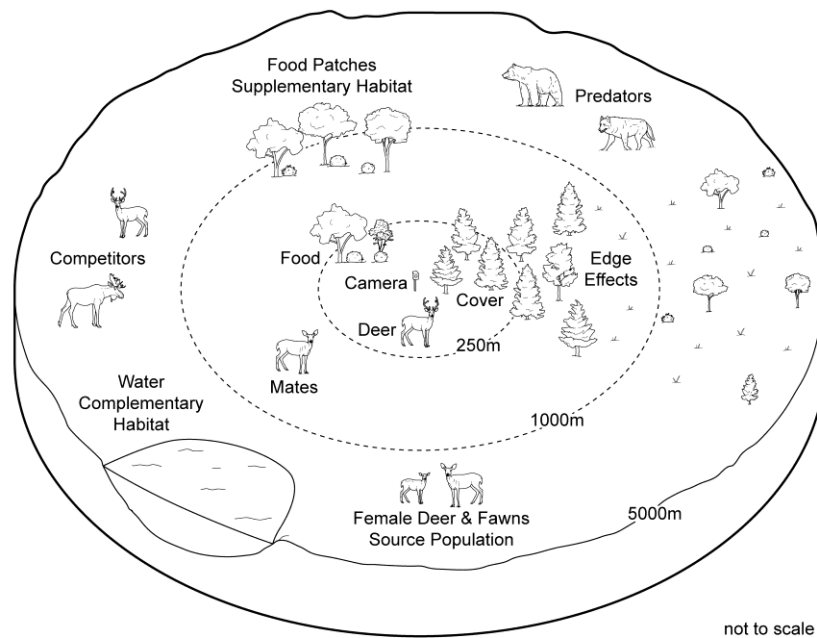
Figure 3-1. Different ecological processes occur at different spatial scales, each involving different landscape features. At small scales – the immediate area around a deer – food and cover be important. At intermediate scales, the presence of potential mates or other conspecifics may be important. Patch edge effects may play a role, as well as complementary or supplementary food sources. At even larger scales, the presence of predators in the landscape, and a source population of conspecifics, may be important. As landscape variables proxy these different processes, the degree to which landscape variables explain deer occurrence is expected to change across scales. (Illustration by Jeff Dixon)

Relative abundance is not always the best indicator of habitat quality (Van Horne 1983). The occurrence of a deer at a site does not always equate to high-quality habitat, as the animal may experience an ecological trap (Schlaepfer et al. 2002, Battin 2004) wherein an animal occupies a site that does not increase its fitness. We can avoid this problem by assessing breeding success – considered to be a much more robust measure of habitat suitability for a species, and more reflective of the habitat's effect on fitness. Research on WTD pregnancy rates and recruitment suggests that female age and body condition affect breeding success (Ozoga et al. 1982, Ozoga and Verme 1986, Verme 1989, DelGiudice et al. 2007), and that body condition is primarily a function of nutrition afforded by available browse (Hewitt 2011). However, there is no research on the landscape-scale distribution of breeding success, and the natural or anthropogenic features that might affect this success. WTD range expansion is obviously a function of reproduction and mortality; examining whether landscape change is associated with increased breeding success helps elucidate the factors contributing to expansion.

We tested five hypotheses:

1. Annual WTD distribution is best described by landscape features measured at large scales, *i.e.* areas > 3000-m radius.

2. Winter WTD distribution is best described by landscape features at small scales, *i.e.* areas of 250-m radius.

3. WTD distribution is explained by a combination of deciduous forest and anthropogenic footprint, as a source of early-seral vegetation.

4. The features explaining WTD in winter differ from those explaining annual distribution, with conifer cover being more important within that season.

5. WTD breeding success remains high after both moderate and severe winters, and is highest in areas with greater deciduous forest cover and human disturbance offering early seral vegetation.

Methods

We analysed each camera image and recorded the presence of each species detected. Where we were not certain of a species' identification, we removed this observation from the dataset, to eliminate the problem of false positives. Missing data from inoperable cameras were removed from the dataset. We used the full three years of camera data to create two different response variables measuring deer distribution. The first variable was *deer relative abundance*, which we indexed by counting the total number of independent camera-detection events, and the number of deer observed in each event (Figure 3-2). We assumed that WTD detections separated by 10 minutes, or with a visibly different deer entering the frame, represented independent visits. The second response variable was *deer persistence*, which we measured as the number of months that a WTD was detected at a camera site over three years.

We reclassified AVI digital forest inventory data into 12 classes that we predicted were potentially important for white-tailed deer (Table 3-1). We reclassified Alberta Biodiversity Monitoring Institute (ABMI) human footprint layer[3] data into 3 classes representing polygonal anthropogenic features – cutblocks, well sites, and other 'block features'. We used a high-resolution linear features layer[4] to classify anthropogenic linear features on the landscape. We buffered these linear features to assign an area of footprint to each. These buffers, described in Table 3-1, are somewhat arbitrary but are the same as those used by Alberta Biodiversity Monitoring Institute for their analyses, so we sought to remain consistent. We used ARCGIS 10.2 and Patch Analyst (ESRI, Inc.) to calculate the percent area of each landscape feature around each camera site. Correlated variables cannot be included in a multivariate model, as they share information about the dependent variable – the problem of multicollinearity (Faraway 2004). As correlated variables measure the same relationships to the response variables, then they are redundant. Models with highly correlated predictors may yield spurious results, showing one variable as important when the correlated variable is driving the ecological relationship. The standard errors of parameter estimates tend to become large, potentially leading to Type II error – failing to identify an existing relationship. To prevent this problem, we tested for correlations among these landscape variables, and omitted correlated variables (r > 0.6) from multiple-variable models (Zuur et al. 2010). This only partly deals with the problem, as correlated variables left

---

[3] 2010 Provincial Human Footprint layer downloaded from:
http://www.abmi.ca/abmi/rawdata/geospatial/gisdownload.jsp?categoryId=3&subcategoryId=7
[4] ABMI and University of Alberta, Integrated Landscape Management Lab

out of the models could still be driving underlying relationships, so the choice of variables to retain is also based on strength of underlying hypotheses.

Table 3-1. Landscape reclassification for camera-based species distribution model analyses. GIS data from multiple sources were reclassified and combined to create 20 different landscape feature categories. We calculated the percent area of each category around each camera site, to create 20 independent variables.

#	Habitat Class	Source[1]	Description[2,3]
1	Upland deciduous	AVI	(Aw, Pb, Bw >=70% canopy), moisture = d or m
2	Lowland deciduous	AVI	(Aw, Pb, Bw >=70% canopy), moisture = w or a
3	Upland mixedwood	AVI	(40% -60%) canopy, moisture = d or m
4	Lowland mixedwood	AVI	(40% -60%) canopy, moisture = w or a
5	Upland spruce	AVI	(Sb, Sw, Fb >=70% canopy), moisture = d or m
6	Lowland spruce	AVI	(Sb,Sw,Fb >=70% canopy), moisture = w or a
7	Pine	AVI	All Pj (>=70%)
8	Tamarack	AVI	All Lt (>=70%)
9	Open wetland	AVI	<6% crown closure; moisture = w or a
10	Upland shrubs	AVI	>25% shrub cover; <6% tree cover; moisture = d or m
11	Water	AVI	Standing or flowing water
12	Cutblocks	ABMI	Forest harvested areas, which regrow trees, and are important for deer in early seral stages.
13	Nonforest	AVI	< 6% canopy
14	Block features	ABMI	Borrow-Pits, Dugouts, Sumps, Industrial Sites, and Other Disturbed Vegetation not falling into other categories
15	Wellsites	ABMI	Petroleum extraction well sites, disturbed forest with canopy removed, areas now grassy or shrubby.
16	3D Seismic	UALF	Intensive (hashmarked) seismic petroleum exploration line *ca.* 1-3 m wide.
17	Cutlines	UALF	Traditional seismic petroleum exploration line *ca.* 7-10 m wide and typically very long.
18	Roads	UALF	All roads including One Lane Gravel, One Lane Paved, Two Lane Gravel, Two Lane Paved, Unimproved Roads
19	Pipelines	UALF	Petroleum pipelines
20	Trails	UALF	Trail + TruckTrail: Unimproved dirt track ca. 5-10 m wide navigable by off-highway vehicle, foot, or horseback, or by truck.

[1]AVI – Alberta Vegetation Index; UALF = University of Alberta Linear Features Map Updated 2012; ABMI = Alberta Biodiversity Monitoring Institute Human Footprint Map Updated 2010.
[2]Aw = aspen, Pb = poplar, Bw = white birch, Sb = black spruce Sw = white spruce, Fb = balsam fir, Pj = jack pine, Lt = tamarack/larch; d = dry, m = mesic, w = wet, a = aquatic
[3]Linear features were buffered for areal calculations as follows: Two Lane Undivided Paved Road: 9m; One Lane Undivided Paved Road: 6m; Rail Line: 5.5m; Rail Line- spur: 5.5m; Two Lane Gravel Road: 7m; One Lane Gravel Road: 5m; Driveway: 2m; Unimproved Road: 6m; Trail: 6m; Truck Trail: 6m; Electrical Transmission Line: 17m; Pipeline: 12m; 3D: 2m; Cutline: 2m.
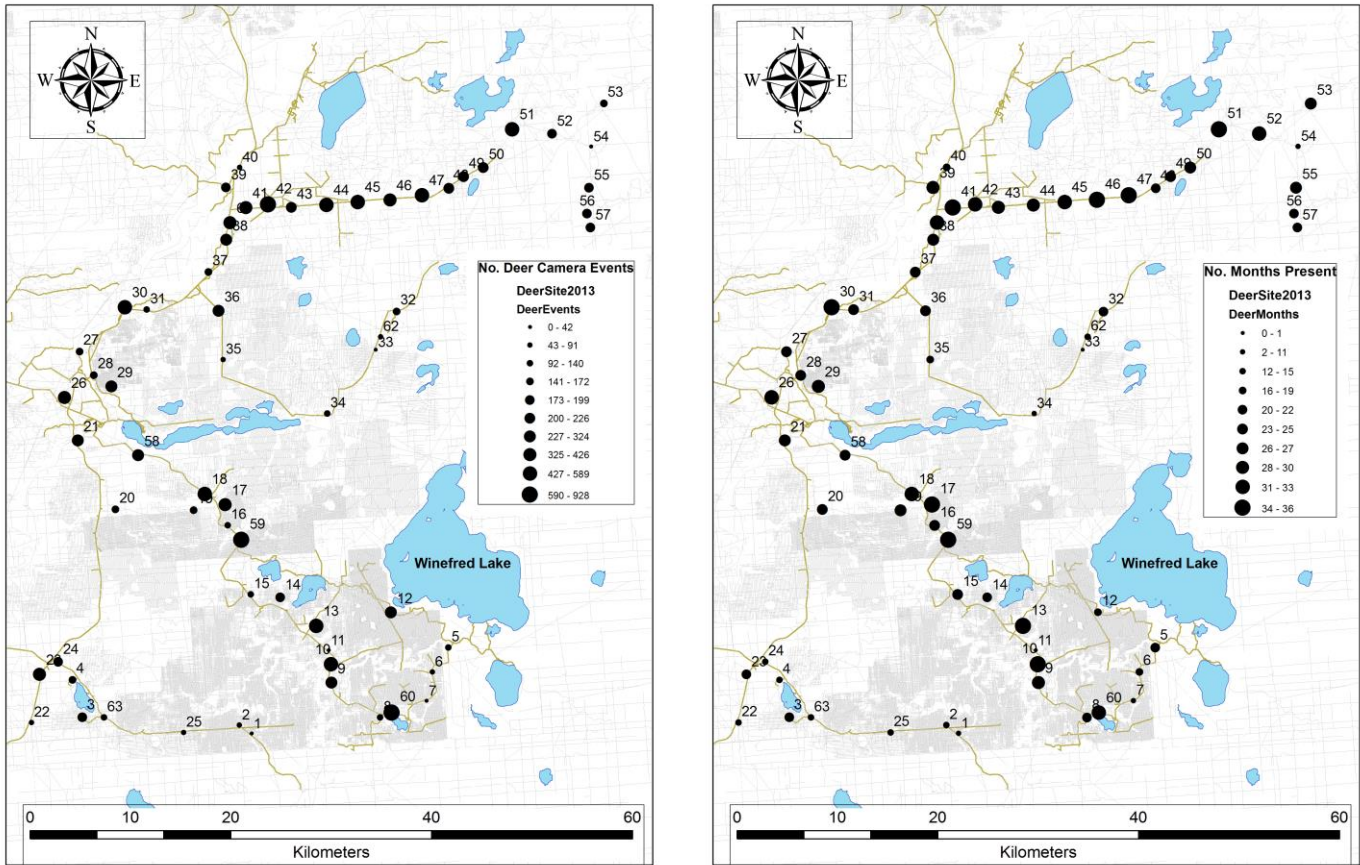
Figure 3-2. Deer relative abundance, measured as the number of deer observed at independent camera events, and deer persistence, measured as the number of months of deer occurrence over three years, at each of 62 camera sites. There is a high degree of concordance between these measures. The background is linear features (grey lines), updated to 2012.

Spatial scale analysis

We quantified the landscape within buffers of different sizes, or *spatial scales* (Figure 3-1). These spatial scales ranged from a 250-m radius circle to a 5000-m radius circle, in 250-m increments, around each camera site. This yielded 20 different spatial scales we could compare to test which scale best explained deer occurrence. At each scale, we modelled deer persistence (0-36, over three years) against all 20 landscape variables using generalized linear models (Binomial errors, logit link) in *R* ver. 3.1.1 (R Foundation for Statistical Computing 2014). These models also included a term for the number of days the camera was active, since, some cameras failed during surveying. Each model produces an AIC score (Akaike Information Criterion) (Burnham and Anderson 2002), which is a function of the number of variables in the model, and the log-likelihood of the model – the amount of variance in the deer data that the model can explain. A model with a low AIC score indicates that this model better explains deer occurrence than a model with a high AIC score. For each of these 20

"scale models", we used the step-AIC function in R package MASS[5] to identify the most parsimonious model that best fit the data. This function uses a backward and forward stepwise regression routine to create models with different combinations of variables, ranks each of these models based on AIC scores, and selects the lowest score. We normalised AIC scores of the best-fit 20 "scale models" as AIC weights (Anderson 2008); AIC weights of a set of models sum to 1.0, and are analogous to the probability that a model is the best one of the set. For example, if the best-fit model has an AIC weight of only 0.2, there is only a 20% chance that it is really best of the lot. If the best model has an AIC weight of 0.9, there is a 90% chance it is really the best. We plotted the 20 AIC weights against the 20 spatial scales to identify a peak, indicating the spatial scale at which landscape explains deer distribution. We repeated this entire procedure using this second response variable, *deer relative abundance* (Figure 3-2), using generalized linear models (square root-transformation, gaussian errors, identity link), to test whether different response variables yielded different scales.

Deer habitat selection models

Once a "best-fit" scale was identified, we used variables measured at this scale in an information-theoretic model selection framework (Burnham and Anderson 2002) to test different hypotheses about the relationship between WTD and landscape features (Table 3-2). Although defining hypotheses and corresponding models *a priori* is a conceptually strong approach (Anderson and Burnham 2002, Burnham and Anderson 2002), it does not always lead to the most parsimonious models that best explain a species' distribution. Crawley (2012) advocates a stepwise regression approach to find the "minimum adequate model" that best explains a species distribution but excludes unnecessary non-significant variables. We used both approaches, and compared stepwise models with the hypothesis-based models (Table 3-2) to determine which had the most support. Because these models were overdispersed (Zuur et al. 2007), we re-ran these models using quasibinomial regression, which accounts and corrects for overdispersion, and obtained parameter estimates from these models. We repeated this procedure again using only data from winter months (January-March each year for 3 years; 0-9 months), to determine if winter habitat associations were different from annual habitat associations (generalized linear models, gaussian errors, identity link).

We graphed univariate relationships between key predictor variables and species occurrence to show the slope and direction of relationships; the grey bands represent 95% confidence intervals of estimates. These plots show the range of independent variables these models were built upon; beyond this range the relationships may change. We used R package *boot* to assess the fit of the AIC-selected best model with 10-fold cross validation (Zhang 1993), a type of bootstrap procedure which fits the model for 10 subsets of testing and training data to assess model prediction error.

---

[5] http://cran.r-project.org/web/packages/MASS/MASS.pdf

Table 3-2. Hypotheses about landscape-scale deer distribution in the northeast boreal forest.

Description	Model #	Hypothesis: WTD distribution is explained by:	Variables (numbers refer to Table 1)
Global model	1	All variables	1-20
Natural landcover	2	Upland deciduous cover	1
	3	All mixedwood cover	3+4
	4	All conifer cover	5+6+7+8
	5	Upland spruce	5
	6	All deciduous + shrubs	1+2+8+10
	7	Wetland	9+11
	8	Upland forest	1+3+5
	9	Lowland forest	2+4+6
Nonforest	10	Early seral	10+12+13+14+15
Forestry	11	Cutblocks	12
Petroleum	12	Wellsites	15
	13	3D seismic	16
	14	Cutlines	17
	15	Pipelines	19
	16	Linear features	16+17+18+19+20
	17	Block features	14+15
Petroleum + Forestry	18	Block features incl. cutblocks	14+15+12
Access	19	Roads	18
	20	Trails	20
	21	Roads and trails	18+20
All anthropogenic	22	All anthropogenic features	12+14+15+16+17+18+19+20
Natural + forestry	23	Upland deciduous and cutblocks	1+12
	24	Shrubs and cutblocks	10+12
	25	Openings and cutblocks	10+12+13
Natural + petroleum	26	Upland deciduous and 3D seismic	1+16
	27	Upland deciduous and cutlines	1+17
	28	Upland deciduous and all anthropogenic	1+12+14+15+16+17+18+19+20
	29	Upland deciduous and all petroleum	1+15+16+17+19
Natural + access	30	Upland deciduous and roads and trails	1+18+20
Best-fit step-AIC model	31	Variables selected by stepwise regression	Varies

Variation in breeding success

We extended the occupancy framework (Chapter 2) to model the dynamics of breeding success by estimating parameters for different age classes using multi-state occupancy models (Nichols et al. 2007, Fisher et al. 2014). Just as species may be detected imperfectly, age-sex classes may also be detected imperfectly, when neither age nor sex is known with accuracy. Using camera imagery, sites can be classified into one of multiple states – such as sites with breeding, or without breeding – which may be observed with error. With repeated surveys we can estimate the probability, for each site, that the species is either wholly absent, present without breeding, or present with breeding; as well as the probability that a species will be detected in each of the two occupied states (Nichols et al. 2007; MacKenzie et al. 2009).

We classified each deer image according to whether an adult female with young of the year (fawns) was present or absent. If a female with fawns appeared in any image within the survey month, we classified that site as "breeding" for that survey. If fawns were not detected, we classified the site as "non-breeding", to create a detection-nondetection dataset with three states: breeding, non-breeding, or no deer detected. "Breeding" sites could be misclassified as "non-breeding" if we missed photographing extant fawns at the cameras, and the models estimate how often this occurred. With this dataset we ran several competing models, each with different assumptions about how detectability, breeding occupancy, and non-breeding occupancy varied through time and in relation to landscape features. We tested whether the probability of detection was either (1) constant, (2) varied among seasons, or (3) varied among surveys. We likewise tested whether site occupancy of breeders and non-breeders was either (1) constant, or (2) varied in relation to landscape features. We used hierarchical models in the Program *Presence* (ver. 6.2) to estimate WTD occupancy (ψ), detectability (p), and breeding state (R), where:

ψ_i = probability that site *i* is occupied, regardless of reproductive state

R_i = conditional probability that young occurred, given that site *i* is occupied

$\psi_{i(breeding)}$ = unconditional probability that site *i* is occupied with breeding = $\psi_i * R_i$

$p(1)_{it}$ = probability that occupancy is detected for site *i*, period *t*, given that true state = 1 (non-breeding),

$p(2)_{it}$ = probability that occupancy is detected for site *i*, period *t*, given that true state = 2 (breeding),

δ_{it} = probability that evidence of successful reproduction is found, given detection of occupancy at site *i*, period *t*, with successful reproduction (Nichols et al. 2007).

Occupancy models provide a per-survey estimate of *p*, and from this we calculated the probability of false absence (PFA) across the three surveys as $[1-p]^3$ (Long et al. 2008). In the event that occupancy models failed to converge and could not estimate ψ and R, we also used generalised linear models (GLMs) to determine whether fawn occurrence varied with landscape features. The GLM approach assumes that detectability over the one-month survey was sufficiently high that the uncorrected number of months with detection is a reliable measure of relative site-use. We summed the number of spring months (April, May, June) with and without breeding across all three survey years creating a 0-9 response variable (3 spring months times 3 years). We modelled number of breeding-months as a binomial count model (GLM; binomial errors, log link) in R ver. 3.1.1 (R Foundation for Statistical Computing 2014) against natural and anthropogenic landcovers, using the same hypotheses we made for adult deer (Table 3-2).

Results

Cross-scale analysis

Of the 20 different spatial scales we examined, landscape measured at the 1000-m radius scale best explained annual deer relative abundance (Figure 3-3a) and deer persistence (Figure 3-3b). In each case this model was supported by over 98% of the evidence (AICw = 0.98 and 0.99, respectively). The 1000-m scale also best explained winter deer persistence (Figure 3-3c), providing strong evidence that variables measured at this scale are affecting deer distribution, regardless how we measured deer, or the time of year we sampled them. We used variables measured at the 1000-m scale in all subsequent species distribution models.
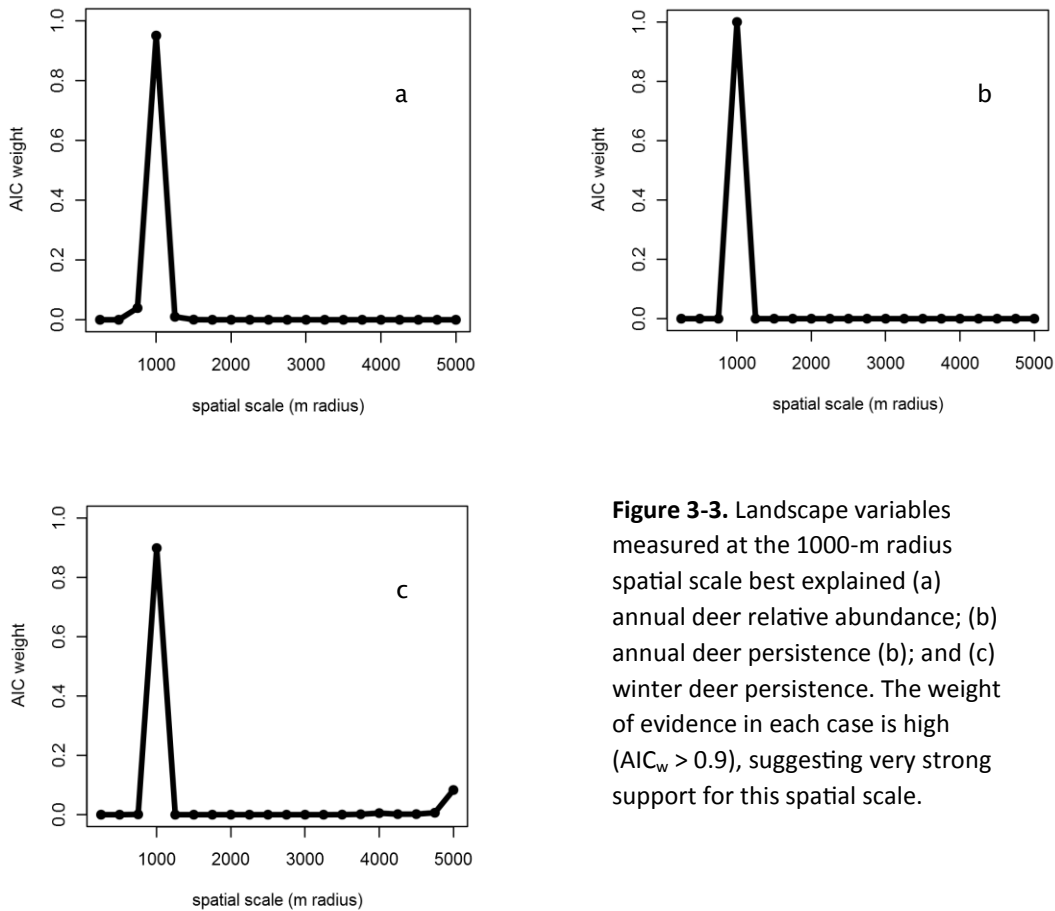
Figure 3-3. Landscape variables measured at the 1000-m radius spatial scale best explained (a) annual deer relative abundance; (b) annual deer persistence (b); and (c) winter deer persistence. The weight of evidence in each case is high ($AIC_w > 0.9$), suggesting very strong support for this spatial scale.

Deer-landscape relationships

There was strong evidence ($AIC_w > 0.99$) that annual *deer relative abundance* was best explained by upland deciduous forest cover and all anthropogenic variables (model 28, Table 3-2). That is, there is a 99% probability that this model better explained deer relative abundance than any other model in Table 3-2, each of which had concomitantly small AIC weights (Figure 3-4a). The relationship between annual deer relative abundance (deer counts) and landscape features are illustrated in Figure 3-4. These results are mirrored for *annual deer persistence*: model 28 is supported by most ($AIC_w > 0.99$) of the weight of evidence (Figure 3-4b). When we examined only *winter deer persistence*, the results are the same; model 28 is supported by most of the weight of evidence (Figure 3-4c).

In other words, whether we measure deer distribution as total counts of deer detections, or months of deer presence; or whether we use all years of data or just winter months; the combination of upland deciduous forest and

anthropogenic features best explains deer distribution in the northeast boreal forest. Deer relative abundance was positively related to upland deciduous forest, cutblocks, well sites, cutlines, pipelines, and block features. Deer abundance was negatively related to 3D seismic, roads, and trails (Tables 3-3 to 3-5).

As expected however, the minimum adequate model selected by the stepwise procedure outperformed all other models for every response variables (AICw > 0.99), and retained slightly different variables than were in model 28 (Tables 3-3 to 3-5). These models performed well. The best-fit model of annual deer relative abundance explained 65.5% of the deviance in the deer data, and had a prediction error of 15%. The best-fit model of annual deer persistence explained 58.9% of the deviance, and carried a prediction error of 0.02%. The best-fit winter persistence model explained 44.8% of the deviance in the winter deer data, and had a prediction error of 0.07%. Though the variables retained in these models are slightly different, they nevertheless reinforce the conclusion that a combination of upland deciduous forest and anthropogenic features – cutblocks, well sites, trails, and block features – best explained annual white-tailed deer relative abundance and persistence. These relationships were also reflected in winter months, wherein cutblocks, trails, and block features best explained deer persistence.
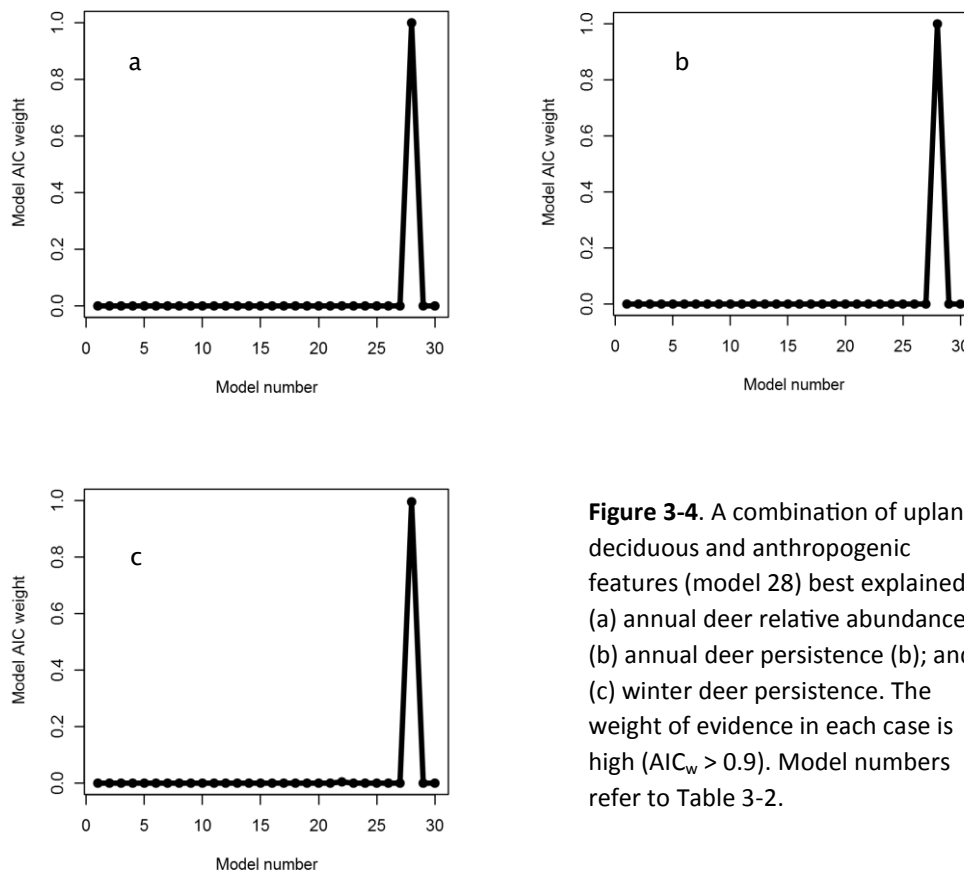
Figure 3-4. A combination of upland deciduous and anthropogenic features (model 28) best explained (a) annual deer relative abundance; (b) annual deer persistence (b); and (c) winter deer persistence. The weight of evidence in each case is high (AIC$_w$ > 0.9). Model numbers refer to Table 3-2.

Table 3-3a. Parameter estimates from the best supported candidate model (#28, Table 2) of annual *deer relative abundance* (number of deer detections over 36 months at camera sites), modelled against landscape features.

Parameter	Estimate	std. error	t-value	p-value
(Intercept)	4.33	3.99	1.09	0.28
Upland deciduous forest	0.13	0.03	4.20	< 0.00
Cutblocks	0.29	0.09	3.43	< 0.00
Well sites	0.62	0.38	1.60	0.11
3D seismic	-0.14	0.29	-0.48	0.63
Cutlines	0.12	1.96	0.06	0.95
Pipelines	1.01	0.39	2.59	0.01
Roads	-0.77	1.40	-0.55	0.58
Trails	-3.29	1.63	-2.02	0.05
Block features	1.56	0.40	3.91	< 0.00
Camera days	0.00	0.00	1.35	0.18

Table 3-3b. Parameter estimates from the best-fit stepwise model of annual *deer relative abundance* (number of deer detections over 36 months at camera sites), modelled against landscape features.*

Parameter	Estimate	std. error	t-value	p-value
(Intercept)	4.17	2.25	1.85	0.07
Upland deciduous	0.15	0.03	4.89	0.00
Upland mixedwood	0.26	0.13	2.09	0.04
Lowland spruce	0.06	0.04	1.54	0.13
Cutblocks	0.30	0.08	3.93	0.00
Well sites	0.56	0.34	1.63	0.11
Pipelines	1.11	0.36	3.03	0.00
Trails	-2.73	1.55	-1.76	0.08
Block features	1.58	0.37	4.30	0.00

Table 3-4a. Parameter estimates from the best supported candidate model (#28, Table 2) of *annual deer persistence* (number of months a deer was present at camera sites, out of 36), modelled against landscape features.

Parameter	Estimate	std. error	t-value	p-value
(Intercept)	0.22	1.01	0.22	0.83
Upland deciduous forest	0.02	0.01	3.53	< 0.00
Cutblocks	0.07	0.02	3.72	< 0.00
Well sites	0.26	0.09	2.92	0.01
3D seismic	-0.02	0.06	-0.37	0.71
Cutlines	-0.19	0.42	-0.46	0.65
Pipelines	0.01	0.08	0.13	0.90
Roads	-0.15	0.30	-0.48	0.63
Trails	-0.88	0.34	-2.63	0.01
Block features	0.41	0.12	3.60	< 0.00
Camera days	0.00	0.00	-0.15	0.88

Table 3-4b. Parameter estimates from the best-fit stepwise model of *annual deer persistence* (number of months a deer was present at camera sites, out of 36), modelled against landscape features.

Parameter	Estimate	std. error	t-value	p-value
(Intercept)	-0.16	0.19	-0.88	0.38
Upland deciduous	0.03	0.01	3.89	0.00
Cutblocks	0.07	0.02	4.27	0.00
Well sites	0.24	0.08	3.06	0.00
Trails	-0.88	0.30	-2.89	0.01
Block features	0.41	0.10	4.06	0.00

Table 3-5. Parameter estimates from the best supported candidate model (#28, Table 2) of *winter deer persistence* (number of months a deer was present at camera sites, out of 36), modelled against landscape features.

Parameter	Estimate	std. error	t-value	p-value
(Intercept)	-2.57	1.71	-1.50	0.14
Upland deciduous forest	0.02	0.01	2.17	0.03
Cutblocks	0.11	0.03	3.65	0.00
Well sites	0.18	0.14	1.24	0.22
3D seismic	-0.03	0.11	-0.24	0.81
Cutlines	-0.29	0.64	-0.45	0.66
Pipelines	0.03	0.13	0.24	0.81
Roads	-0.03	0.48	-0.06	0.95
Trails	-1.61	0.56	-2.87	0.01
Block features	0.54	0.17	3.21	0.00
Camera days	0.00	0.00	0.90	0.37

Table 3-5a. Parameter estimates from the best-fit stepwise model of *winter deer persistence* (number of months a deer was present at camera sites, out of 36), modelled against landscape features.
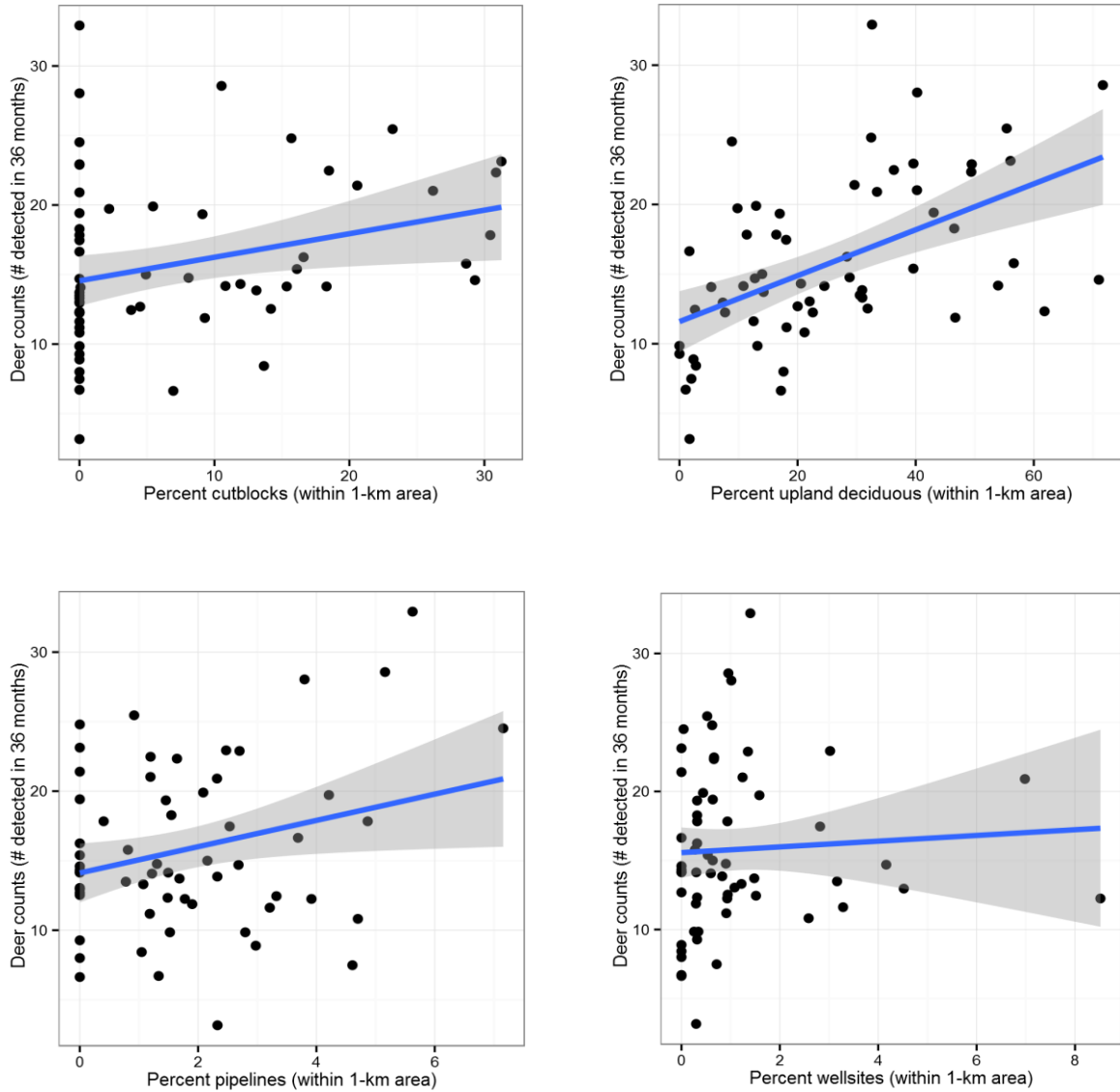
Parameter	Estimate	std. error	t-value	p-value
(Intercept)	-1.30	0.31	-4.20	0.00
Upland deciduous	0.02	0.01	2.47	0.02
Cutblocks	0.10	0.02	4.02	0.00
Trails	-1.32	0.47	-2.78	0.01
Block features	0.59	0.15	4.05	0.00

Figure 3-5. The relationship between annual deer relative abundance (# counts at each camera site over three years) and some landscape features, from the best-supported candidate model (#28, Table 3-2). These graphs show univariate relationships, rather than the relationships from the multi-variable models, for illustration.

Evidence of breeding

Of 112,648 deer images, 12,460 images (11.1%) had evidence of young of the year. This included single fawns (92.9%), twins (7.6%) and triplets (0.6%). There was a marked drop in the distribution of successful breeding across years. Of 62 sites, successful breeding was detected at 36 sites (58.1%) in 2012, 22 (35.5%) in 2013, and 12 (19.4%) in 2014. Among all years pooled together, 45 of 62 sites (72.6%) had evidence of breeding in at least one year.

White-tailed deer breeding distribution

Reproductively successful deer – does with fawns – were predicted by occupancy models to be widespread across the study area in spring 2012 following the mild winter (ψ_b = 0.89, SE = 0.14), as well as the springs of 2013 (ψ_b = 0.98; SE = 0.02) and 2014 (ψ_b = 0.95; SE = 0.03) following the severe winters. However, these models were unstable, and convergence on a maximum likelihood estimate could not be reached in all cases. This, and the fact that the breeding occupancy estimates do not fit with the observed decline in the distribution of breeding among years, suggests more work is needed to understand dynamics in reproduction across this landscape. Moreover, we were unable to use occupancy models to determine whether the fraction of occupied sites with breeding varied with landscape covariates, as there was very little variation in breeding success across sites (as measured by occupancy, which seems to be the wrong tool in this case). Models failed to converge and estimates of occupancy and probability of breeding were unreliable in the models with covariates. However, the probability of false absences for deer with fawns was $\leq$ 0.002 in all years, suggesting that we reliably detected fawns when they occurred, and that uncorrected presence-absence data could be used with generalized linear models to examine fawn occurrence.

We used observed number of months of breeding (0 to 9) in generalized linear models to test whether breeding success varied spatially as a function of natural and anthropogenic landscape features. The best-supported generalised linear model (AICw = 0.80; Figure 3-6) suggests the percent of deciduous forest cover, 3D seismic lines, traditional seismic lines, and pipelines best explained the occurrence of white-tailed deer with fawns. All variables were significantly positively related to fawn occurrence (Table 3-6).
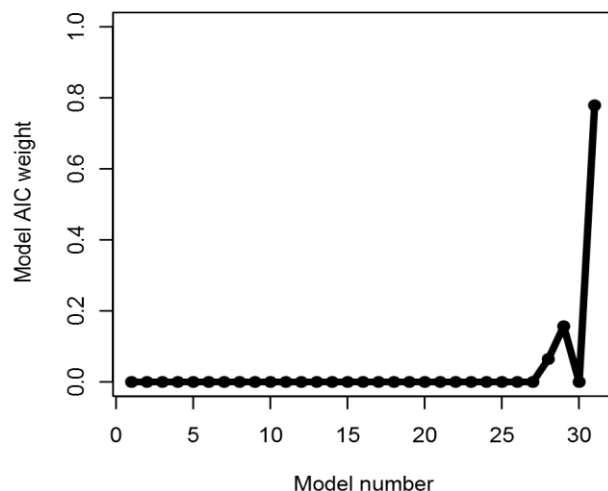
Figure 3-6. A combination of upland deciduous and anthropogenic features (model 31) best explained the occurrence of white-tailed does with fawns. The weight of evidence is high (AIC$_w$ > 0.8). Model numbers refer to Table 3-2.

Table 3-6. Parameter estimates from the best supported candidate model of *spring fawn occurrence* (number of spring months of detections over 3 years), modelled against landscape features.

Parameter	Estimate	std. error	z-value	p-value
(Intercept)	-2.49	0.19	-13.03	< 0.00
Upland deciduous forest	0.014	0.003	4.48	< 0.00
3D seismic lines	0.10	0.03	3.47	< 0.00
Cutlines	1.15	0.20	5.66	< 0.00
Pipelines	0.08	0.03	2.55	0.01

Discussion

Upland deciduous forest and anthropogenic features were the best predictors of white-tailed deer relative abundance and persistence, both annually and in winter. In all models, deer were more likely to occur where there was more upland deciduous forest in the landscape. This result is perhaps intuitive. Abundant forage is critical to deer persistence; white-tailed deer diet is dominated by the leaves and stems of woody deciduous plants (as well as grasses and forbs); conifer needles offer comparatively low nutritional value (Moen 1978, Hewitt 2011). Upland deciduous forest provides abundant ungulate browse in the boreal forest. Moreover, areas of anthropogenic footprint such as cutblocks tend to regenerate into young, early-successional species that also provide abundant forage (Fisher and Wilkinson 2005). We expected that forest cutblocks from timber harvest would drive this relationship, as white-tailed deer were frequently observed in cutblocks during the aerial survey over the study area this year (L.D. Roy, pers. obs.). Although WTD are indeed using cutblocks, the area covered by other anthropogenic footprint – well sites, industrial block features, and pipelines, always explained deer occurrence better than cutblocks alone. The cumulative effects of multiple resource sectors that have so radically altered the Alberta boreal landscape (Pickell et al. 2013, Pickell et al. 2015) collectively increase the amount of the landscape covered by early seral vegetation, augmenting natural deciduous landcover, providing abundant deer browse. These landscape features markedly increase both the abundance and persistence of white-tailed deer in the boreal landscape.

Some anthropogenic features had a negative effect on WTD distribution. No matter how measured, WTD tended to avoid areas with high proportion of roads and trails. "Roads" provide motorized access; "trails" are cleared linear features accessible by foot and off-road vehicle, and provide human access into forested areas that is not easy or possible in intact areas. The consistent negative relationship with trails suggests deer avoid these features, perhaps because they perceive these as high-risk areas. Although human access into forested areas is recognized as a key factor in game management, surprisingly little research has been devoted to understanding the effect of industrial access on wildlife distribution (Trombulak and Frissell 2000). Some research in Alberta shows recreational access can have a significant effect on ungulate distribution (Muhly et al. 2011, Rogala et al. 2011), and we can hypothesize that with extensive human

presence on this landscape – petroleum industry workers, hunters, and recreational outdoorsmen – increased access may be deterring WTD use of some areas. From a management perspective, this relationship is worth further consideration.

The most pervasive anthropogenic features in the landscape were cutlines (traditional seismic lines) and 3D seismic. Adult deer avoided 3D seismic, though the effect was not significant, suggesting 3D seismic is not having a great effect on adult WTD distribution. However, 3D seismic did have positive and significant association with deer reproductive success. How 3D seismic is bolstering reproductive success is unknown, though early seral vegetation on the line borders may play a role. Traditional seismic lines were likewise significant predictors of deer reproductive success. The effect of traditional cutlines was weak for adults, though the relationship between WTD and cutlines changed depending on how we measured it. Deer abundance was greater in areas with more cutlines, but deer persistence was lower in these areas. This changing direction suggests that deer congregate near these areas but only shortly, because they either (1) leave quickly, or (2) suffer mortality. These linear features increase predation rates of wolves on woodland caribou (Whittington et al. 2011, McKenzie et al. 2012), and it is reasonable to assume that wolves using cutlines may likewise predate WTD. If deer are attracted to cutlines (increasing abundance) but then are predated (reducing persistence), cutlines may pose an ecological trap (Schlaepfer et al. 2002). However, the positive relationship between seismic lines and reproductive success suggest exactly the opposite: females occurring in areas with high densities of lines are more likely to produce fawns.

White-tailed deer habitat relationships vary seasonally in other regions (DeYoung 2011, DeYoung et al. 2011), and so we expected different habitat relationships in winter than in the full-year period. This was not the case, except for a few variables. Relationships remained the same in winter as they were year-round. In fact, the stepwise model of winter deer persistence selected fewer variables than did the stepwise model of annual deer persistence, suggesting fewer features are important in winter: upland deciduous forest, cutblocks, trails, and block features. Concordance between annual and winter models suggests that the primary factors driving deer distribution in this landscape remain constant among seasons: an abundance of available deciduous and early seral forage, and avoidance of human access.

The rapid recolonization after overwinter reduction observed in Chapter 2 suggests that the landscape provides abundant forage upon which white-tailed deer may quickly capitalize. Given this rapidity, a high degree of overwinter survival is likely an important component of that recolonization. Our analysis of habitat associations of does with fawns suggests breeding success may also play an important role. Many sites in this landscape supported successfully breeding deer immediately after moderate and severe winters, and models (tentatively) predict that breeding is widespread in all three years. Pregnancy induces markedly greater metabolic costs on female deer (Pekins et al. 1998, Ditchkoff 2011). If WTD females in this landscape were metabolically stressed after severe winters, female mortality, small fawns with low survival (Ditchkoff 2011), and starvation-induced abortions (Worden 1992, in Pekins et al. 1998) might be expected to reduce reproductive success. We observed female overwinter mortality (Chapter 4), but obviously we have no evidence of fawn survival or of pregnancy and abortion rates, which would require luteal, protein assay, or ultrasound examination (e.g. Andelt et al. (2004)). Further research is required to resolve these mechanisms.

Notwithstanding, we found no evidence that overwinter mortality (or other mechanisms of population reduction) were extensive enough to markedly reduce population distribution. Instead, we found that although the distribution of fawning decreased through time in conjunction with severe winters, fawning was still widespread and WTD distribution

remained stable. Fawning success was greater in areas with more deciduous forest and anthropogenic features associated with early seral vegetation (seismic lines, pipeline rights-of-ways). Nutrition has widely known effects on ungulates' probability of pregnancy, over-winter survival, parturition, and neonatal survival (Parker et al. 2009, Hewitt 2011). Greater nutrition from abundant available forage can prevent metabolic stress and increase survivorship and reproductive success (Hewitt 2011), although this relationship is not straightforward. Forage biomass is in itself not a good predictor of deer nutrition, as forage distribution relative to inedible vegetation plays a significant role (Spalinger and Hobbs 1992). Edible forage is concentrated in cutblocks and industrial block features, and this concentrating effect may be important. This may be especially true in spring, during green-up, when energetic demands of gestation are great (Pekins et al. 1998).

In summary, our conclusions about white-tailed deer distribution and habitat relationships are consistent across different metrics of abundance, and between age-sex classes. Our research strongly suggests that resource extraction on this boreal landscape is providing nutritional subsidies that provide for stable deer distributions over time – even after severe winters. The expansion of white-tailed deer is a continental-scale issue ongoing for over a century (Côté et al. 2004, Heffelfinger 2011). It has occurred despite heavy hunting in some regions, and despite a massive expansion in urban and rural residential landscapes. The conversion of mature forest, especially conifer forest into species that provide ample deer forage is a primary mechanism of this continental expansion. Our research shows that the very unique forms of anthropogenic disturbance in this boreal forest landscape are contributing to WTD expansion in the northerly region of the species' range. From a management perspective, managing for increased human access to facilitate wildlife harvest may be one way of managing white-tailed deer populations in the boreal forest. However, the influence of early seral vegetation is pervasive, suggesting that to be effective over the long term, white-tailed deer population management through increased harvesting may have to be augmented by landscape management.

CHAPTER 4: WHITE–TAILED DEER SPACE–USE AND RESOURCE SELECTION IN THE BOREAL FOREST

Introduction

Animals depend on multiple resources for survival, and the adaptation of a species to its available resources underpins niche theory and most of ecology (Grinnell 1917, MacArthur 1968, Chase and Leibold 2003, Soberon 2007). Optimal foraging theory dictates that an animal will use its environment to obtain resources in a way that maximizes its fitness and minimizes mortality (Fretwell and Calver 1969, Fretwell 1972, Pianka and Parker 1975, Pyke et al. 1977, Krebs 1978, Huey and Pianka 1981, Pianka 1981). Consequently, individuals' space-use and resource selection have underpinned much of wildlife ecology research for the last two decades or more (Millspaugh and Marzluff 2001, Boyce et al. 2002, Manly et al. 2002, Johnson et al. 2006, Millspaugh et al. 2006). Though advances in monitoring technologies such as camera traps have increased research examining species-habitat relationships at population and landscape scales (Fisher et al. 2011, O'Connell et al. 2011, Burton et al. 2015), the examination of individual's space use remains a key pursuit in ecology.

Conceptually, an individual's selection of resources is expected to scale up to home-range selection, and thence to population distribution. Johnson (1980) suggested there is a "natural ordering" of these selection processes across space. First-order selection defines the full species range of an organism. Second-order selection defines the selection of a home-range from within that species range. Third-order selection defines the selection of habitats or features (such as forest types) within that home range (Johnson 1980). This conceptual framework has been widely adopted as a foundation for explaining species' resource selection across different spatial scales (Rettie and Messier 2000, Bowyer and Kie 2006), although the observed patterns of selection across scales have been revealed as much more complex than this simple hierarchy would suggest (Wheatley and Johnson 2009, Fisher et al. 2011). For example, a deer's selection of an individual forage plant within a deciduous stand does not easily scale up to explain the selection of forest types within a home range, or its selection of a home range within the boreal forest. An entire sub-field of ecology has emerged to understand why processes change across spatial scales (Wiens 1989, Kotliar and Wiens 1990, Wiens et al. 1993, Schneider 2001, Scott et al. 2002). Nevertheless, resource selection and space-use by individuals does provide a useful piece of the puzzle that is species' population distribution. We sought to understand space-use and resource selection by white-tailed deer in Alberta's boreal forest, to test whether conclusions made at the scale of populations are consistent with individuals' selection of resources.

White-tailed deer may be one of the most captured, collared, and radio-tracked of North American mammals. Scores of studies have examined white-tailed deer space use across their continental range from Florida to Canada; unsurprisingly, these studies reveal a remarkable degree of variability (Stewart et al. 2011). In general, white-tailed deer space-use is affected by the usual suspects: available forage, water, and escape cover, though the exact features providing these requirements vary across habitats (Stewart et al. 2011). Moreover, white-tailed deer sexually segregate (McCullough et al. 1989, Kie and Bowyer 1999, DePerno et al. 2003), further affecting space-use by individuals. Sexual segregation and space-use is density- dependent (Kie and Bowyer 1999), complicating generalizations. White-tailed deer movement and

resource selection also changes seasonally, but not in a uniform way. Some deer individuals are obligatory migrators, moving between distinct summer and winter ranges; some are conditional migrators, moving only under specific environmental conditions relating to temperature or snow depth; some are residents and do not move at all (Sabine et al. 2002, Grovenburg et al. 2009). Finally, landscape structure is known to affect mule deer (*Odocoileus hemionus*) space-use (Kie et al. 2002) and this also holds true for white-tailed deer (Long et al. 2005) – meaning that space-use is expected to vary with the degree of habitat fragmentation and loss from anthropogenic landscape development.

All of this variability – even within populations and landscapes – means that generalizations about deer space-use are elusive; predictions about expanding populations in new environments are even less reliable. Very little is known about space use and resource selection by white-tailed deer in northern boreal forests, where they are relative newcomers. How do Alberta boreal deer populations use and share their space? What resources do they select or avoid? How does resource selection change across seasons? We endeavored to answer these questions by capturing, collaring, and mapping locations of white-tailed deer females.

Methods

We captured and collared white-tailed deer in our study area in the northeast boreal forest (Figure 4-1), in the vicinity of our camera array to support density estimates (Chapter 5). We fitted deer with LOTEK Iridium Track M 3D telemetry collars[6]. The collars weigh 840 g (approximately 1.5% of body weight) with a centre collar size of 44 +/- 7 cm. These collars use the Iridium satellite system to download GPS (Geographic Positioning System) locations from the collars, and transmit these data to the user's computer *via* email. Collars were programmed to record a location every two hours (12 locations per day), and provided approximately two years of battery life.

We captured six white-tailed deer females using net-guns from a helicopter[7] in March 2012 and January 2013 (Appendix 2). In February 2013 we switched to ground capture to better target deer within our camera array. We tried stalking deer with a tranquilizer gun, but this proved ineffective. We also attempted to capture deer using rocket-net on baited stations, but this was likewise ineffective. Finally, we used Clover traps (Clover 1956) equipped with TrapSmart[TM]

devices (Vernon, NJ, USA), which sends an email to a cellphone when the trapdoor closes. Clover traps are expected to minimize stress on deer relative to other modes of capture (Delgiudice et al. 1990a, DelGiudice et al. 2001, Haulton et al. 2001). Capture and handling protocols were reviewed and approved by AITF's Animal Care Committee, and permitted by Alberta Environment and Parks.

---

[6] http://www.lotek.com/iridium-animal-collars.htm

[7] Bighorn Helicopters, Cranbrook, British Columbia
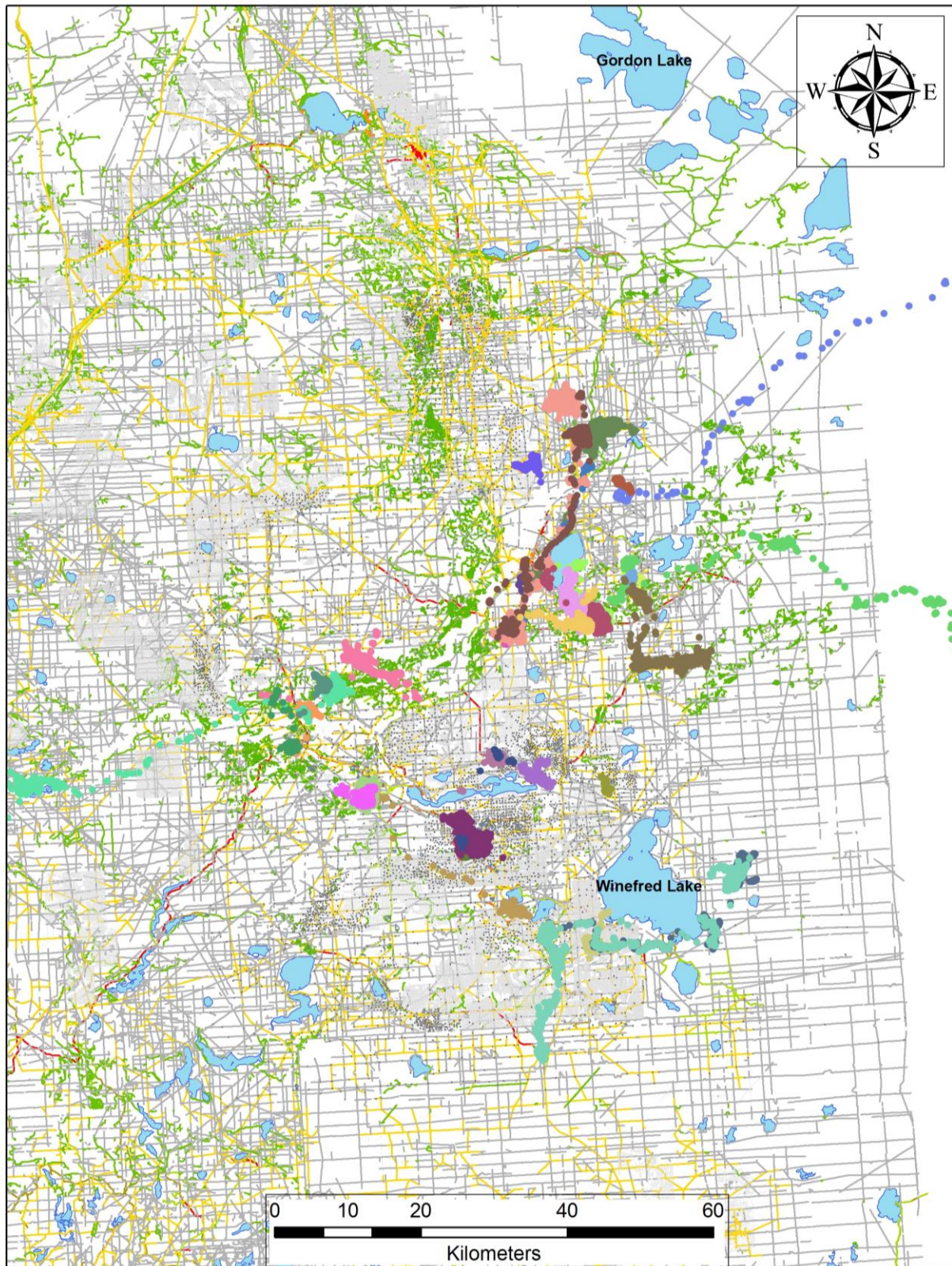
Figure 4-1. Satellite collars (coloured dots, unique to each female) were deployed across the study area in the vicinity of anthropogenic features including cutblocks (green), 3D seismic (light grey), cutlines (dark grey), pipelines and roads (yellow-red spectrum according to width), and well sites (small squares).

Traps were placed in locations that cameras or snow tracking data indicated were populated by female white-tailed deer, and which were within the vicinity of our camera-trapping array. Traps were deployed and pre-baited in November, and set and monitored in shifts through the winter, for a total of 222 trap-days. Captured animals were physically restrained, assessed for signs of health, ear tagged, fitted with the collar, and then released. GPS locations of collared animals were compiled in ArcGIS 10.2 (Esri, Inc) and analyzed.

GPS bias analysis

GPS satellite collars provide location data with a high degree of precision, but habitat-selection models generated from collars may be biased if collars are more successful at achieving satellite fixes in some habitats than in others. Failed fixes can result from different canopy densities or terrain ruggedness (D'Eon et al. 2002, Frair et al. 2004, James III et al. 2005), collar position (D'eon and Delparte 2005) or a function of programming (*e.g.* different fix rates set across diurnal cycles or across seasons; (Horne et al. 2007)). Some brands of GPS collar are more sensitive to GPS bias than are others (Hebblewhite et al. 2007). To quantify the degree of GPS bias potentially occurring in this study, we used stationary collars to quantify fix failures and obtain a measure of bias. Following the methods of Frair et al. (2004), we deployed stationary collars at multiple sites within different forest stands characteristic of the study area.

Home range analysis

We estimated home-range sizes using minimum convex polygon and kernel home-range estimators (Worton 1989). We used the 95% isopleth, describing 95% of the location volume, as an estimate of each individual's home range. Location data were autocorrelated – that is, a location was dependent on the location before it, because they were obtained over short (2-hr) intervals – but Fieberg (2007) showed that autocorrelation does not affect kernel density estimates. We calculated home-range sizes using the R package *adehabitatHR* (Calenge 2006) and examined the distribution of these sizes relative to the numbers of locations taken, and looked for differences among seasons.

Resource selection functions

We used resource selection functions (Manly et al. 2002) to test whether boreal white-tailed deer individuals selected or avoided natural and anthropogenic landscape features. Resource selection functions (RSFs) can employ several different models to assess selection or avoidance (Johnson et al. 2006). We opted to use a logistic regression-based model to compare used sites (deer telemetry locations) with unused but available sites within the same landscape. We collected 108,327 deer locations within the Alberta provincial boundary during the study period. As we did not have landscape data for neighboring Saskatchewan, where some deer migrated into (Figure 5-1), we truncated the data at the border. We created a minimum convex polygon around the outermost locations. Within this polygon, we generated an equal number (108,327) of random locations and treated these as available locations. A complementary analysis using step selection functions (Thurfjell et al. 2014) was undertaken in a separate analysis and is included as Appendix 3.

In ArcGis 10.2, we quantified the % dominant canopy species in forested stands in which the location fell (*e.g.* aspen overstorey with 30% canopy) based on Enhanced Alberta Vegetation Inventory (AVIE) data[8]. We used the Alberta Biodiversity Monitoring Institute (ABMI) human footprint layer[9] data to quantify distance to nearest polygonal anthropogenic features – cutblocks, well sites, and other polygonal 'block features'. We used a high-resolution linear features layer[10] to quantify distance to nearest anthropogenic linear features (*e.g.* cutline; Table 4-1). When features overlapped or were adjacent to one another, they were assigned precedence as described in Appendix 1. The search algorithm required exceptionally long time periods to locate rare linear features that were far from deer locations, so we truncated the searchable area to within 20-km of the study area. Linear features beyond this distance were recorded as 20-km away. We assumed that features beyond this distance are unlikely to influence deer habitat selection, and could find no literature to the contrary. Locations that fell physically within a feature were recorded as 0-m distant from that feature. Composite variables were created for those landscape features that were poorly represented in the landscape (Table 4-1), for which we calculated the minimum distance to any feature within that composite variable. We standardized all variables by subtracting the mean and dividing by standard deviation using the scale() function in R (R Foundation for Statistical Computing 2014). This centers the value of each variable on 0.0 and allows comparison of effect sizes (analogous to the slope of the line between deer and the landscape variable).

Correlated variables share information, therefore including them in the same model may yield spurious results. Correlation is often typical of landscape data; for example, some anthropogenic features may be more likely to occur in some forest types. To prevent problems induced by collinearity, we explored the data and tested for correlations among landscape variables using the Zuur et al. (2010) protocol. Using Pearson correlation coefficients (r^2) matrices and multi-panel scatter plots, we reduced variables within each category by retaining only those variables that were correlated with an $r^2 < 0.70$. This cutoff retained some partially correlated variables that were of ecological significance. We used variance inflation factor (VIF) estimation to examine the effects of including partially correlated variables in multivariate models (Zuur et al. 2010). Using a cut-off value of VIF < 3 – a generally accepted threshold to minimize the effects of collinearity in models (Craney and Surles 2002) – we used a stepwise approach to further reduce the number of variables retained for a global model. The final list of independent variables is listed in Table 4-1; we used these variables in resource selection functions. Regression models assume that observations are independent of one another (Bolker et al. 2009). This is obviously not the case for telemetry data, in which multiple observations (thousands) are obtained from a single animal. Each location is constrained by, and hence correlated with, the previous location – a problem known as serial autocorrelation (Fieberg et al. 2010). Moreover, each animal's unique behavior will dictate its choice of resources, such that a location from one animal is not directly comparable to a location from a different animal (Aarts et al. 2008, Koper and Manseau 2009). Treating each location as the sampling unit is a classic example of pseudoreplication (Hurlbert 1984). To

---

[8] AVIE data were created and provided by Alberta Environment and Parks.
[9] 2010 Provincial Human Footprint layer downloaded from:
http://www.abmi.ca/abmi/rawdata/geospatial/gisdownload.jsp?categoryId=3&subcategoryId=7
[10] ABMI and University of Alberta, Integrated Landscape Management Lab

overcome this problem, we adopted mixed effects models, which treat each individual as a "random effect", essentially calculating a different intercept for each animals' resource selection (Gillies et al. 2006, Aarts et al. 2008, Koper and Manseau 2009). We used generalized linear mixed effects models (binomial errors, logit link) (Zuur et al. 2009, Zuur et al. 2013) to test whether white-tailed deer were closer to, or further from, each of these features than expected by chance. We formulated several hypotheses about how we expected white-tailed deer to respond to natural and anthropogenic features. Each hypothesis was characterized by a separate statistical model (Table 4-2). We ranked the weight of evidence for each model (and corresponding hypothesis) using an information theoretic approach (Burnham and Anderson 2002).

Table 4-1. Natural and anthropogenic features derived from Alberta Vegetation Index (AVIE) data, and ABMI Human Footprint data. These variables were used in multiple models to test predictions about white-tailed deer resource selection (Table 4-2). All anthropogenic features were measured as "distance to the nearest feature of this type".

Variable Name	Description
CUTBLOCKS	Forest harvesting areas with mature trees removed and saplings regrowing
CUTLINE	Traditional seismic petroleum exploration line *ca.* 7-10 m wide
3D SEISMIC	Intensive (hashmarked) seismic petroleum exploration line *ca.* 1-3 m wide
ELECTRICAL	Electrical transmission line and grassy right of way
HIGH.DENSITY	High density industrial sites, representing high human activity (*e.g.* oil drilling camp)
INDUSTRIAL.MINE	Borrow Pits, Industrial Sites, Mine Sites, Well Sites, Peat Mines
NEAREST.BLOCK[+]	CutBlocks, High Density, Other Disturbed, Industrial Mine, Settlement, Wellsite
NEAREST.LINEAR[+]	Cutline, Cutline3D, Electrical, Pipeline, Trail, Truck Trail, Rail, Road
OTHER.DISTURBANCE	Recreation areas and other vegetated areas created for human use, including golf courses, grave yards, vegetated edges of airports, and any other disturbed areas with vegetation
OTHER.LINEAR[+]	All roads including one and two lane, paved and gravel, railways, and winter roads
PIPELINE	Petroleum pipeline and grassy right of way
RAIL	Railway line and associated vegetated right of way
ROAD	Hard surface road, Roads including vegetated verge, Unimproved (gravel) roads
SETTLEMENT[+]	Cultivated Areas, Municipal Areas, Urban Areas, Rural Residential Acreages
TRAIL	Unimproved dirt track ca. 5-10 m wide navigable by off-highway vehicle, foot, or horseback
TRUCK TRAIL	Unimproved dirt track navigable by truck
PCT_AW*	Trembling aspen *Populus tremulodies*
PCT_BW	White birch *Betula papyrifera*
PCT_FB	Balsam fir *Abies balsamea*
PCT_LT	Tamarack *Larix laricina*
PCT_PB	Balsam poplar *Populus balsamifera*
PCT_PJ	Jack pine *Pinus banksiana*
PCT_SB	Black spruce *Picea mariana*
PCT_SW	White spruce *Picea glauca*

[+]These are composite variables; measuring the distance to the closest of any of these features, regardless of type. *PCT refers to the *percent* of the forest canopy overstorey dominated by this leading tree species. We also included variable denoted uPCT, referring to the percent of the forest understorey dominated by each of these tree species.

Table 4-2. Hypotheses about landscape-scale deer distribution in the northeast boreal forest, grouped by similar types of natural and anthropogenic features. Variable names refer to Table 4-1.

General Hypothesis	Model set	Model	Model variables	Hypothesis: habitat use by white-tailed deer is predicted by…
	Global Model	1	CUTBLOCKS + HIGHDENSIT + OTHERDISTU + INDUSTRIALMINE + SETTLEMENT + CUTLINE + CUTLINE3D + ELECTRICAL + PIPELINE + TRAIL + TRUCKTRAIL + RAIL + ROAD + OTHERLINEAR + PCT_AW + PCT_BW + PCT_PB + PCT_PJ + PCT_SB + PCT_SW + PCT_FB + PCT_LT + UPCT_AW + PCT_BW + UPCT_PB + UPCT_PJ + UPCT_SB + UPCT_SW + UPCT_FB + UPCT_LT	All natural and anthropogenic variables.
Polygon (or block) disturbances provide early seral vegetation and hence a forage subsidy for deer.	Anthropogenic Footprint_Block	2	CUTBLOCKS + HIGHDENSIT + OTHERDISTU + INDUSTRIALMINE + SETTLEMENT + WELLSITE	Distance to all polygonal human footprint features.
		2a	NEAREST BLOCK FEATURE	Distance to the nearest block feature, regardless of type.
		3	INDUSTRIAL MINES	Petroleum extraction features with grass and shrubs not trees, often maintained in a disturbed state.
		4	WELL SITES	Distance to well sites, disturbed and grassy or shrubby; cameras suggest they are important for deer.
		5	CUTBLOCKS	Distance to forest harvested areas, which regrow trees, and are important for deer in early seral stages.
		6	SETTLEMENT	Distance to residential areas and urban town sites, which provide early seral vegetation and possibly refuge from predators.
		7	OTHER DISTURBANCE	Distance to other human footprint disturbance, which may have some unknown effect.
Linear disturbances change how deer move but also change how predators move, so are associated with predation risk and may be avoided.	Human Footprint_Linear	8	CUTLINE + CUTLINE3D + ELECTRICAL + PIPELINE + TRAIL + TRUCKTRAIL + RAIL + ROAD	All linear features.
		8a	NEAREST LINEAR FEATURE	Distance to nearest linear feature, regardless of type.
		9	CUTLINE + CUTLINE 3D + ELECTRICAL + PIPELINE	Industrial linear features.
		10	RAIL	Railway lines only.
		11	ROAD	Road features only.
		12	TRAIL + TRUCKTRAIL	Trail features only, as trails provide human access into forests but without the vehicle hazard danger, so act differently than roads.
	Distance to nearest SAGD features	13	CUTLINE, CUTLINE3D, WELLSITES	Petroleum extraction features.

		14	CUTLINE	Traditional seismic lines, which facilitate wolf movement and may be avoided.
		15	CUTLINE3D	3d seismic lines may act differently than regular seismic (cutlines).
Deer select habitats based on overstorey composition; they select deciduous but avoid conifer.	Vegetative overstorey	16	PCT_AW + PCT_BW + PCT_PB + PCT_PJ + PCT_SB + PCT_SW + PCT_FB + PCT_LT	All forest cover overstorey types.
		17	PCT_PJ + PCT_SB + PCT_SW + PCT_FB + PCT_LT	Conifer forest overstorey cover.
		18	PCT_AW + PCT_BW + PCT_PB	Deciduous forest overstorey cover.
Deer select habitats based on understorey composition, targeting stands with deciduous understorey.	Vegetative understory	19	UPCT_AW + UPCT_BW + UPCT_PB + UPCT_PJ + UPCT_SB + UPCT_SW + UPCT_FB + UPCT_LT	All forest cover understory types.
		20	PCT_PJ + PCT_SB + PCT_SW + PCT_FB + PCT_LT	Conifer forest understory cover.
		21	PCT_AW + PCT_BW + PCT_PB	Deciduous forest understory cover.
Stand characteristics predict deer occurrence.	Successional stage	22	SERAL STAGE + HEIGHT + DENSITY	Stages and characteristics of forest stand structure (categorical).
		23	FC_DOM + HEIGHT + DENSITY	Dominant cover class, average height of tree cover, and percent of ground covered.
		24	FC_DOM	Dominant cover class only.
		25	HEIGHT	Average stand height of leading dominant and co-dominant tree cover.
		26	DENSITY	Percentage of ground covered by tree crown cover.
		27	SERAL STAGE	Stage of ecological succession and average birth year of stand using 10yr origin classes.
Cumulative Effects Models	Cumulative Effects	28	COMBINATION OF THE BEST FIT VARIABLES FROM EACH MODEL SET	The combined effect of the best supported models.
Do deer use linear features more frequently near other sources of disturbance (early successional forage)?	Interactions	29	BEST SUPPORTED OVERSTOREY FEATURES * BEST SUPPORTED LINEAR FOOTPRINT FEATURES + BEST SUPPORTED OVERSTOREY FEATURES * BEST SUPPORTED BLOCK FOOTPRINT FEATURES. = MODEL 16 * MODEL 8 + MODEL 16 * MODEL 2	Footprint x habitat interaction.
		30	CUTLINE * WELLSITES + CUTLINE3D * WELLSITES	Linear features x block features interaction.
		31	CUTLINE * CUTBLOCKS + CUTLINE3D * CUTBLOCKS	Petroleum and forest harvesting, acting synergistically.

Each model produces an Akaike's Information Criterion (AIC) score (Burnham and Anderson 2002), which is a function of the number of variables in the model, and the log-likelihood of the model – the amount of variance in the deer telemetry data that the model can explain. A model with a low AIC score indicates that this model better explains deer locations than a model with a high AIC score. We normalised AIC scores as AIC weights (Anderson 2008); AIC weights of a set of models sum to 1.0, and are analogous to the probability that a model is the best one of the set. For example, if the best-fit model has an AIC weight of 0.3, there is a 30% chance that it is the best-fit model. If the best model has an AIC weight of 0.8, there is an 80% chance it is the best-fit model.

Results

White-tailed deer captures

We captured 6 white-tailed deer females *via* helicopter net-gunning in 2012. All of these collars immediately failed (Figure 4-3). The collar problems were identified by the manufacturer and rectified; new collars were used in subsequent deployments. We tried helicopter captures again in 2013 and captured 5 females; all but one died shortly thereafter (Appendix 2). The low success rate and high mortality rate of known-fate deer lead us to *not* recommend helicopter captures for boreal white-tailed deer. We captured white-tailed deer 74 times with Clover traps in 222 trap nights (Table 4-3). We collared 29 females. Clover trapping proved a far more effective way to capture boreal deer than other methods attempted.

Table 4-3. Capture rates of boreal white-tailed deer using baited Clover traps.

| Age-sex class	Number captured
collared females	29
captured males	10
captured fawns	29
recaptured fawns	2
recaptured collared does	3
total captures	73
total trap nights	222
total captures / 100 trap nights	32.8
total collars / 100 trap nights	13.1

Location data

Satellite location data were collected for 38 white-tailed deer females. A total of 111,978 telemetry locations were obtained, with a mean of 2946 per collared deer (range = 133 - 12,236; Figure 4-2 a,b). Periods of data collection – from date of capture to date of mortality or collar fail, or to June 4, 2015 for active collars – ranged from 15 to 778 days (mean = 221, median = 162, sd = 192 days; Figure 4-3).
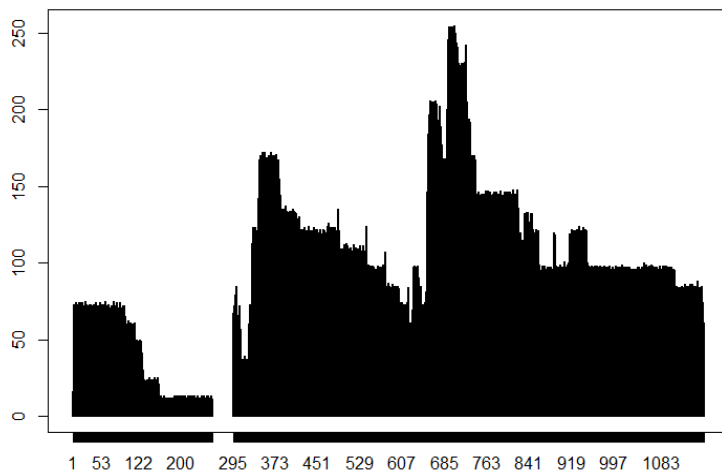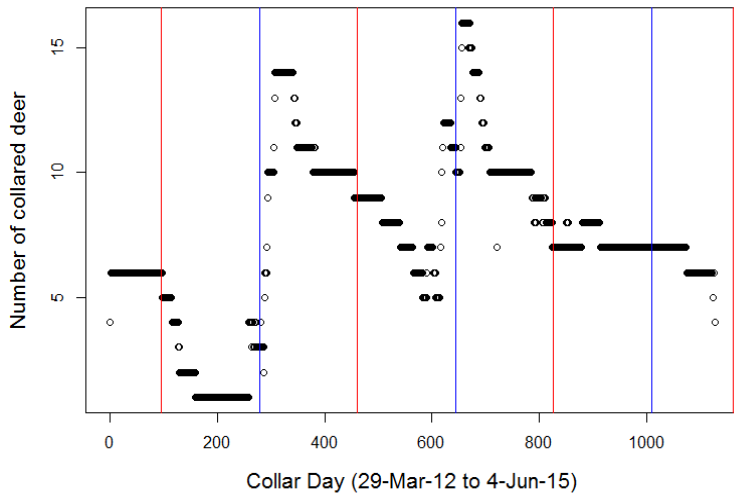
Figure 4-2. (a) The number of collared deer for which location data were collected throughout the study period. Reference lines indicate July 1 (red) and January 1 (blue) of each year, from 2012-2015. (b) The total number of telemetry locations collected each day, indicating the monitoring intensity over the study period.
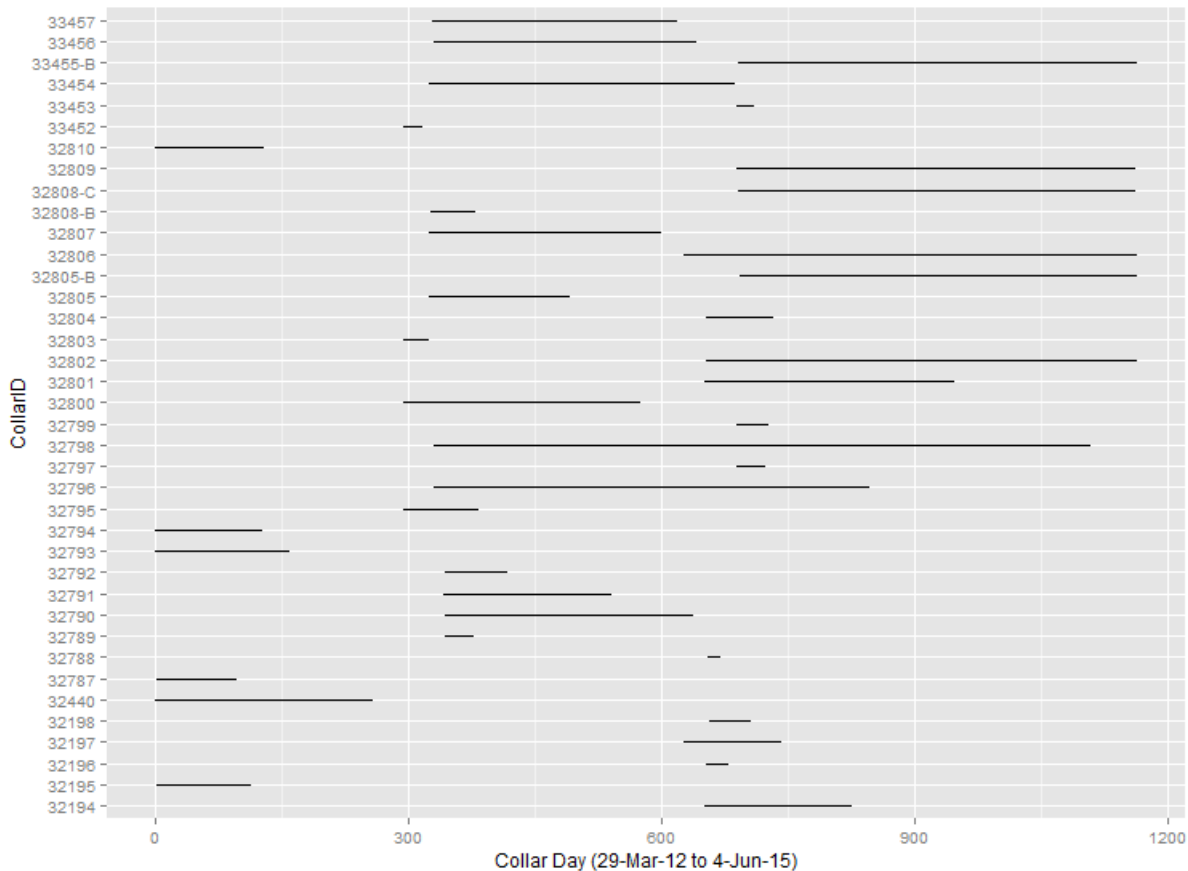
Figure 4-3. The duration that each individual female (CollarID) was monitored varied markedly, as some died quickly whereas others remained alive throughout much of the study.
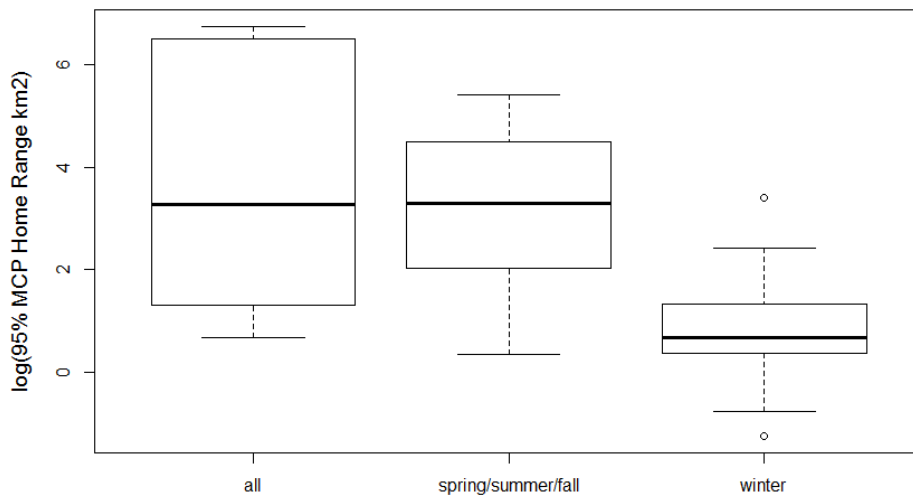
Home range sizes

There was considerable variation in extent of movement across the 38 collared deer, with 95% Minimum Convex Polygon (MCP) home ranges spanning from 0.29 to 850 km^2 (mean = 84, median = 5.1, sd = 183). Most individuals had small home ranges while a few covered very large areas during the period of data collection (Figure 4-4). Ten of the collared females undertook large seasonal movements to cover total areas greater than 75 km^2. Among the remaining 28 monitored deer, mean 95% MCP was 7.3 km^2 (median = 3.5, sd = 9.4). Home range sizes were highly correlated whether estimated by MCP or by 95% and 50% kernel density (not shown). As would be expected, home range size (or extent of movement) was correlated with length of observation period and number of locations; however, the correlation was not very strong ($r <$ 0.35; Fig. 4-5), implying that other factors influenced variation in movement behaviours. Grouping deer by the season(s) in which they were monitored showed that deer monitored primarily during winter had much smaller home ranges sizes (mean = 4.0 km^2, sd = 6.1, n = 23) than deer monitored between spring and fall (mean = 56.7 km^2, sd = 73.8, n = 9) or across the entire year (mean = 267 km^2, sd = 384.0, n = 6; Fig. 4-6). Similarly, an analysis of mean step lengths showed that, on average, deer moved to a greater extent during summer than winter (Fig. 4-7; further details in Appendix 3). Further analysis is warranted of individual variation in home range sizes, using standardized time periods, as well as in location of ranges and seasonal changes.
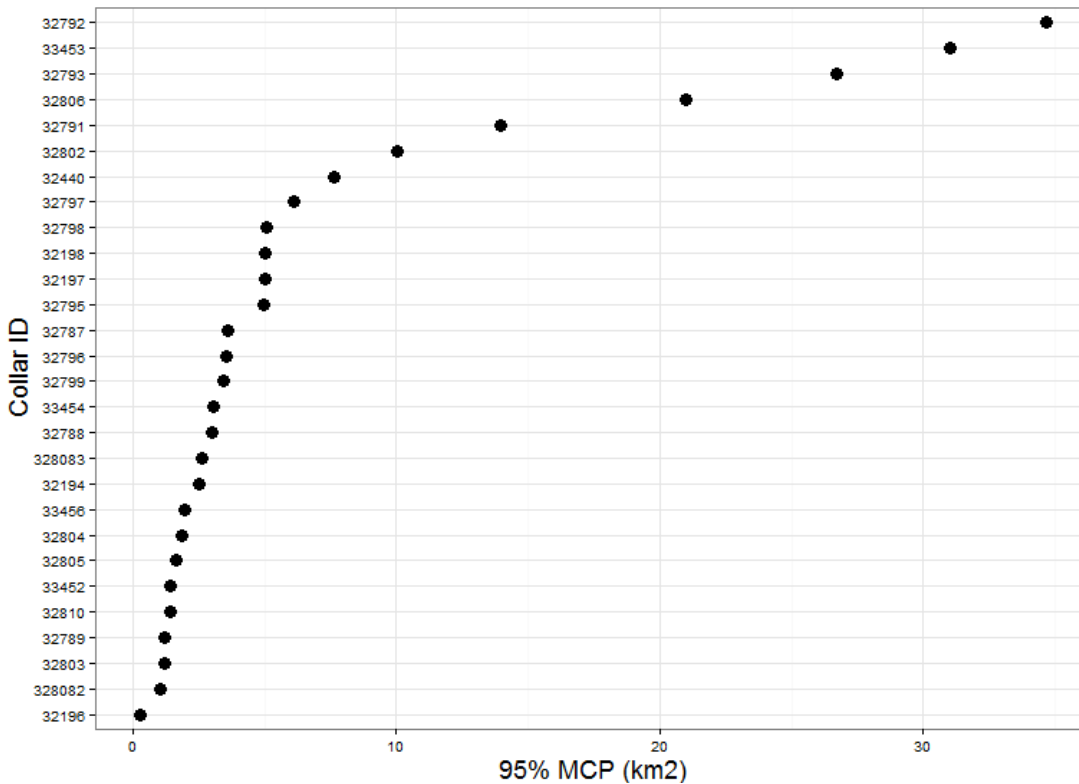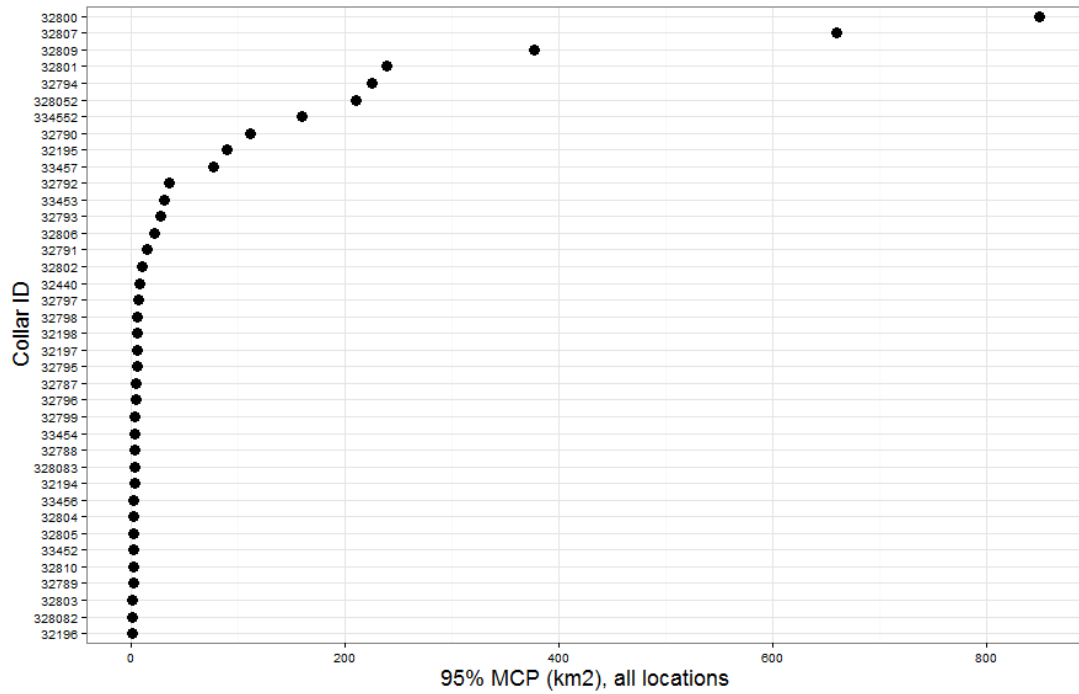
Figure 4-4. Distribution of home range sizes (estimated by 95% MCP) across: TOP, all collared female deer over the entire period that they were monitored (note that these include seasonal migratory movements for some deer); BOTTOM, only those with non-migratory ranges less than 50 km2.
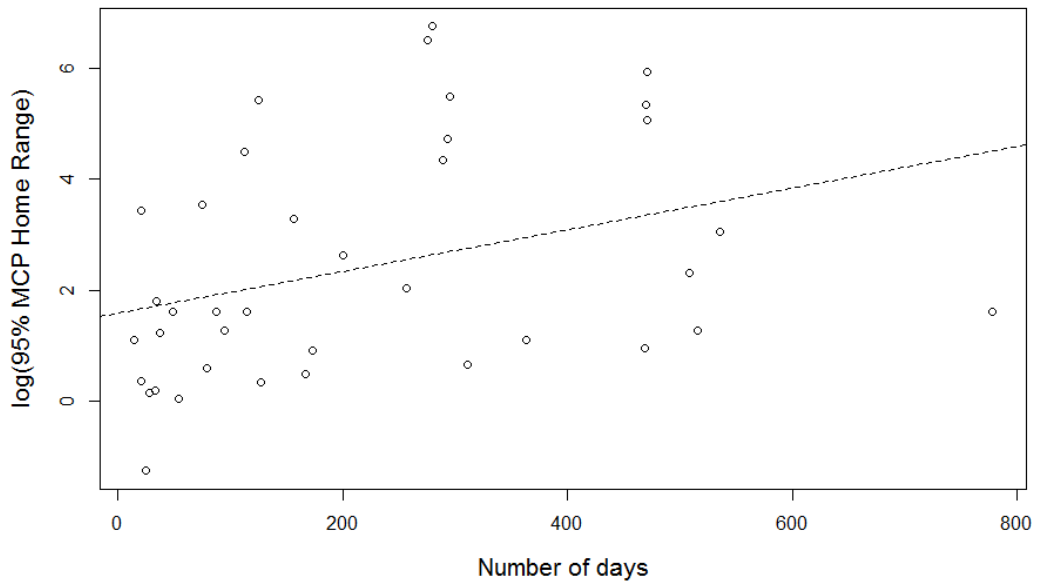
Figure 4-5. Correlation between 95% MCP home range size and number of days of GPS monitoring for collared deer.

Figure 4-6. Variation in home range size by season(s) in which deer location data were collected.
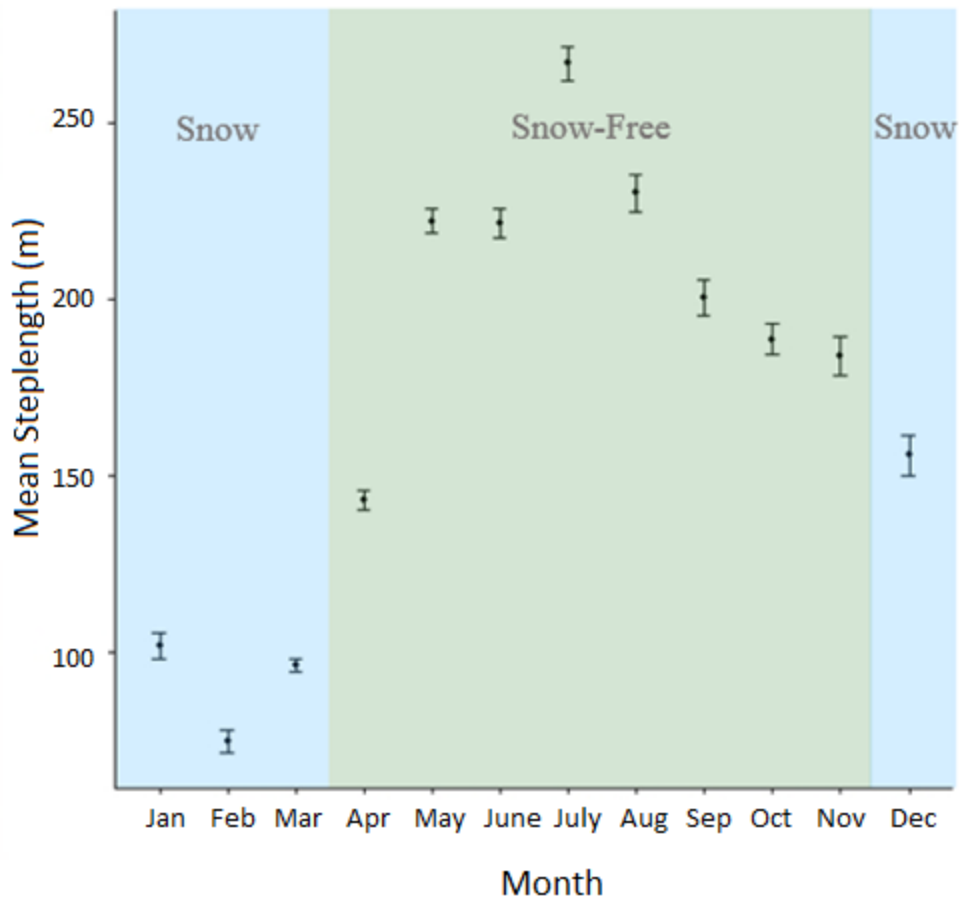
Figure 4-7. Mean step lengths (across 2-hour fix intervals) for collared deer during different months. See Appendix 3 for more information about step lengths and step selection functions.

Resource selection functions

We ranked multiple models in a nested approach (Table 4-2) to test hypotheses about how white-tailed deer females selected or avoided natural and anthropogenic landscape features. Within each block of models describing a common type of features (linear, forest overstorey, *etc.*), the most complex model of each set was definitively best-supported (Table 4-4). Within each model group, the most complex model was best-supported (highest AIC weight). Support for the best model was unambiguous, as AIC_w ~ 1.0 in each case. Among the best-supported models within each group, the cumulative effects model best described white-tailed deer resource selection, with AIC_w ~ 1.0.

Table 4-4. Ranking of white-tailed deer resource selection models, within nested groups of similar landscape features. Model numbers refer to models described in Table 4-1.

Model Group	Model number	AIC	ΔAIC	AIC$_w$
Block features	Model 2	250007.5	0.0	1.00
	Model 2a	273978.7	23971.2	0.00
	Model 3	300334.7	50327.2	0.00
	Model 4	280927.6	30920.1	0.00
	Model 5	299897.6	49890.1	0.00
	Model 6	280311.7	30304.2	0.00
Linear features	Model 8	244572.7	0.0	1.00
	Model 8a	275901.6	31328.9	0.00
	Model 9	275562.7	30990.0	0.00
	Model 10	293288.1	48715.4	0.00
	Model 11	286339.8	41767.1	0.00
	Model 12	258667.9	14095.2	0.00
SAGD features	Model 13	276817.2	0.0	1.00
	Model 14	296032.8	19215.6	0.00
	Model 15	299371.1	22553.9	0.00
Forest overstorey	Model 16	257765.2	0.0	1.00
	Model 17	274790.1	17024.9	0.00
	Model 18	264957.1	7191.9	0.00
Forest understorey	Model 19	291352.5	0.0	1.00
	Model 20	293309.8	1957.3	0.00
	Model 21	298316.4	6963.9	0.00
Successional stage	Model 22	187539.9	0.0	1.00
	Model 23	195156.6	7616.7	0.00
	Model 25	275144.3	87604.4	0.00
	Model 26	208852.7	21312.8	0.00
	Model 27	246968.3	59428.4	0.00
Cumulative effects and interactions	Model 28	186655.6	0.0	1.00
	Model 29	194019.3	7363.7	0.00
	Model 30	274169.1	87513.5	0.00
	Model 31	294815.2	108159.6	0.00

Ranking of best-supported models from each group

Model Group	Model number	AIC	ΔAIC	AIC$_w$
Cumulative effects	**Model 1 / 28**	**192900**	**0.0**	**1.00**
Block features	Model 2	250008	57107.6	0.00
Linear features	Model 8	244573	51672.8	0.00
SAGD features	Model 13	276817	83917.3	0.00
Forest overstorey	Model 16	257765	64865.3	0.00
Forest understorey	Model 19	291353	98452.6	0.00

The cumulative effects model suggested white-tailed deer resource selection in this boreal landscape is dictated by a number of natural and anthropogenic factors (Table 4-5). Deer selected several natural features: aspen stands, white and black spruce stands, and stands with larch understorey selected (parameter estimate > |0.1|). Deer weakly avoided a few natural features, most strongly black spruce and larch overstoreys. Deer were closer than expected to several anthropogenic features: forest harvesting cutblocks, trails, well sites (Figure 4-8), roads, and pipelines. Deer were farther than expected from 3D seismic lines (Figure 4-8) and high density industrial sites. Stands with jack pine overstorey and industrial mine sites were not significantly selected nor avoided.

Table 4-5. Parameter estimates from the best-supported resource selection function of female white-tailed deer in the northeast boreal forest of Alberta, Canada, from telemetry locations spanning across all seasons. With the exception of the intercept, variables are arranged from strongest positive parameter estimates to strongest negative parameter estimates. A positive relationship between deer locations and "distance to" anthropogenic features indicates deer were farther from that feature than expected by chance.

Variable	Parameter estimate	Std. error	z value	Pr(>|z|)	Significance[+]
(Intercept)	-0.294	0.091	-3.22	0.00129	**
ELECTRICAL	1.087	0.016	70.10	< 2e-16	***
PCT_AW	0.569	0.008	73.36	< 2e-16	***
HIGH.DENSITY	0.464	0.012	37.93	< 2e-16	***
PCT_SW	0.216	0.006	35.36	< 2e-16	***
UPCT_LT	0.214	0.006	33.01	< 2e-16	***
PCT_BW	0.119	0.006	21.62	< 2e-16	***
CUTLINE3D	0.107	0.014	7.47	7.85E-14	***
UPCT_PJ	0.063	0.006	11.16	< 2e-16	***
UPCT_PB	0.045	0.007	6.09	1.10E-09	***
UPCT_SW	0.031	0.007	4.56	5.12E-06	***
PCT_PJ	0.003	0.007	0.48	0.63175	NS
INDUSTRIAL.MINE	-0.014	0.013	-1.10	0.27031	NS
UPCT_BW	-0.015	0.006	-2.31	0.02087	*
UPCT_AW	-0.029	0.007	-3.97	7.25E-05	***
PCT_PB	-0.045	0.005	-8.31	< 2e-16	***
PCT_FB	-0.047	0.006	-7.53	4.93E-14	***
SETTLEMENT	-0.074	0.013	-5.55	2.90E-08	***
UPCT_SB	-0.080	0.007	-12.12	< 2e-16	***
UPCT_FB	-0.084	0.009	-9.82	< 2e-16	***
CUTLINE	-0.144	0.008	-17.43	< 2e-16	***
PCT_LT	-0.166	0.007	-22.40	< 2e-16	***
PCT_SB	-0.243	0.007	-35.32	< 2e-16	***
PIPELINE	-0.363	0.018	-20.04	< 2e-16	***
WELLSITE	-0.405	0.014	-29.90	< 2e-16	***
ROAD	-0.491	0.013	-39.20	< 2e-16	***
TRUCKTRAIL	-0.530	0.017	-31.59	< 2e-16	***
OTHER.DISTURBED	-0.812	0.010	-78.71	< 2e-16	***
RAIL	-0.853	0.012	-71.63	< 2e-16	***
CUTBLOCKS	-0.899	0.011	-84.06	< 2e-16	***
TRAIL	-1.051	0.009	-115.26	< 2e-16	***

+Significance codes: ~0***, 0.001**, 0.01*, 0.05[@], 0.1[NS]
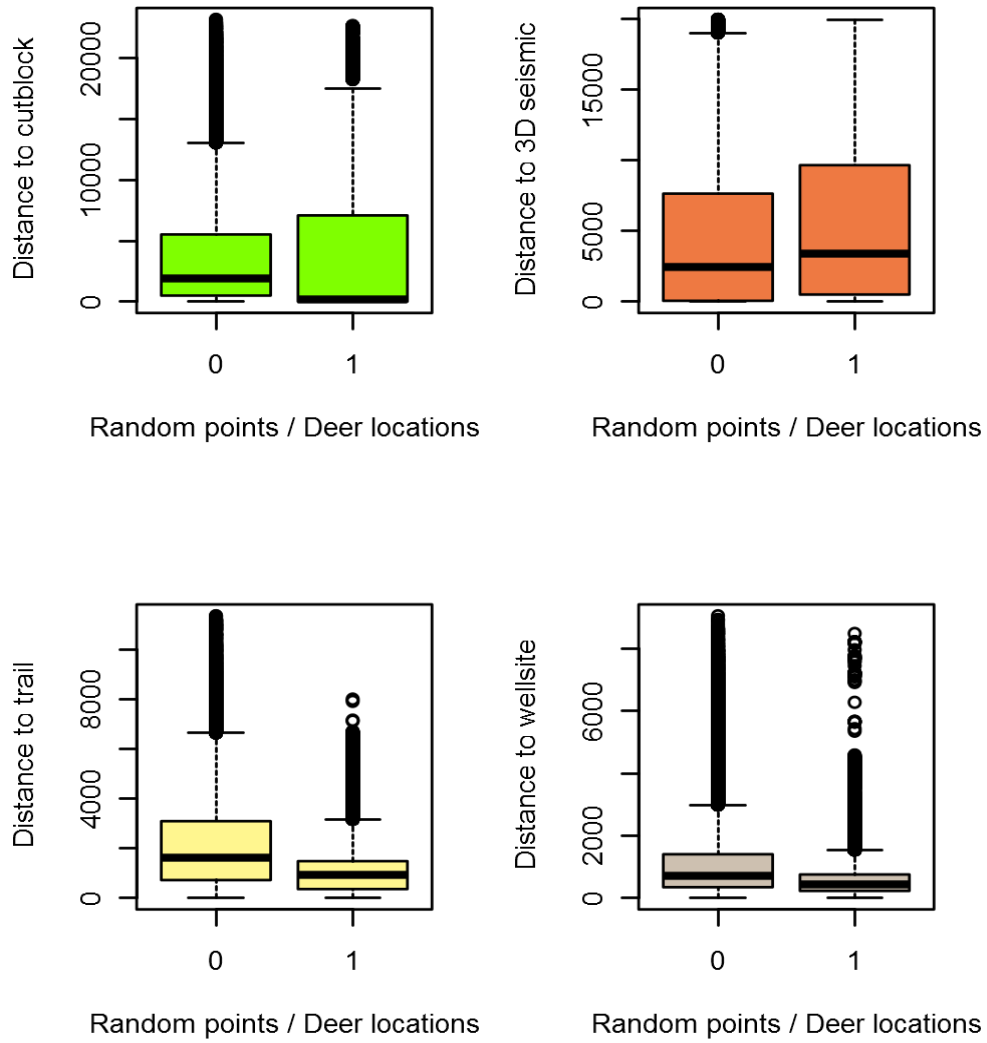
Figure 4-8. Boxplots of random locations (0) and white-tailed deer telemetry locations (1) and in relation to some landscape features that were significantly selected or avoided. Deer locations were closer to cutblocks (upper left panel), farther from 3D seismic lines (upper right), closer to trails, and closer to well sites than were random locations.

Discussion

White-tailed deer space-use in the boreal forest was highly variable among individuals. This is consistent with similar studies from across WTD range (DeYoung et al. 2011), which show WTD home ranges vary from 1 – 20 km^2. Deer are also highly variable in their seasonal space-use patterns, with some individuals migrating every winter, some staying resident every winter, and some migrating only under certain conditions (conditional migration) (Sabine et al. 2002). If we exclude long-distance movements, boreal female WTD home ranges averaged around 7 km^2 in our study (+/- 9 sd, although the large variability in length and timing of collar monitoring across individuals makes standardization more difficult). This information helps us to estimate white-tailed deer abundance (Chapter 5), but otherwise does not yield much useful information about the factors contributing to white-tailed deer expansion. A more in-depth examination of variation in home-range size among individuals, with respect to the habitat composition and degree of anthropogenic alteration, might yield more insights (Fieberg and Börger 2012).

Female white-tailed deer selected forest stands with high percentages of deciduous trees (aspen and birch), but also upland conifer (white spruce). Stands with conifer understoreys were also selected. We predicted that deer would be associated with deciduous stands, as these provide browse species commonly used by white-tailed deer across their northern range (Hewitt 2011). Conifer cover, including conifer understorey, catches snowfall and reduces snow depth on the ground. Lower snow depth reduces metabolic costs on deer (Ditchkoff 2011, Hewitt 2011), and these snow refuges are often selected by deer (Stewart et al. 2011). However, deer avoided lowland coniferous stands such as black spruce and tamarack, which typically contain little available browse. Forested stands providing a mix of browse and snow refuge are selected in this boreal landscape, fitting with our hypotheses.

Deer were significantly farther than expected from electrical lines, high density industrial sites, and 3D seismic lines. The latter is of particular interest as these features are so spatially intensive across the south and centre of the study area. At this time we cannot suggest why this avoidance occurs.

White-tailed deer were closer than expected to anthropogenic features that replace mature forest with early seral vegetation: cutblocks, well sites, and pipelines. Cutblocks are known as high-quality deer habitat (Fisher and Wilkinson 2005), and our results are consistent with many studies before us on this point. Well sites, in comparison, are small polygonal areas with grassy or shrubby cover surrounded by mature forest. We hypothesized that the juxtaposition of escape cover and abundant browse provided by well sites would be heavily selected by WTD. Our hypothesis was supported, and this conclusion also fits with the landscape-scale association between well sites and WTD relative abundance modelled from camera data (Chapter 3). Together, these results support our hypotheses that white-tailed deer are selecting deciduous forest and disturbed areas with early seral vegetation.

However, deer were also closer than expected to several linear features: trails, truck trails, and roads. This result result runs counter to expectations. Linear features provide early seral vegetation, but also human access, and are the primary areas where accidental mortalities (road kills) and hunting mortalities reportedly occur. Moreover, wolves travel linear features searching for prey, as travel is easier and search times are reduced; therefore predation rates on caribou are

greater (Whittington et al. 2011, McKenzie et al. 2012) and it is very likely that predation rates on deer are likewise greater. These results suggest white-tailed deer do not, apparently, exhibit trade-offs in habitat selection (*sensu* Fretwell and Calver 1969, Fretwell 1972, Pyke et al. 1977) by avoiding areas with higher mortality risk. It is important to note that this analysis includes all deer data from all years, conducted using a simple approach, and is only a first examination of white-tailed deer habitat selection. Further analysis of seasonal data, using more precise analyses such as step selection functions, may yield different conclusions.

As the spatial use of landscapes by white-tailed deer is pervasively variable among (and within) regions (Stewart et al. 2011), there is no straightforward comparison between our results and those from other studies. In highly fragmented mixed forest-agricultural landscapes in South Dakota, white-tailed deer movements were heavily influenced by anthropogenic footprint: row crops, pasture, and grassland (Grovenburg et al. 2009). Like boreal deer and those in New Brunswick (Sabine et al. 2002), South Dakota deer exhibited mixed migration strategies – some deer were resident, some obligate, and some conditional migrators. In mixed agricultural-Carolinian forests in New York, white-tailed deer selected for deciduous forest and agricultural features throughout the year, and coniferous forest in winter (Williams et al. 2012). Williams *et al.* concluded that deer perceive heterogeneity and move among patches differently with changing resources within patches. We opted to use an annual resource selection function to provide a cohesive overview of deer selection in the boreal forest. Movement and selection within long time periods such as ours is likely a function of seasonally changing browse availability, predation risk, social dynamics, and annual density (Gautestad and Mysterud 2005). Shorter time frames, especially those tied to specific seasons, are likely tied to a smaller range of variables. Winter may be particularly important for white-tailed deer as this is a period of great stress, and presumably strong selection (Beier and McCullough 1990). Our camera-based species distribution models did not show a marked difference between annual and winter distribution, but our boreal white-tailed deer telemetry data could be further mined to examine seasonal space-use shifts.

The nature of the anthropogenic footprint in the Alberta boreal landscape also makes comparisons difficult, as most studies have been conducted in forested or mixed forest-agricultural landscapes. However, recent mule deer (*Odocoileus hemionus*) research has explicitly examined species' response to petroleum extraction footprint. In Colorado, anthropogenic footprint altered mule deer space-use and home-range philopatry (Northrup et al. 2015a). Northrup et al. (2015b) found that mule deer strongly avoided well pads and roads, resulting in the effective loss of 50% of critical winter range. Conversely, we observed selection of wellpads and roads by white-tailed deer. Mule deer also altered their diel behaviour, avoiding human activity more during the day than at night. Behavioural responses to features may be manifested by boreal white-tailed deer, and this is also worth future examination. The different responses to human activity between the two species may in part drive the declines in mule deer and increases in white-tailed deer observed in landscapes across western North America.

The conclusions about white-tailed movement and resource selection lend support to our overarching hypothesis that landscape development for resource extraction from multiple industrial sectors is altering landscape function, allowing for persistence of white-tailed deer, even after severe winters. The final piece of evidence with which we can test this overarching hypothesis arises from an examination of white-tailed deer densities before and after severe winters.

CHAPTER 5: ESTIMATING WHITE–TAILED DEER DENSITY IN THE BOREAL FOREST

Introduction

Estimating and monitoring the abundance of white-tailed deer populations in Alberta's boreal forests is an important management challenge. Reliable abundance estimation facilitates effective management of white-tailed deer harvest (Hansen 2011), and understanding the expansion of white-tailed deer populations is an important aspect of conservation efforts for woodland caribou (Latham et al. 2011, Boutin et al. 2012). Many different methods have been used to estimate the abundance of white-tailed deer populations (e.g. DeYoung 2011). In Alberta, white-tailed deer population monitoring has typically used aerial survey transects and a modified Gasaway sampling technique to estimate abundance (a.k.a. stratified random block survey; e.g. Chapman & Gilligan 2013). These aerial ungulate surveys have primarily focused on moose populations, and a key challenge for deer monitoring is that their sightability from aerial transects may be very low in boreal forest. More recently, distance sampling methods have been used to try to improve estimates by explicitly modelling detectability (Buckland et al. 2001; Peters et al. 2014; Burgar & Sztaba 2015). However, there remain challenges associated with distance-based estimation methods and they have not yet been proven for estimating white-tailed deer density in Alberta's boreal forests.

Camera traps (CTs) are a valuable non-invasive survey tool increasingly used to monitor wildlife populations (Burton et al. 2015). Fisher & Burton (2012) suggested that CTs may provide an alternative approach to monitoring white-tailed deer and other mammals in Alberta's boreal forests, and the Alberta Biodiversity Monitoring Institute recently changed their mammal monitoring program from one based on snow tracking to one based on CTs. Camera trapping readily provides an index of relative abundance (*i.e.* detection rate) that is potentially useful for monitoring population changes over time (Carbone et al. 2001, O'Brien 2011). However, such indices rely on the questionable assumption of equal detectability over areas or time periods being compared, and thus require either calibration with robust estimates of abundance, or a more direct estimation of detection probability (Anderson 2001; MacKenzie & Kendall 2002; Sollmann et al. 2013a).

Occupancy estimation provides a formal approach to estimate detection probabilities (MacKenzie et al. 2006), and thus occupancy has been recommended as a state variable for monitoring wildlife populations at regional scales (e.g. Noon et al. 2012; see also Chapter 2). However, occupancy is a relatively coarse metric describing species distribution or habitat use, and it does not provide detailed information on population abundance within occupied areas. Methods have been developed to estimate local (site-level) abundance based on detections from point surveys such as camera trapping (*e.g.* Royle 2004; Chandler et al. 2011; Denes et al. 2015). Nevertheless, these techniques require assumptions that may not be realistic for relatively wide-ranging species that are not easily individually identified (*e.g.* white-tailed deer), such as independence of detections among surveys and sites (but see Duquette et al. 2014).

Capture-recapture techniques are frequently used to estimate wildlife density from CT data, but these techniques also traditionally depend on accurate identification of individuals (Foster & Harmsen 2012; Burton et al. 2015). Such "marked" approaches are difficult to apply on "unmarked" species such as white-tailed deer, for which reliable identification of individuals from photographs is difficult. Jacobson et al. (1997) proposed a population estimator for white-tailed deer using data from camera surveys in which individual males were identified using antler variation (see also Watts et al. 2008). Such an approach has potential, but Moore et al. (2013) showed the method underestimated known deer populations by 32% on average. Furthermore, it relied on baited sites, which can be problematic, particularly when data on multiple species is also being collected (e.g. McCoy et al. 2011; Burton 2014). Recent extensions of spatial capture-recapture (SCR) models have been proposed for estimating density of unmarked or partially marked wildlife populations (Chandler & Royle 2013; Sollmann et al. 2013b; Royle et al. 2014). These show promise but have not been widely tested. The goal of this study is to test the utility of these new techniques for estimating white-tailed deer density in the project study area in northeastern Alberta (Chapter 1).

Methods & Results

### *Spatial and temporal variation in deer relative abundance*

The camera trap survey was initiated in October 2011 and completed in October 2014, covering a continuous 3-year sampling period (1101 sampling days; Fig. 5-1). During this period, data were collected from 62 camera stations for a total sampling effort of 60,937 camera trap-days (accounting for inactive days due to camera malfunctions; see Chapter 1 for further details on the camera trap methods).
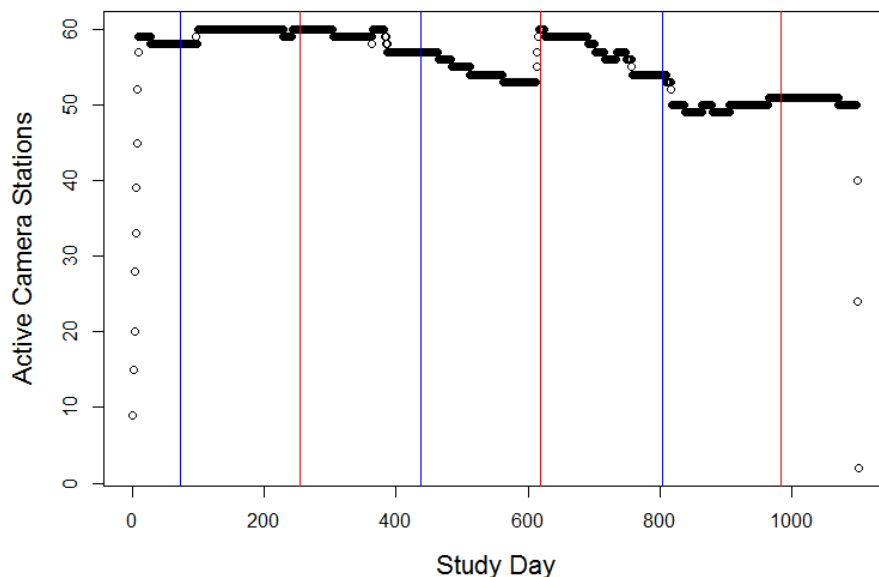

Figure 5-1. Number of camera stations active on each day of the study period, from 22 October 2011 (Day 1) to 26 October 2014 (Day 1101). Blue lines indicate January 1 and red lines indicate July 1 for each year (2012-2014).

We calculated a count of deer detections for each day and station by defining a detection event as a photograph, or sequence of photographs, of an individual deer staying within the camera detection zone. Each individual captured in the photograph was counted, and when all individuals left the photographic frame, the next photograph was counted as a new detection event (with no minimum threshold of elapsed time). We calculated a total count that included all photographed deer regardless of age, and a second count that excluded fawns (young of year) for the purpose of density estimation (see below). The total count of deer detections, summed across all stations and days, was 17,359 (15,609 excluding fawn detections). Note that this is not an estimate of abundance as it includes the same individuals counted multiple times. We divided the daily count of deer detections by the number of active camera stations per day (Fig. 5-1), or number of active days per station, to create temporal and spatial indices of deer relative abundance that accounted for variation in sampling effort (cf. O'Brien et al. 2003). However, we emphasize that the relationship between the index and *true* deer abundance is not known since the index does not distinguish individuals (and thus double-counts individuals) nor does it account for detectability (defined as the probability of detecting an individual given its occurrence at the sampled site). As such, this simple index reflects both the local abundance of deer around camera stations and the behavioural activity of those deer (e.g. habitat use, movement; Burton et al. 2015).

Assessing variation in the count index across camera stations and sampling days can give insight into changes in deer abundance and habitat use across space and time. As implied above, we highlight the implicit assumption that detection probability is constant across the spatial or temporal bounds of comparison, and thus urge caution in making inferences about abundance or habitat use without testing this assumption (see Chapter 2 on estimating detectability through occupancy modelling). There was considerable variation in the deer count index across camera stations during the study period (Figs. 5-2, 5-3); hypotheses about environmental variables potentially underlying this spatial variation are investigated in Chapter 3.
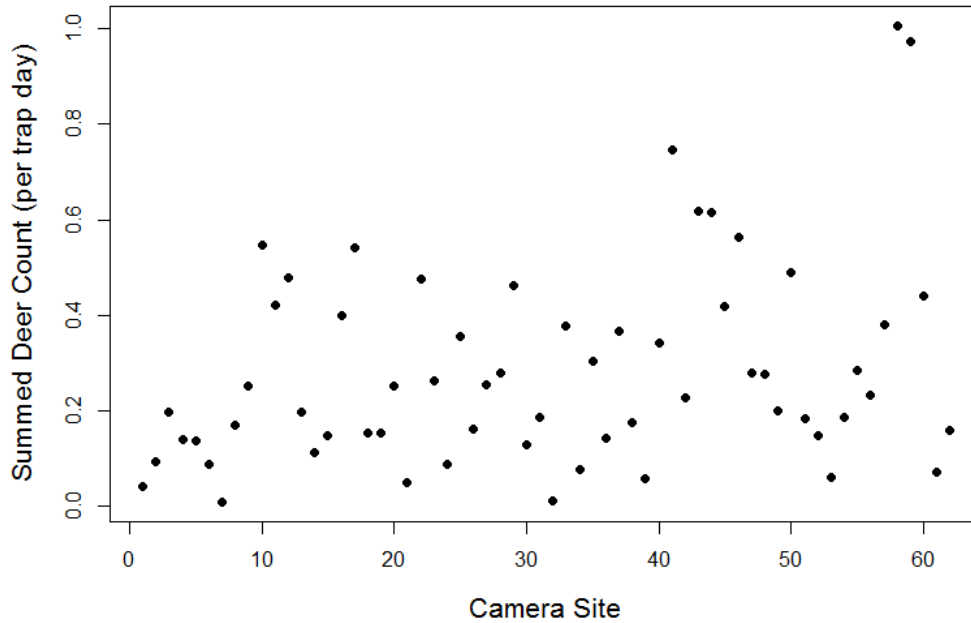
Figure 5-2. Variation in the total count of white-tailed deer detection events across camera sampling sites summed over the entire survey period, and corrected for the number of active sampling days for each site.
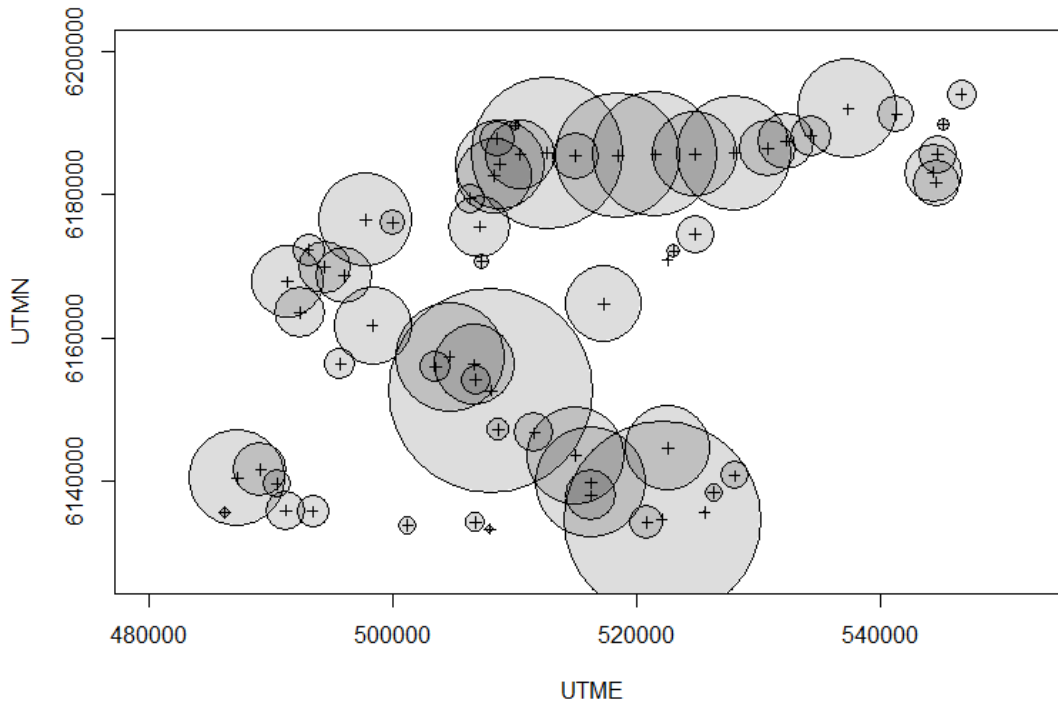

Figure 5-3. Spatial variation in the index of white-tailed deer relative abundance (count per camera-day) across camera sampling sites over the entire survey period (axes are UTM coordinates of camera stations).

There was also considerable variation in the daily deer count over the 3-year study period (Fig. 5-4). This variation likely reflects seasonal variation in both local abundance and movement; for instance, deer survival and movement rates are lower during winter, while fecundity and movement are higher during snow-free periods (Chapter 4). Detection rates were also generally lower in the second and third years of the study, corresponding to more severe winters in the region relative to the first year (colder winters with more snow; Fig. 2-2). This pattern motivates the hypothesis that deer density declined in the study area as a result of increased winter severity—a hypothesis we aimed to test through more robust density estimates (see below).
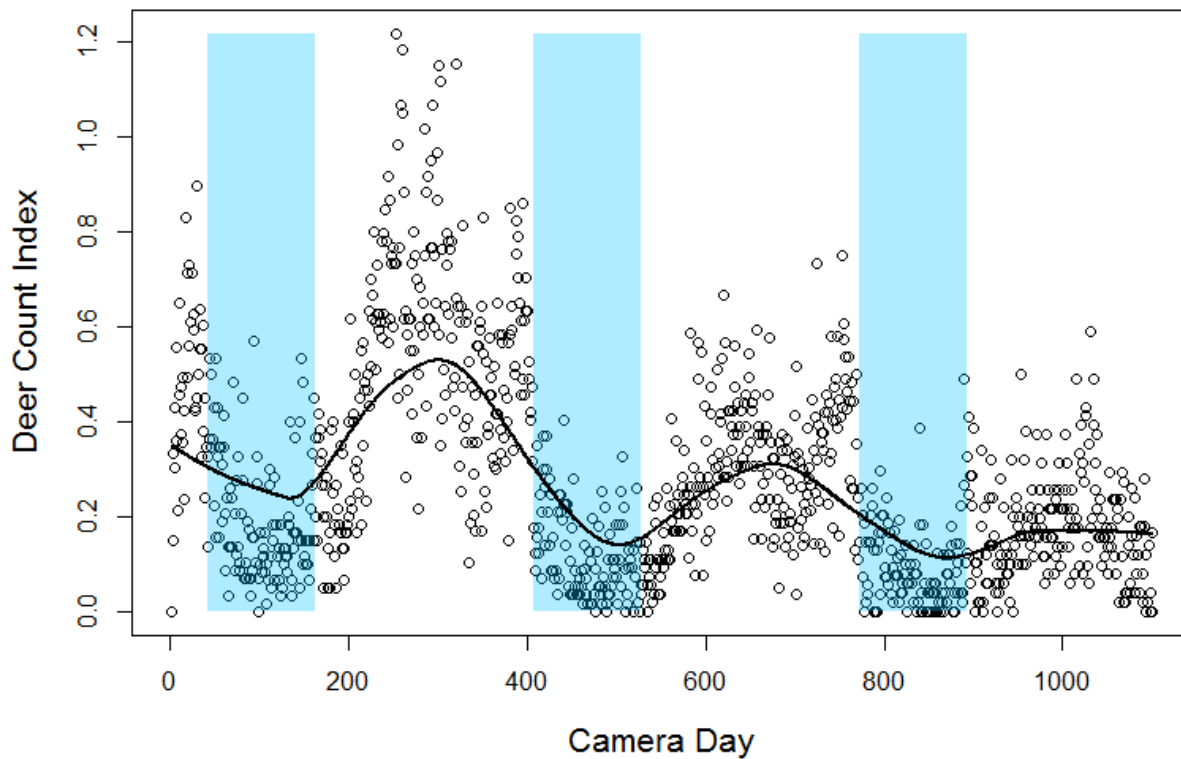
Figure 5-4. Variation in the daily count of deer detections across the three-year survey duration (counts summed over all active camera stations each day and divided by the number of active stations. Day 1 = 22 October 2011). Blue shading represents winter periods (Dec-Mar) and the solid line is a lowess smoother of the count index.

The spatio-temporal patterns in deer detections also indicate that deer relative abundance declined during winter periods and later in the study (Fig. 5-5). However, these patterns support the conclusion that deer recovered quickly after the severe winters, both in terms of the number of sites used and relative use (or local abundance) at sites (see Chapters 2,3).
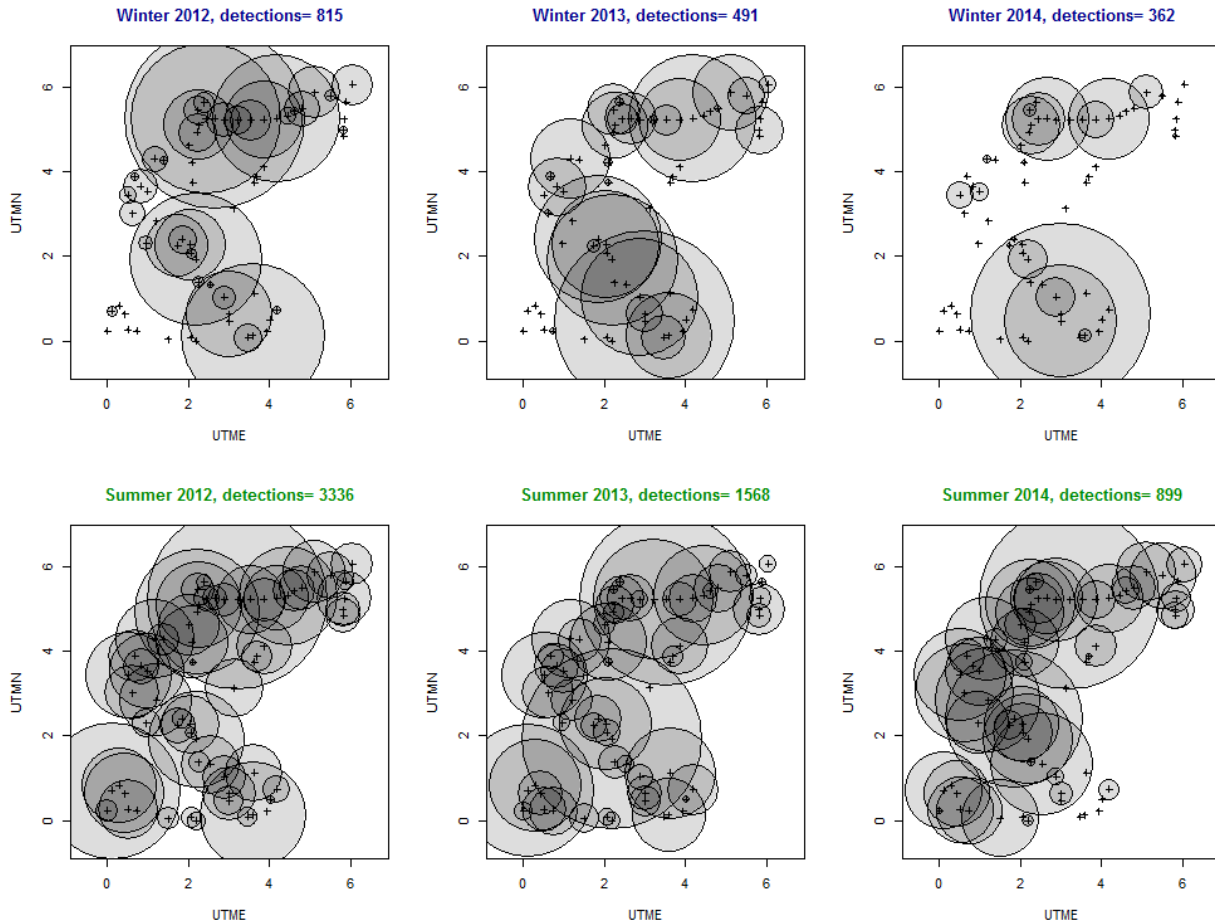
Figure 5-5. Spatio-temporal patterns of white-tailed deer detections across camera sampling sites during the study period, showing declines in relative abundance across years but seasonal increases from winter to summer. Each plot shows the relative number of deer detections (size of circle) at individual camera sites (crosses) for a specific time period. The top row shows relative abundance patterns across winter periods (January-March) for each year of the study; the bottom row shows patterns for summer periods (June-August). The total number of deer detections is indicated for each period. Plot axes give the standardized UTM coordinates for camera stations.

Estimating deer density using an unmarked spatial count model

A robust method for estimating deer population density is required to reliably assess population dynamics. This includes using an estimator that accounts for detection heterogeneity to calibrate a relative abundance index (such as the detection rate described above) if such an index is to be used to assess spatial or temporal trends (e.g. Rovero & Marshall 2009). Chandler & Royle (2013) proposed a spatially explicit model for estimating density in unmarked populations (*i.e.*, for which individuals are not marked or otherwise identified). Their approach builds on recently developed spatial capture-recapture (SCR) models, which improve on traditional capture-recapture models by explicitly accounting for effective sampling area and spatial heterogeneity resulting from interactions between animal movements and sampling locations (Efford 2004; Royle et al. 2014). The spatial count (SC) model for unmarked populations uses spatial correlation in counts from relatively closely spaced sampling units to model the location of individual activity centres, and thereby estimate

distance-related heterogeneity in detection. Density is then calculated by counting the number of estimated activity centres (Chandler & Royle 2013; Royle et al. 2014). Essentially, the model extends the SCR framework by considering individual detection histories to be latent, or unobserved, variables that result in the observed count of detections.

The SC model uses an approach called data augmentation whereby a maximum hypothetical population size, M, is specified for the given study area. M should be greater than the expected true population size, N, encompassing both real, detected individuals and *potential* individuals with all-zero detection histories (Royle et al. 2014). The model then estimates the number of individuals that exist within the sampled population; that is, the proportion of M that make up N. The model is formulated in a hierarchical structure consisting of:

- z_i, an auxiliary variable indicating if individual i is a member of the population N, which is modelled as a Bernoulli variable dependent on probability ψ,

$$z_i \sim Bernouilli(\psi)$$

- the latent encounter history, y, of individual i at site j on occasion k, which is modelled as a Poisson variable dependent on z_i and the individual encounter rate, λ_{ijk},

$$y_{ijk} \sim Poisson(\lambda_{ijk} z_i)$$

- the encounter rate is in turn modelled as a function of the baseline encounter rate at a camera trap, λ_0, and a distance function describing how encounter rate declines with increasing distance between the trap location, x_j, and the individual's activity centre, s_i (i.e. home range centre),

$$\lambda_{ijk} = \lambda_0 exp(-\parallel x_j - s_i \parallel^2)/2\sigma^2$$

where σ is the scale parameter determining the rate at which the encounter rate decreases with distance (assuming a Gaussian or bivariate normal model of space usage in this case),

- and the observed count, n_{jk}, is then calculated as the sum of all latent encounter histories over the M potential individuals,

$$n_{jk} = \sum_{i=1}^{M} y_{ijk}$$

The SC model can be implemented in a Bayesian framework using Markov Chain Monte Carlo (MCMC) estimation, with prior distributions specified for the parameters ψ, σ, and λ_0. It also requires specification of a state-space, S, representing the region containing the potential locations of individual activity centres, s_i. This should be chosen to be sufficiently large to include all animals with a non-negligible probability of being detected by camera traps during the sampling period (Royle et al. 2014).

The SC model makes several assumptions that should be carefully considered, including demographic and geographic closure over the sampling period, random distribution of activity centres, encounter probability declines with distance from home range centre, and independence of encounters among and within individuals (see Royle et al. 2014 for further discussion of these assumptions and the expected degree of model robustness to violations).

As an initial test of this method, we applied an SC model to a subset of the camera survey data roughly corresponding to the period for which the last aerial-based estimate of deer population density was made. An aerial survey of Wildlife Management Unit (WMU) 517 was conducted in January 2013 by Alberta Environment and Sustainable Resource Development (AESRD, now Alberta Environment & Parks, AEP; Chapman & Gilligan 2013). The white-tailed deer population was estimated to be 693 (± 367, 90% C.I.), corresponding to a density of $0.15/km^2$, which provides a basis for comparison with our initial estimate (although we note that the true population density remains unknown).

We used the daily deer detection count for each of 57 camera stations for a 57 day period from 1 December 2012 to 26 January 2013. This period was chosen as a compromise between having a relatively large sample of detections and reducing potential bias due to violating model assumptions, such as geographic and demographic closure. We excluded fawns from the count as we felt they were likely to violate the assumption of independence among detections of different individuals (i.e. fawns are more likely to be detected with their mothers), so the resulting estimates are for the deer population ≥ 1 year old. We added a 10-km buffer to the locations of the outermost camera stations, creating a rectangular state-space of $6,482$ km^2, and specified a maximum population size of 2,000 deer across the entire state-space (which corresponds to a maximum potential density of 0.31 deer/km^2. Note that the state-space is not exactly the same as the area covered by WMU 517, which was the focus of the AESRD aerial survey). We specified uninformative (vague) prior distributions and random initial values for the estimated parameters of σ (scale parameter), λ_0 (baseline encounter rate), and ψ (probability that a potential individual is included in the sampled population). The derived parameter N reflects the estimated number of individual activity centres (i.e. individual deer) and is converted to density by dividing by the area of the state-space.

We found estimating parameters of this SC model to be very computationally intensive due to the large number of potential latent encounter histories that need to be assessed across the large state-space. We successfully ran a model using the program JAGS version 3.4.0, executed with the package *rjags* (Plummer 2014) within program *R* version 3.3.1 (R Core Team 2014). The model run consisted of 2 MCMC chains of 10,000 samples each after an initial burn-in of 1,000 iterations, and it took 166 hours to run (~ 7 days) on a Dell Precision M3800 laptop with dual 2.20 GHz processors and 16 GB of RAM. The model produced reasonable estimates of σ (scale parameter) and λ_0 (baseline encounter rate) but a diffuse posterior distribution for N (number of deer in the state-space; Fig. 5-6). The posterior mean and SD for N was 1,412 ± 366 deer (95% C.I. = 697 – 1,969), corresponding to an estimated mean density of 0.22 ± 0.06 white-tailed deer/km^2 (95% C.I. = 0.11 – 0.30), but the posterior distribution was truncated at our specified maximum "augmented" population size of 2,000 (M), and the MCMC chains did not fully converge (Fig. 5-6).
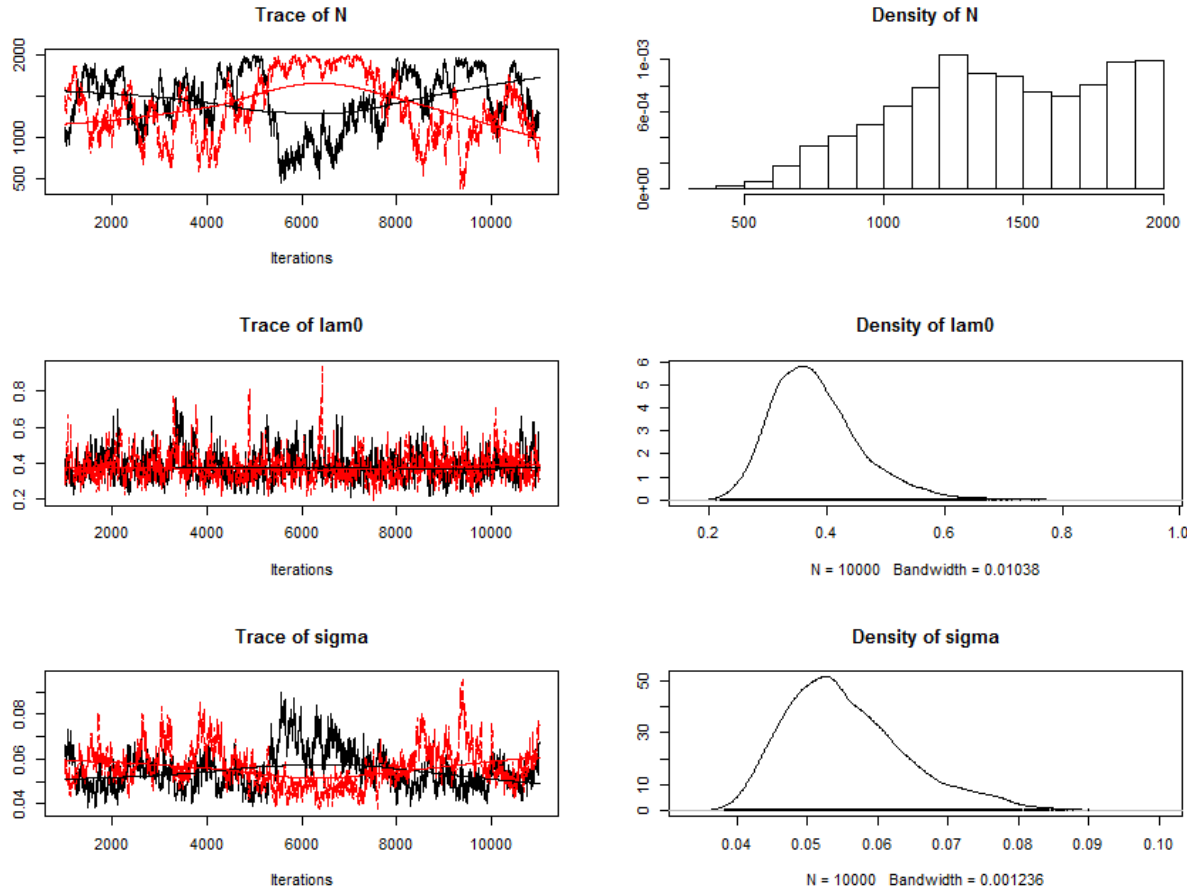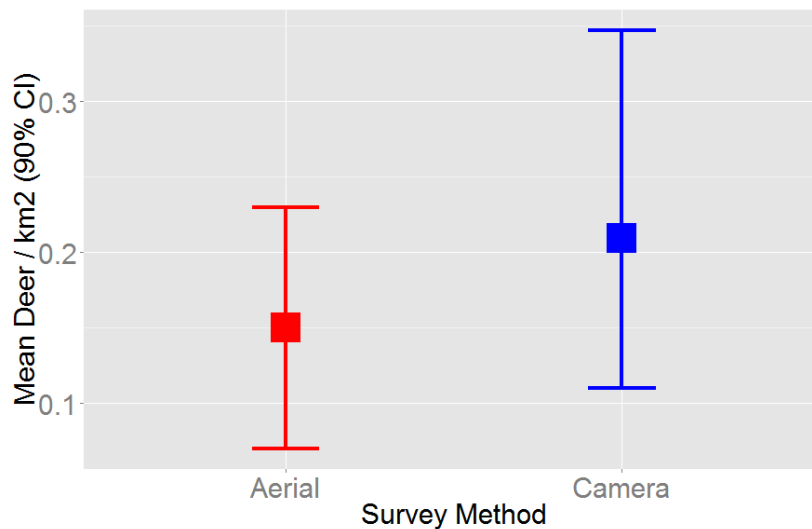
Figure 5-6. Results of white-tailed deer density estimation using a spatial count model for camera trap detections over the period Dec. 2012 – Jan. 2013. Markov Chain Monte Carlo iterations (*Left*, showing both chains) and posterior probability densities (*Right*) for the estimated parameters N (number of deer), λ_0 ("lam0", baseline encounter rate), and σ ("sigma", scale parameter).

Estimates of σ can be converted to home range area, assuming a bivariate normal model of space usage (Royle et al. 2014). Estimates from this model correspond to a mean of 5.8 km^2 (± 0.14 sd, median = 5.5, 95% CI = 3.4 – 11.0), which appear reasonable based on telemetry analysis of female deer home range sizes (Chapter 4).

In order to try to improve on this initial SC estimate, we ran another model using a larger augmented population size (M = 2500) and an informative prior on σ based on observed home range sizes of collared deer [*dgamma*(3,70)]. This model took 45 days to complete and showed better convergence but did not significantly change the accuracy or precision of the resulting density estimate (mean = 0.21 deer/km^2, 95% CI = 0.098 – 0.36; Figs. 5-7, 5-8; Table 5-1).
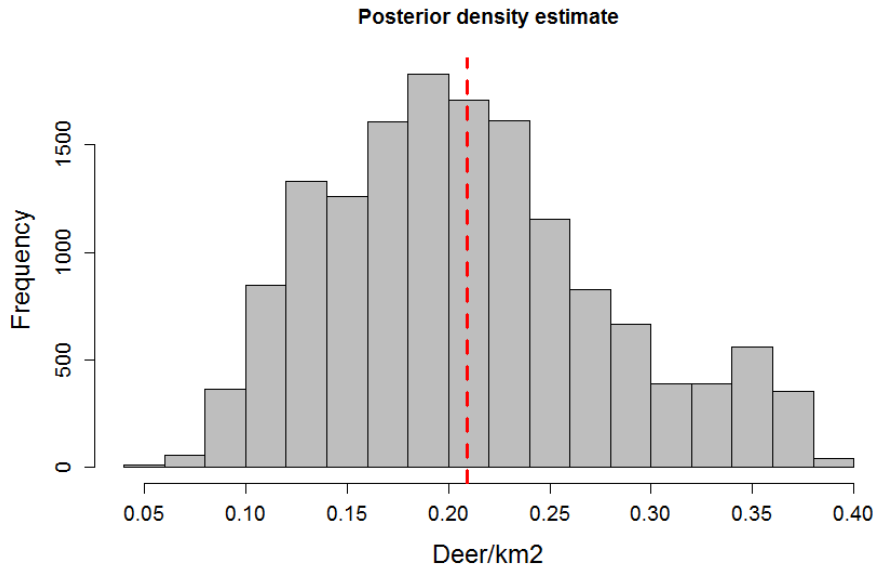
Figure 5-7. Posterior estimate of white-tailed deer density from a Spatial Count (unmarked) model applied to camera-trap data for the period 1 December 2012 to 26 January 2013.

Figure 5-8. Comparison of white-tailed deer density estimates from the AEP aerial survey (January 2013) and the camera-trap sampling (December 2012 – January 2013). Uncertainty is shown using 90% confidence intervals, as reported in the AEP report (Chapman & Gilligan 2013).

Given the long computation times for this implementation of the SC model in JAGS, we evaluated alternative implementations using a custom MCMC algorithm developed by Royle et al. (2014), namely the function *scrUN* from the *scrbook* R package. Computation times using this algorithm remained slow but were faster than the JAGS implementation. However, the estimates generally failed to converge and did not seem reliable – they produced very different estimates than the spatial mark-resight models described below. For instance, even when using an informative prior for sigma (based

on observed home range sizes), SC estimates of density using the *scrUN* function sometimes differed by more than an order of magnitude from the SMR density estimates. We therefore urge caution in applying this estimation approach and suggest that more evaluation is needed for the SC models of unmarked populations. Other authors have similarly reported challenges with obtaining reliable estimates from SC models applied to realistic datasets (e.g., Chandler & Royle 2013; Sollmann et al. 2013a,b) .

Despite the encouraging result that our estimate of white-tailed deer density from the SC model corresponded reasonably well with the AEP aerial survey estimate (Fig. 5-8), we conclude at this time that the SC models are of uncertain reliability for broader application. There may not be enough information in typical camera survey datasets to reliably estimate sigma and lambda without additional information from marked individuals. We suggest that further assessment of the SC models is warranted, including evaluation of different MCMC implementations (e.g. Nimble), greater iterations to more thoroughly assess convergence, and tests against known populations—ideally real populations of known density, but simulated populations could also be used. Notwithstanding these recommendations for further research on SC models, we focused the remainder of our effort for this report on assessing the utility of spatial mark-resight models that use additional information on marked individuals.

Estimating deer density using a spatial mark-resight model

Spatial mark-resight (SMR) models represent a hybrid between the spatial count (SC) models of unmarked individuals (described in previous section) and the spatial capture-recapture (SCR) models of marked individuals (wherein all detected animals are individually identified; Royle et al. 2014). The data underlying SMR models include individual encounter histories across sites and occasions for a subset of the sampled population that is marked, as well as the spatial counts of all unmarked individuals across those sites and occasions. SMR models build on traditional mark-resight models (e.g. McClintock & White 2012) by explicitly modelling the locations of detections, thereby linking abundance estimates to a clearly defined area and facilitating unambiguous estimates of density (Sollmann et al. 2013a,b).

In the SMR model, individual encounter histories, y_{ijk}, are partially latent, with only those for the m marked animals being observed. The observed count, n_{jk}, is modelled as the sum of all latent encounter histories over the $M\text{-}m$ potential unmarked individuals in the state-space, and a Bayesian framework (using Metropolis-within-Gibbs Markov chain Monte Carlo sampling) is used to estimate model parameters (as described above; see also Chandler & Royle 2013; Sollmann et al. 2013a,b; Royle et al. 2014).

In our study, the marked subset of the population consisted of collared female deer (see Chapter 4). Encounter histories (i.e. camera detections) and telemetry relocations for these deer were modelled in combination with the camera-specific counts of unmarked deer, using a custom MCMC algorithm implemented in the *scrPID.tel* function from the *scrbook* R package (Royle et al. 2014). To evaluate the SMR models, we first identified periods of sampling with suitable numbers of collared deer exposed to, and detected by, the camera array (Fig. 5-9). In order to maximize use of data while minimizing the potential for model violations, we sought to choose relatively short periods (e.g. 2-3 months) that maximized the

number of collared deer monitored and their camera detections while minimizing violations of the assumption of population closure (e.g. mortality or migration of collared deer, fawning period).
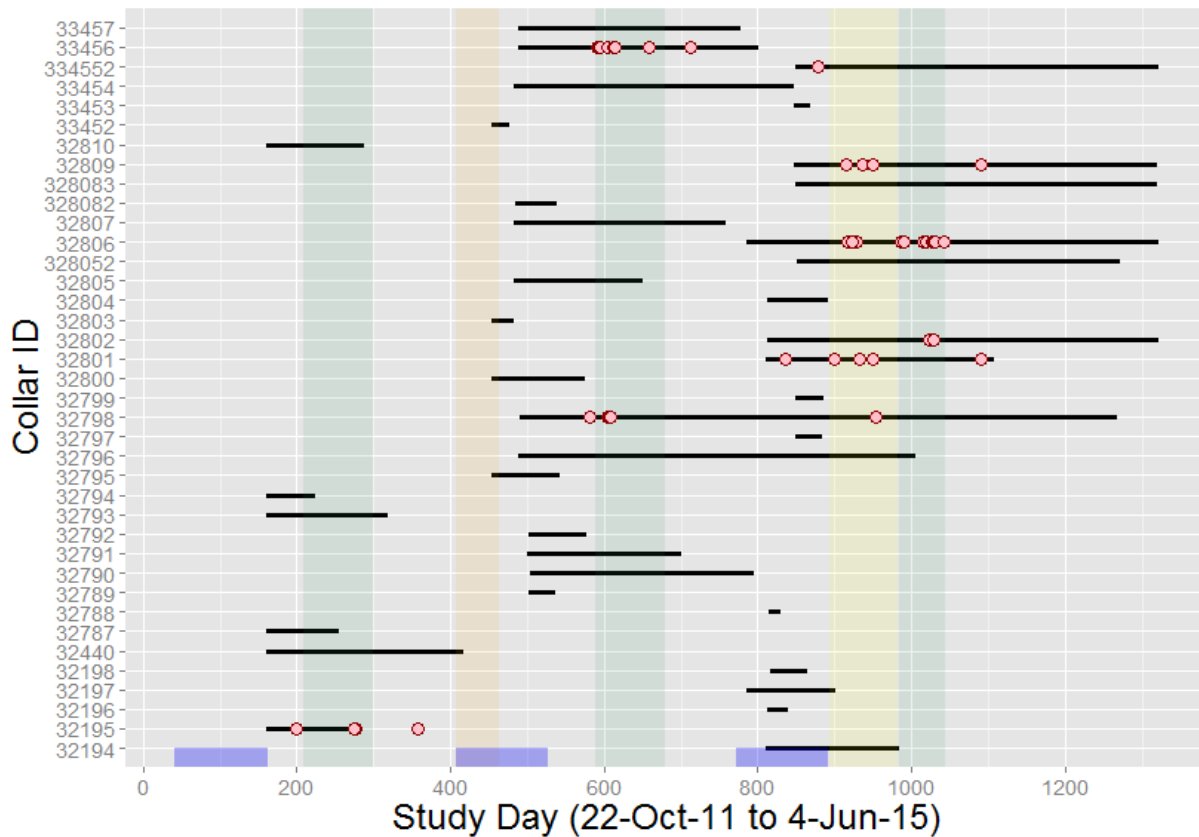

Figure 5-9. Periods of monitoring for satellite-collared deer (y-axis, black lines) over the duration of the study (x-axis), with red points indicating camera detections of collared deer. Green shading denotes three periods for which spatial mark-resight density estimates were made to allow comparison of density across years. Migratory movements of collared deer during the yellow-shaded period led to a poor estimate of density. Orange shading indicates the period for which a spatial count model was used to estimate density for comparison with the January 2013 AEP aerial survey. Blue shading at the bottom corresponds to December to March winter periods in each of the three main study years (2011-2014).

Based on a more complete evaluation of space use by the collared deer (Chapter 4), we expanded the state-space for the SMR models to encompass a 10,000 km^2 area defined by adding a 20-km buffer to the outermost camera locations in the sampling array (although we note that future work should consider reducing computation time by using an irregularly shaped state-space that more closely matches the area sampled by the camera array). We chose the period from 1 April to 30 June 2014 ("Spring 2014") for the first SMR estimation, as it represented a period with the most collared deer monitored and detected by cameras (study days 893-983, 10 collared deer and 50 active camera stations; Fig. 5-9). The model was run with a single MCMC chain of 11,000 iterations (2,000 discarded as burn-in), using the *scrPID.tel* function, with the maximum potential unmarked individuals set at *M* = 2000.

This period produced a very low mean density estimate of only 0.037 deer/km^2 (95% CI = 0.028 – 0.049; Fig. 5-10), much lower than the mean density of 0.21 deer/km^2 estimated from the SC model for Winter 2012-13 (Fig. 5-7; Table 5-1).

However, further evaluation of the telemetry data revealed that this estimation period included large, seasonal migratory movements by several deer (Fig. 5-11), resulting in a very high estimate for σ, the spatial scale parameter (Fig. 5-12). This large estimate corresponds to an unrealistically large home range size (> 600 km^2) and indicates that this period of estimation violated a key assumption of the modelling framework, namely that home ranges (activity centres) were stable and the population was closed to immigration or emigration from the state space. We conclude that the density estimate was very sensitive to this model assumption, and therefore that the Spring 2014 period was not appropriate for estimating deer density using this approach.
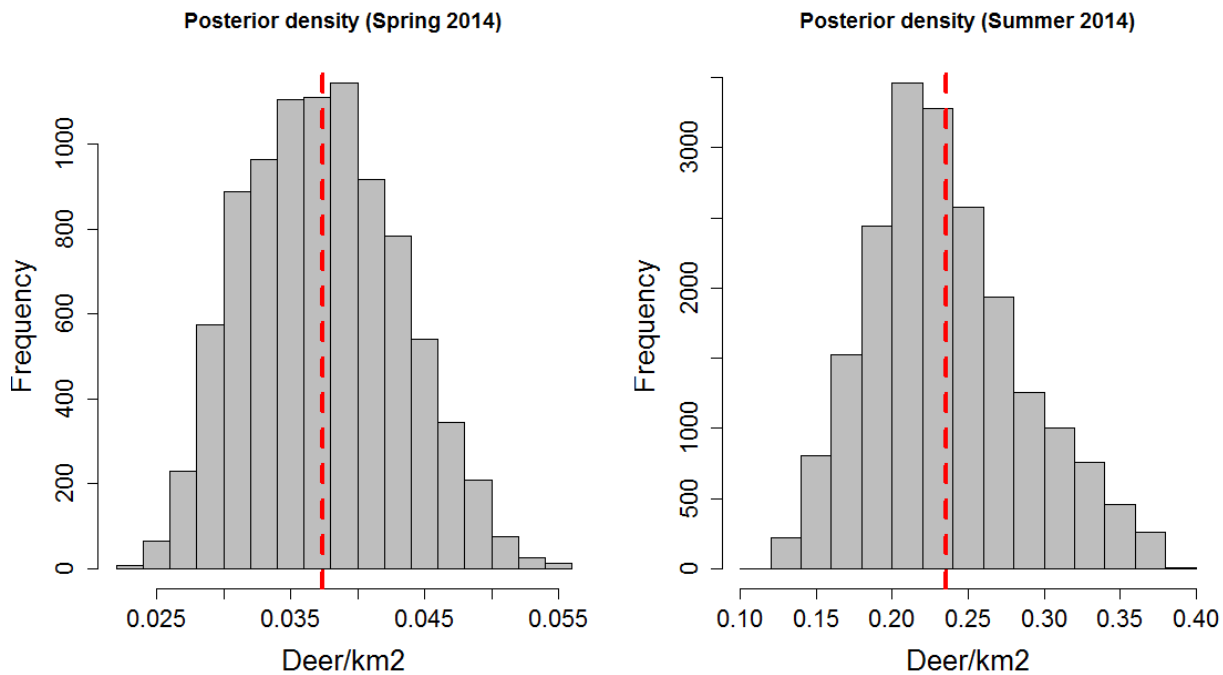

Figure 5-10. Posterior distributions of the SMR deer density estimates for the periods 1 April to 30 June 2014 ("Spring 2014", left), and 1 July to 31 August 2014 ("Summer 2014", right). Dashed red lines denote the posterior means. Further evaluation indicated that the Spring 2014 estimate was biased low due to seasonal migratory movements of some collared deer (and thus violation of the model's assumption of closure and stable home ranges).
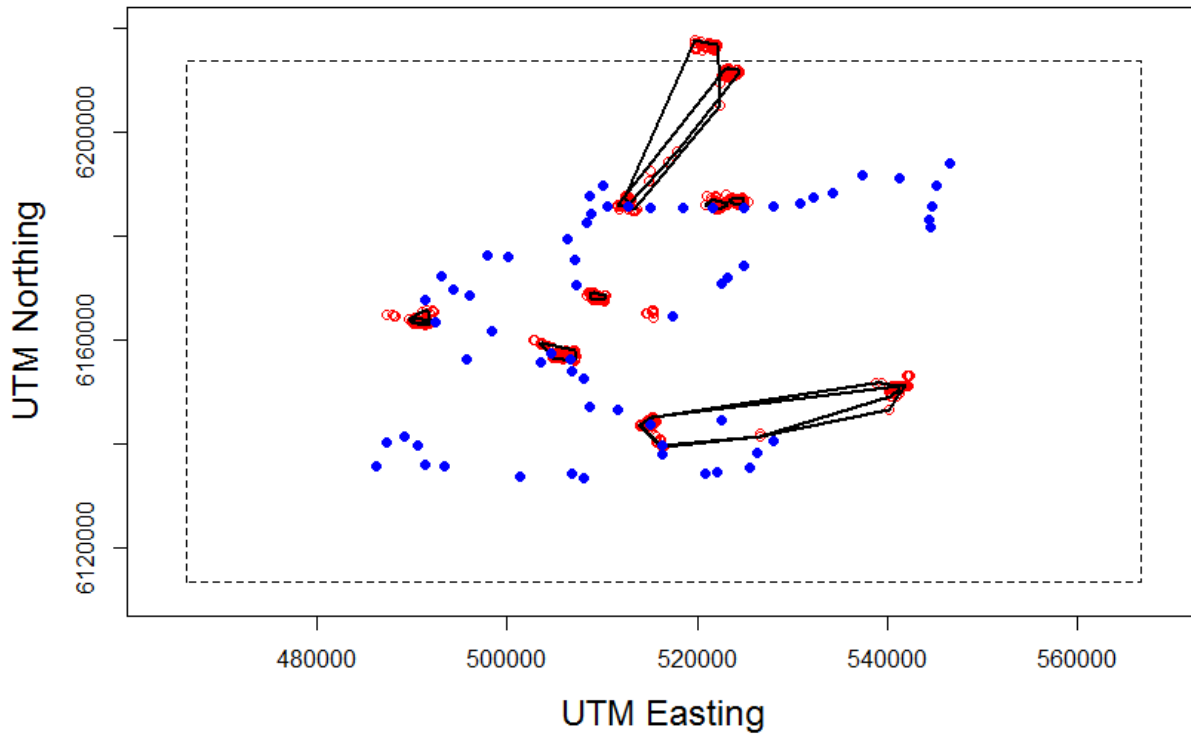
Figure 5-11. Telemetry locations (red points) and minimum convex home ranges (black lines) of collared deer for the Spring 2014 estimation period (1 Apr – 30 June 2014), relative to the camera array (blue points) and state-space (dashed box). This shows that seasonal migratory movements occurred during this period (large polygons), and thus that model assumptions of stable home ranges and population closure were violated.
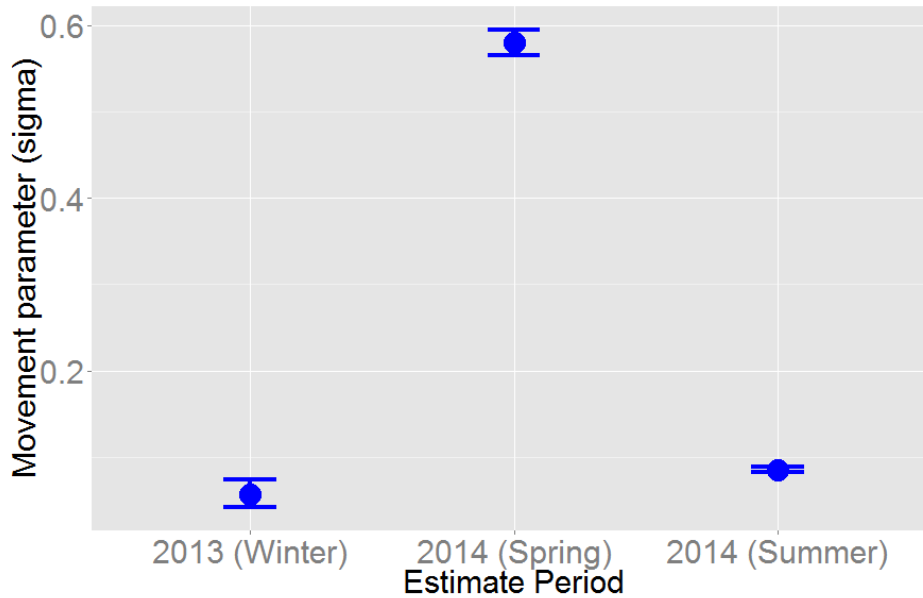
Figure 5-12. Estimates of σ, the spatial scale (movement) parameter, for the SC model in Winter 2012-13 and the SMR models in Spring and Summer 2014 (posterior mean and 90% C.I.). The Spring 2014 period included large, seasonal migratory movements by deer, resulting in a very large estimate of σ (corresponding to a home range of > 600 km^2), and a low estimate of density (Fig. 5-10). By contrast, estimates of σ for the other periods were more consistent with non-migratory deer home ranges (e.g. 5-15 km^2), and thus did not violate model assumptions.

We then shifted the estimation period to later in that year ("Summer 2014": 1 July - 31 August, study days 984-1045), which represented a period with similar camera and telemetry data for collared deer (Fig. 5-9), but during which deer did not make large, migratory movements (Fig. 5-12). We ran 21,000 MCMC iterations (discarding 1,000 as burn-in) and increased M to 4000. The resulting density estimate for this period was more similar to the SC estimate for the winter 2012-13 (mean = 0.24, 90% CI = 0.16 − 0.33; Fig. 5-10, Table 5-1), and the estimate of sigma was more in line with expectations of stable home range size (mean sigma = 0.06, equivalent to a bivariate normal home range size of 13.8 km^2; Fig. 5-12). This result reinforced our interpretation that the SMR model is sensitive to seasonal migratory movements (i.e., non-stable home ranges during estimation period). It also suggested that the deer population did not decline between the Winter 2012-13 and Summer 2014 periods.

In order to further evaluate the SMR estimation method and investigate temporal trends in deer density within the study area, we next estimated density for the periods from *a)* 16 May to 16 August 2012 ("Summer 2012"), and *b)* 24 May to 31 August 2013 ("Summer 2013"; study days 208-300 and 581-680, respectively). These periods were chosen to maximize the number of collared deer and their detections by cameras (Fig. 5-9) while avoiding long-distance seasonal movements (determined by inspecting telemetry locations, as in Fig. 5-11). The comparison across the three summer periods, from 2012 to 2014, allowed a test of the hypothesis that deer abundance declined in the study area due to the severe winters of 2012-13 and 2013-14 (Fig. 2-2).

We implemented these models in a similar manner as described for the previous SMR models, with the exception that we ran 30,000 iterations and increased M to 10,000 for the Summer 2012 model (based on results of an initial run in which the posterior estimate of N was truncated at 5,000; this longer version of the model took 12 days to complete). The resulting mean posterior density estimate for Summer 2012 was 0.46 deer/km^2 (95% CI = 0.32-0.64; Fig. 5-13), and for Summer 2013 mean density was estimated as 0.25 deer/km^2 (95% CI = 0.17 − 0.35; Fig. 5-13; Table 5-1). These results suggest that the deer population did decline in abundance over the severe winter of 2012-13, but remained relatively constant after the following winter of 2013-14, which was also more severe than average (Fig. 5-14).
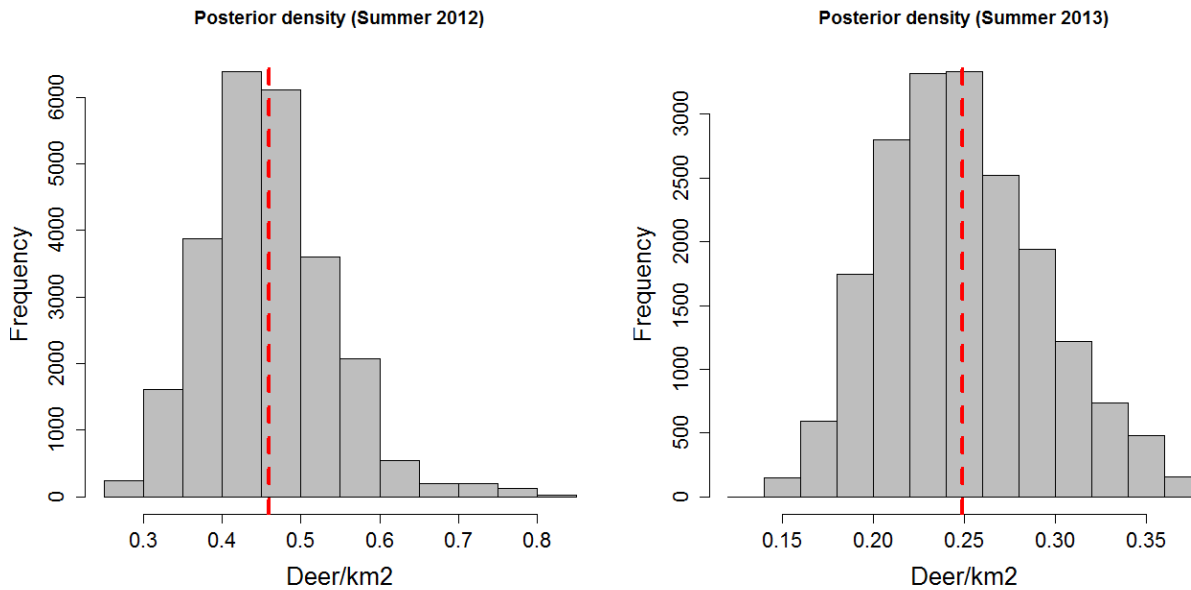
Figure 5-13. Posterior distributions of the SMR deer density estimates for the periods 16 May to 16 August 2012 ("Summer 2012", left), and 24 May to 31 August 2013 ("Summer 2013", right). Dashed red lines denote the posterior means.
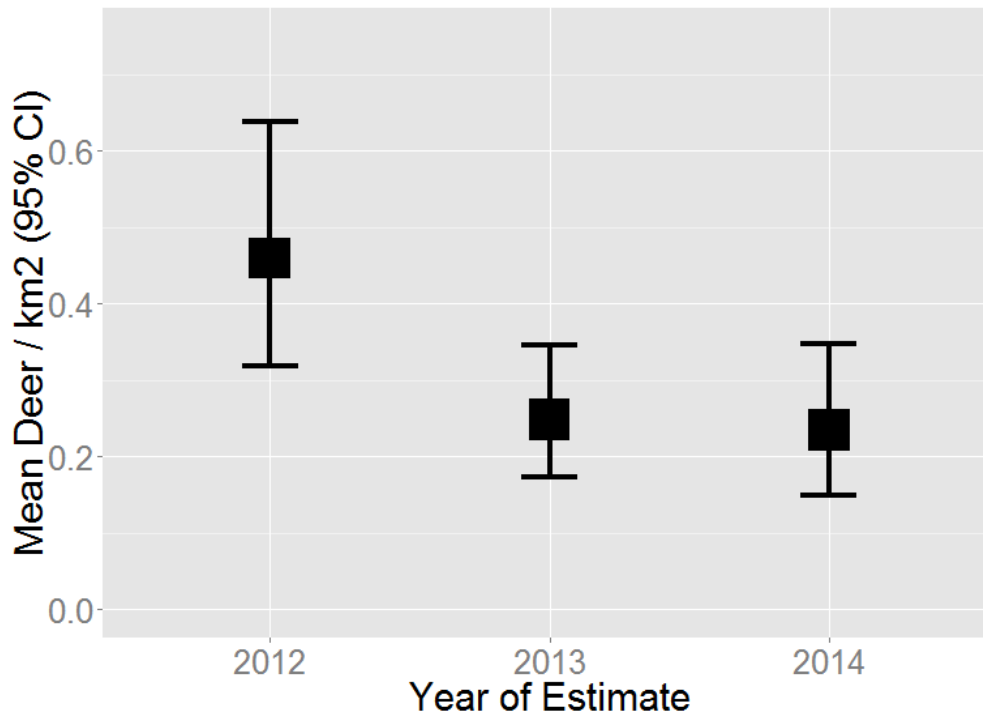
Figure 5-14. White-tailed deer population density estimates from the spatial mark-resight models for the three summer periods: 16 May to 16 August 2012, 24 May to 31 August 2013, and 1 July to 31 August 2014.

Table 5-1. Summary results of the main density estimation models applied to the white-tailed deer dataset (SC = spatial count model on unmarked sample; SMR = spatial mark-resight model on partially marked sample).

Model type	Estimation Period	Number of collared deer (marked individuals)	Number of active camera stations	Density Mean deer/km^2 (95% CI)	Scale Mean sigma (95 % CI)	Detectability Mean lam0 (95% CI)	Comment
SC	1-Dec-2012 to 26-Jan-2013	0	57	0.21 (0.10 – 0.36)	0.057 (0.040 – 0.077)	0.39 (0.27 – 0.58)	Compares well with AEP aerial survey estimate of 0.15/km^2, but SC models are difficult
SMR	1-Apr-2014 to 30-Jun-2014	10	50	0.037 (0.028 – 0.049)	0.58 (0.56 – 0.60)	0.017 (0.013 – 0.021)	Estimate sensitive to migratory movements (violation of model assumption)
SMR	1-Jul-2014 to 31-Aug-2014	8	51	0.24 (0.15 – 0.35)	0.086 (0.082 – 0.089)	0.19 (0.12 – 0.28)	Estimate considered more reliable since no migratory movements of collared deer
SMR	24-May-2013 to 31-Aug-2013	8	53	0.25 (0.17 – 0.35)	0.12 (0.11 – 0.12)	0.13 (0.09 – 0.19)	Suggests density declined over severe 2012-13 winter
SMR	16-May-2012 to 16-Aug-2012	5	60	0.46 (0.32 – 0.64)	0.073 (0.070 – 0.077)	0.39 (0.28 – 0.53)	Suggests density declined over severe 2012-13 winter

Conclusions

Our evaluation of spatial count and spatial mark-resight models suggest that camera-based density estimation using spatial capture-recapture methods hold considerable promise for surveying white-tailed deer populations in the boreal forest. Camera-based surveys provide different information than aerial-based surveys (which are currently required for management), and each has its advantages. Camera-based surveys have the potential to significantly augment population information obtained from a region, especially in areas where poor sightability that varies among habitats renders the statistical reliability of aerial surveys questionable. With the initial research work completed, an inexpensive and efficient protocol for data collection and analysis is definitely feasible. We recommend that camera-based surveys be adopted as test cases in adjacent areas to develop and evaluate this method for future surveys.

Our SC estimate of deer density was comparable to the AEP aerial survey estimate in January 2013 (Fig. 5-8), suggesting the camera-based approach provides an alternative means of monitoring deer populations, particularly when considering the additional data generated by camera surveys (this report; Fisher & Burton 2016). Nevertheless, SC models appear to be sensitive to the MCMC algorithm used, as evidenced by the discrepancy in density estimates obtained when we changed from implementing models in JAGS to using the custom *scrUN* function. This sensitivity, and the performance of SC models more generally (including computational efficiency), warrants further evaluation, and is indeed at the cutting-edge of camera trap and SCR research (Royle et al. 2014).

Capitalizing on the additional information obtained through GPS-collaring a subset of deer improved our ability to estimate deer density. Incorporating the telemetry locations and camera detections of these known individuals into SMR models provided a stronger basis for modelling the movements and detectability of deer, as has been seen in other studies (e.g. Chandler & Royle, Sollmann). However, we found that the SMR models can be very sensitive to long-distance, migratory movements that violate the model assumption of stable activity centres and population closure within the state-space (Fig. 5-12). It is therefore important to restrict survey periods for density estimation to those with the greatest likelihood of meeting such assumptions. When we used 2-3 month summer sampling periods, when deer were not expected (or observed) to migrate, we generated reasonable estimates of density across the three years of the study. These estimates suggest that deer density declined by almost half in the study area across the severe winter of 2012-13 (Fig. 5-14), when accumulated snow on the ground reached a height of almost double the 30-year average for the region (Fig. 2-2). This is consistent with the hypothesis that winter severity limits deer populations, as has been suggested in other studies (Dawe et al. 2014; Serrouya et al. 2015). However, deer density appeared to hold stable across another severe winter in 2013-14, suggesting some resilience in this population, which is consistent with our observations that deer distribution and *relative* abundance rebounded across the study area during snow-free seasons (Figs. 5-4, 5-5 and Chapter 2). Encouragingly, the trend in SMR density estimates across years was similar to that observed in the camera detection rates (Fig. 5-4), suggesting that the latter could be useful as a coarse index of changes in deer population abundance over time (although we suggest caution and further evaluation before relying on such a relative abundance index to infer trends in density).

We recommend that research be continued to further evaluate these SC and SMR modelling approaches. Firstly, comparing SC and SMR estimates to independent density estimates provides an important means of assessing their accuracy and precision. Unfortunately we could not attempt an SMR model to coincide with the January 2013 AEP aerial survey, due to a lack of collared females during this period (Fig. 5-9). It would be useful to pursue opportunities to facilitate methodological comparison, such as by deploying camera arrays to coincide with aerial ungulate surveys being undertaken by AEP in the oil sands region (e.g. Burgar & Sztaba 2015). It may also be worthwhile to compare results of the SC and SMR models to those of other recently developed methods that can be applied to similar camera and telemetry data (e.g. Rowcliffe et al.2008; Ivan et al. 2013; Tingley et al. 2015).

Tests of model accuracy and precision should also be done using simulated datasets, where true density is known and individual factors can be varied (e.g. movement behaviours, sampling design). This would also allow more detailed evaluation of optimal sampling frameworks. It is important to bear in mind that the camera trap sampling design for this study preceded development of these SC and SMR modelling methods, and was in fact designed with different sampling objectives (e.g. occupancy). Simulation studies using observed detection rates could help assess how different designs affect model performance—for instance, whether a denser camera array (i.e. more systematic grid with tighter spacing) could provide SC models with more power to reliably model movement, detection and the location of activity centres. Similarly, our study had a relatively small proportion of marked individuals at any given time, and few camera recaptures for each (Fig. 5-9), so simulation could help evaluate the number of marked individuals to target to optimize SMR model performance (Chandler & Royle 2013).

Further testing of the sensitivity of models to key assumptions (*e.g.* demographic closure, movement behaviour) could also be done through empirical comparisons of estimates from different periods, datasets, methods, and species (including other collared species detected during this study). As one example, our marked subset included only female deer, which may exhibit different movement behaviours from males. Next steps may include individually identifying bucks based on antler characteristics, and incorporating identified individuals into SMR models to account for such potential sex-specific behaviours.

We also recommend further evaluation of options to reduce model computation times and test consistency, such as omitting unsampled portions of the state-space, customizing MCMC algorithms, and running models in parallel on multiple processors or within a faster programming environment like Stan or Nimble (Royle et al. 2014; P. de Valpine unpublished report). Once the density estimation models have been carefully evaluated and fine-tuned, the results can be used to parameterize SC and SMR simulation models to refine camera trap study designs for future density surveys of white-tailed deer and other species in Alberta's boreal and beyond. Building on these closed population models, the use of open or integrated population models also holds considerable promise for long-term monitoring of population dynamics (e.g. Chandler & Clarke 2014; Whittington & Sawaya 2015).

SUMMARY CONCLUSIONS

1. White-tailed deer are widespread through the study area in Alberta's northeast boreal forest.

2. WTD distribution shrinks more markedly in more severe winters, but rebounds quickly in each spring, regardless of winter severity.

3. WTD distribution is positively related to anthropogenic features generated by forest harvesting and petroleum extraction, as well as upland deciduous forest.

4. Individual WTD selected anthropogenic features associated with early seral vegetation, including those stemming from forest harvesting, petroleum exploration and extraction, and transportation infrastructure.

5. WTD density dropped markedly after a severe winter, but then remained stable following a second severe winter.

6. Camera-based surveys and spatially explicit mark-resight models offer a way of enumerating deer density in environments where aerial surveys miss many animals due to poor sightability.

7. In summary, we suggest there is strong evidence that white-tailed deer expansion in the boreal forest is due to an interaction between less severe winters following climate change, and a substantial forage subsidy provided by widespread anthropogenic features. There is no evidence to suggest this issue is mainly a result of climate change, or of landscape change, but instead is like due to the interacting effects of climate and landscape change. This research suggests landscape management, in addition to population management, will be a key component of a white-tailed deer management strategy.